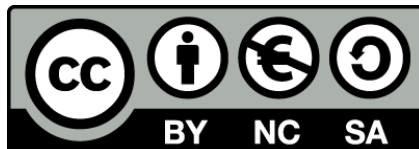




UNIVERSITAT_{DE}
BARCELONA

Enhanced recording paradigms and advanced analyses of peripheral nerve fibers *SPIike software*

Federico Ponente



Aquesta tesi doctoral està subjecta a la llicència **Reconeixement- NoComercial – Compartir Igual 4.0. Espanya de Creative Commons.**

Esta tesis doctoral está sujeta a la licencia **Reconocimiento - NoComercial – Compartir Igual 4.0. España de Creative Commons.**

This doctoral thesis is licensed under the **Creative Commons Attribution-NonCommercial-ShareAlike 4.0. Spain License.**

Federico Ponente

**Enhanced recording
paradigms and advanced
analyses of peripheral
nerve fibers**

SPiike software



Sleeping seal

[<https://www.nature.com/articles/d41586-019-03839-z>]



UNIVERSITAT_{DE}
BARCELONA

Enhanced recording paradigms and advanced
analyses of peripheral nerve fibers
SPiike software

PhD in Biomedicine, research line of Neuroscience
Facultad de Medicina, Universitat de Barcelona

Author:
Federico PONENTE

Ponente Federico

Supervisor:
full professor Xavier GASULL CASANOVA

ACADEMIC YEARS 2017-2021

Copyright ©2017–2021 Federico PONENTE

All rights reserved. No part of this publication may be produced or transmitted in any form or by any means, electronic or mechanical, including photocopying recording or any information storage and retrieval system, without the prior written permission of the writer.

Abstract

The aim of this work is to investigate the human nociceptive system at the peripheral level. Researchers are still debating how the pain perception arises from this very intricate network. The human perception is the most elusive part of our knowledge since different subsystems are involved. The external information such as noxious stimuli must be processed at the peripheral level and through signal cascades and transduction this signal must reach the brain. At the brain level the information is processed and some decisions are taken, such as the well-known fight-or-flight response.

In the introduction, the author describes how the human nociceptive system works and in which way the noxious stimulus is converted into a signal understandable by the brain. Several cortical and subcortical areas are involved in this signal processing and going deeper in this assembly line the information becomes more abstracted. The whole pathway is fundamental for pain perception, however some diseases start at the peripheral level. This in turn makes wrong signals reaching the brain. The brain is then processing information that are not real and the responses do not suit with the needs. Therefore, the peripheral system must be investigated and understood firstly, since some central diseases may have a peripheral component as well. With this purpose in mind the microneurography technique has been used. This technique has got some complexity and a computer-aided system must be implemented. The hardware aims to filter out the noisy signal and perform recording and stimulation of the neural fibers. The software is instead used to make the stimulation and recording as automatic as possible in a way that researchers do not have to deal with a lot of parameters and steps to carry out this powerful but also time consuming technique. Some software are already available in the market however even if they work fine with slow conduction fibers such as C-fibers they cannot cope with faster neurons (e.g. *A δ fibers*). The aim of this work is to create a software (i.e. SPiike) able to stimulate and record every type of fibers implementing advanced analysis technique as well. Furthermore, considering that some *in vivo* experiments have been pursued within the project to check the functionality of the software, more specifically in rats

and mice, the comparison between human nociceptors and mouse nociceptors is depicted in this section.

In the method section, the experimental approach is described step by step. This is composed by several systems that work together for the stimulation, recording and analysis of the neural fibers. The control and acquisition module is composed by the software and a data acquisition board that trigger the stimulator and record the filtered signal. The stimulation module is composed by a stimulator that can be tuned as wish through dedicated knobs. Then the stimulus is delivered to the animal model (or the human patient) and the signal is recorded though a microelectrode inserted into the sciatic nerve. The amplification module is filtering out the noisy signal and is feeding a audio monitor for helping the researcher during the insertion of the electrode inside the nerve and it provides support during the whole experiment giving insights on fiber discharges. In this section the whole setup is described in details as well as the devices needed for the recording. Furthermore, the software development that is the core of this project is described as well, with all the considerations that must be considered during coding. Indeed, the flow chart must be followed methodically in order to minimize bugs and errors that may arise in the final product. Thus a description of the compiler and the Matlab IDE is given along with system and software requirements for the making of the SPiike software. Eventually the explanation of embedded functionalities and capabilities of SPiike is depicted in the final part of this section. This software is indeed able to stimulate slow conducting fibers as well as faster ones, and enhanced analysis techniques such as supervised machine learning are implemented.

In the results section, the graphical user interface of the Spiike software is reveled. It resembles the one of another software already available in the market, with a filtered signal and a raster plot embedded on it. However, this software is more user-friendly and it accounts with icons and drop-down menus that enhance the experience of the users during the use of the tool, making their interactions smooth and intuitive. The SPiike software is subdivide into two different tools, a recording module and a analysis module. The former allows the stimulation and recording of neural fibers with a stimulation frequency up to 1000Hz and some online analysis can be conducted to have insights on fibers type and behavior. The analysis module is instead a more powerful analysis environment that can retrieve the dataset recorded with the other module or with the LabChart software. Advanced analysis techniques are implemented in this module, this is meant to speed up fiber classification and analysis.

Conclusion and discussion provide a overview on some results. These will be compared to those obtainable through other software available in the market. In this

section, pros and cons of the new implemented software, SPiike, will be described as well.

Acknowledgement



UNIVERSITAT DE
BARCELONA

“ *The wisdom of the body is responsible for 90% of the hope of patients to recover. The body has a super wisdom that is in favor of life, rather than death. This is the power that we depend on for life. All doctors are responsible for letting their patients know of this great force working within them.*

— **Dr. Richard Cabot**
Harvard Medical School

To my family, in particular to my mother Silvina Bruera and my father Francesco Paolo Ponente. Basically, because I owe it all to you.

I would also like to thank the European Commission for the funding to this project that assisted me in the development of this work as well as all staff of the PAIN-Net consortium that allowed me to be here.

I am grateful for the university members of Xavier Gasull lab, in which I spent most of the time of my writing and the members of my late work laboratory at Neuroscience Technologies SLP for the experiments carried out over there. In particular to the researchers Elizabeth Garcia-Perez and Romà Solà as well as the other fellow of the Pain-Net program Lenin Reyes-Haro.

With a special mention to my supervisor Xavier Gasull for useful advices during the whole PhD period.

I thank you all for your support.

Contents

| | |
|---|-----------|
| Abstract | V |
| Acknowledgement | IX |
| 1 Introduction | 5 |
| 1.1 The human nociceptive system | 5 |
| 1.2 The nociceptors | 6 |
| 1.3 Nociceptive transduction | 7 |
| 1.3.1 Transient receptor potential (TRP) | 7 |
| 1.3.2 Acid-sensing ion channels (ASICs) | 8 |
| 1.3.3 G-protein coupled receptors (GPCRs) | 8 |
| 1.3.4 High threshold mechanoreceptors (HTMRs) | 9 |
| 1.3.5 Low threshold mechanoreceptors (LTMRs) | 9 |
| 1.3.6 Tropomyosin receptor kinase (TRK) and REarranged during Transfection (RET) | 9 |
| 1.4 Action potential generation and propagation | 11 |
| 1.5 Nociceptive transmission | 12 |
| 1.5.1 Spatial and temporal summation | 12 |
| 1.5.2 Peripheral modulation of pain (Gate control theory) | 13 |
| 1.6 Central pain pathways | 15 |
| 1.6.1 The sensory discriminative component | 15 |
| 1.6.2 The affective-motivational component | 16 |
| 1.7 Sensitization | 16 |
| 1.7.1 Peripheral sensitization | 17 |
| 1.7.2 Central sensitization | 17 |
| 1.7.3 Central modulation of pain | 18 |
| 1.8 Neuropathic pain | 19 |
| 1.8.1 Diseases | 19 |
| 1.8.2 Diagnostic tools | 19 |
| 1.9 Microneurography | 20 |
| 1.9.1 Procedure | 20 |
| 1.9.2 First attempts | 21 |
| 1.9.3 The electrode | 21 |
| 1.9.4 Single unit discrimination of fiber impulses | 23 |

| | | |
|----------|---|-----------|
| 1.9.5 | Medical and ethical considerations | 25 |
| 1.10 | Human vs. rodent nociceptors | 26 |
| 1.10.1 | TrkB and TrkC against TrkA expression | 26 |
| 1.10.2 | TRPV1 against TrkA expression | 27 |
| 1.10.3 | RET against TrkA expression | 28 |
| 1.10.4 | Na _v 1.6- Na _v 1.9 against TrkA expression | 30 |
| 1.10.5 | Overall view | 30 |
| 1.11 | Software used in microneurographic recordings | 31 |
| 1.12 | The work done | 32 |
| 2 | Objectives | 37 |
| 3 | Methods | 41 |
| 3.1 | Introduction | 41 |
| 3.2 | Stimulation paradigms | 42 |
| 3.2.1 | High voltage constant current stimulator - Digitimer [®] DS7a . | 43 |
| 3.2.2 | DAQ for control NI - National Instruments [®] PCI 6221 and BNC-2110 | 43 |
| 3.3 | Animal models | 44 |
| 3.3.1 | Homeothermic blanket system - Harvard Apparatus [®] | 45 |
| 3.4 | Microneurography recording | 46 |
| 3.4.1 | Electrode - FHC [®] Microelectrode Neurography | 46 |
| 3.4.2 | Micromanipulator - Tritech Research [®] MM-3 | 47 |
| 3.4.3 | Headstage - ADInstruments [®] MLT185 Neuro Amp EX Headstage | 47 |
| 3.4.4 | Amplifier - ADInstruments [®] Neuro Amp EX | 47 |
| 3.4.5 | Audio Monitor - Natus [®] Grass AM10 | 48 |
| 3.4.6 | Noise Eliminator - Digitimer [®] Hum Bug | 49 |
| 3.4.7 | DAQ for acquisition NI - National Instruments [®] PCI 6221 and BNC-2110 | 49 |
| 3.4.8 | DAQ ADI - ADInstruments [®] PowerLab | 49 |
| 3.4.9 | DAQ ADI - ADInstruments [®] LabChart | 50 |
| 3.5 | Software development | 51 |
| 3.5.1 | Matlab | 51 |
| 3.5.2 | Compiler | 52 |
| 3.5.3 | Waterfall model | 54 |
| 3.6 | System and software requirements | 55 |
| 3.6.1 | Sample rate and aliasing | 55 |
| 3.6.2 | Data acquisition toolbox | 56 |
| 3.6.3 | Guide | 59 |
| 3.7 | Analysis and program design | 60 |
| 3.7.1 | Spike design | 60 |
| 3.8 | Recording module - Spiike | 62 |

| | | |
|----------|---|-----------|
| 3.8.1 | Raster plot | 62 |
| 3.8.2 | Activity-dependent slowing and marking technique | 63 |
| 3.8.3 | Recovery cycle | 64 |
| 3.8.4 | Stimulation frequency up to 1kHz - $A\delta$ fibers | 65 |
| 3.9 | Analysis module - SPiike | 65 |
| 3.9.1 | Analysis module | 65 |
| 3.9.2 | Unsupervised machine learning algorithm, 1 ^o step - Principal component analysis (PCA) | 66 |
| 3.9.3 | Unsupervised machine learning algorithm, 2 ^o step - K means clustering | 68 |
| 3.9.4 | Fiber ADS analysis | 69 |
| 3.9.5 | LabChart recordings | 69 |
| 3.9.6 | Fibers activity | 70 |
| 3.9.7 | Instantaneous firing rate (IFR) | 70 |
| 3.10 | Coding | 70 |
| 3.11 | Testing | 72 |
| 3.12 | Operations and maintenance | 73 |
| 3.13 | Discoveries | 74 |
| 4 | Results | 79 |
| 4.1 | SPiike software | 79 |
| 4.1.1 | Graphical user interface | 79 |
| 4.1.2 | Standalone application | 81 |
| 4.1.3 | Comparison with another software | 83 |
| 4.2 | SPiike, recording module | 83 |
| 4.2.1 | Menu and toolbar - SPiike recording module | 84 |
| 4.2.2 | Basic recording technique - <i>C fibers</i> | 88 |
| 4.2.3 | Improved recording technique - <i>Aδ fibers</i> insights | 88 |
| 4.2.4 | ADS stimulation of C-fibers | 88 |
| 4.2.5 | ADS stimulation of $A\delta$ -fibers | 90 |
| 4.2.6 | Marking technique of C-fibers and $A\delta$ -fibers | 91 |
| 4.2.7 | Recovery cycle of C-fibers | 91 |
| 4.3 | SPiike, analysis module | 91 |
| 4.3.1 | Menu and toolbar - SPiike Analysis module | 92 |
| 4.3.2 | Spike sorting and fiber classification – C-fibers of a mouse recording | 94 |
| 4.3.3 | Spike sorting and fiber classification – C fiber vs. $A\delta$ -fiber | 98 |
| 4.3.4 | Statistical analysis of Adelta fibers | 99 |
| 4.4 | Spike extraction - an example of a cold hyperalgesia patient | 101 |
| 4.4.1 | Fiber activity | 101 |
| 4.4.2 | Instantaneous firing rate (IFR) | 102 |
| 4.4.3 | IFR statistical analysis | 103 |

| | | |
|----------|---|------------|
| 4.4.4 | Correlation between SPiike and QTrac outcomes | 104 |
| 5 | Discussion | 111 |
| 5.0.1 | SPiike overview | 111 |
| 5.0.2 | Recording module | 113 |
| 5.0.3 | Stimulus waveforms | 115 |
| 5.0.4 | Analysis module | 117 |
| 5.0.5 | A δ -fibers insight | 119 |
| 5.0.6 | Comparison between microneurography and other techniques | 121 |
| 5.0.7 | Overview of microneurography | 121 |
| 5.0.8 | Comparison between <i>in vivo</i> and <i>ex vivo</i> software | 122 |
| 5.0.9 | SPiike advantages over QTrac | 123 |
| 5.0.10 | Software validation - Correlation between SPiike and QTrac . | 124 |
| 5.0.11 | Acknowledgments | 125 |
| 6 | Conclusions | 129 |
| | Bibliography | 135 |
| | Publications | A |

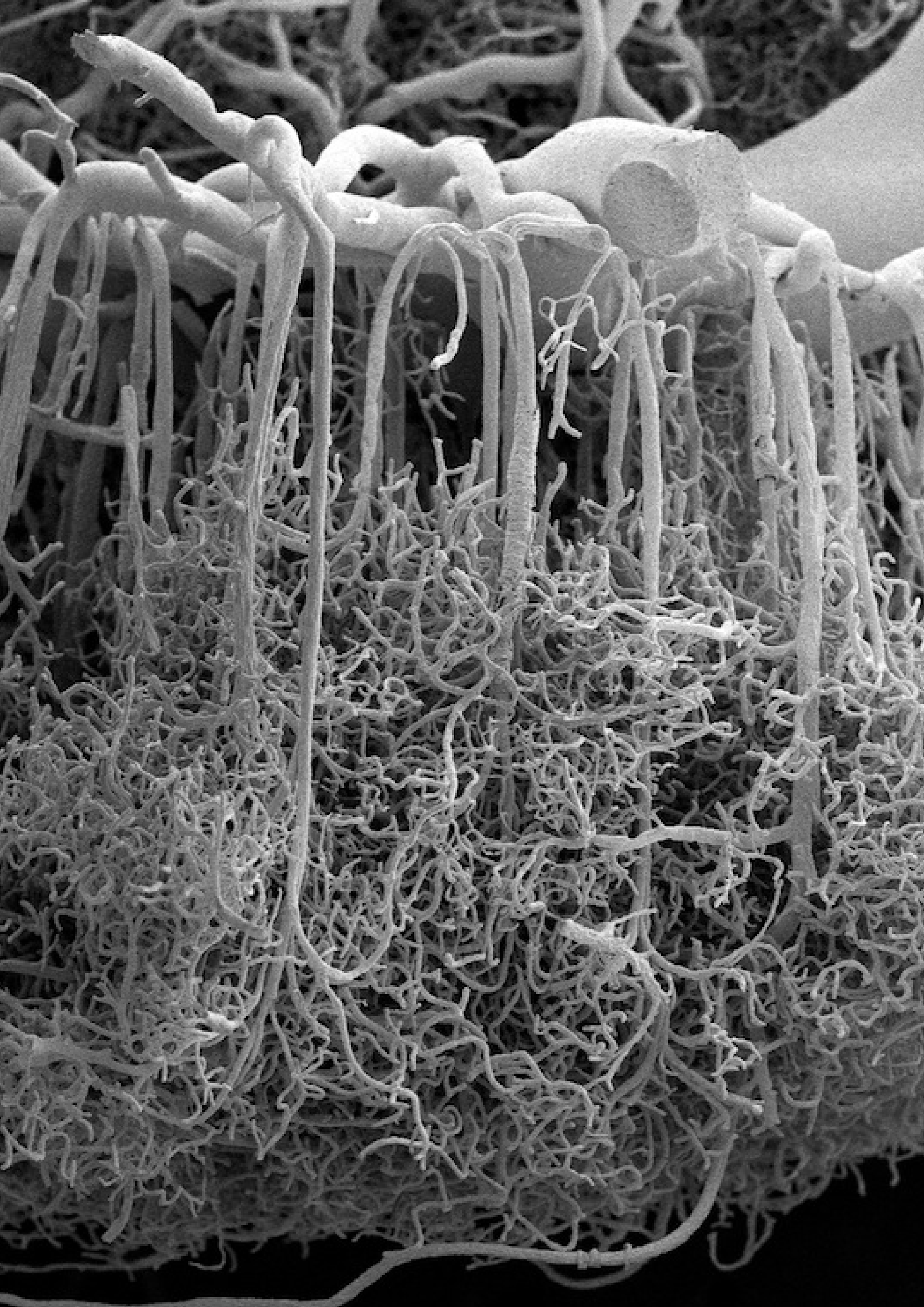
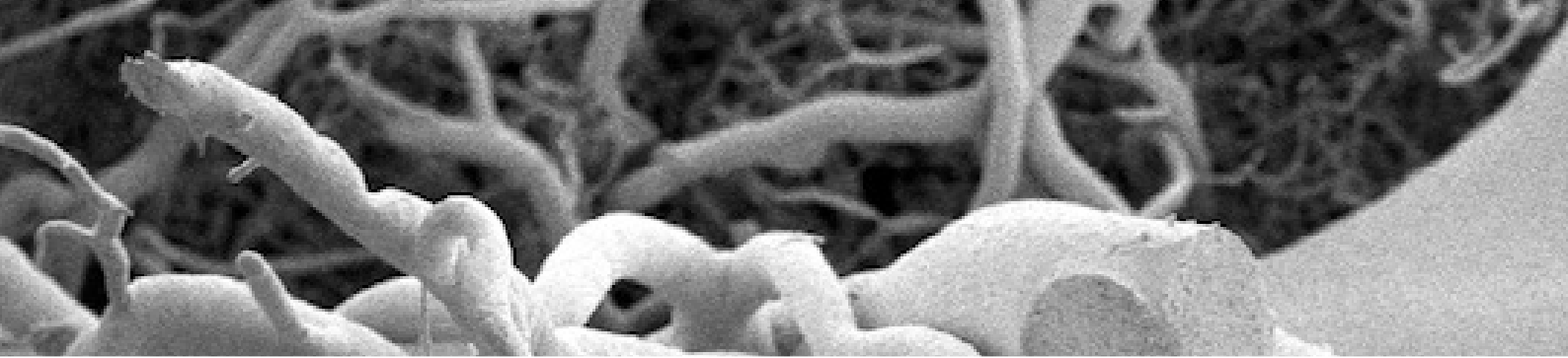


Image of blood vessels into the Brain

[<https://s-media-cache-ak0.pinimg.com/564x/75/c9/ed/75c9ed93a4a90622ca9cd4d314ebe886.jpg>]



1

Introduction

1.1 The human nociceptive system

The human body can sense external stimuli allowing us to navigate the environment that surround us. However, sometimes it has to warn us about dangerous situations unleashing the fight-or-flight response. A straightforward assumption could be that the somatosensory system upon intense stimulation might discharge more and generate pain sensations. However, the human body has got an additional pathway to warn the brain about noxious stimuli. This is called nociceptive system, and the receptors that convey this information are called nociceptors (*noc*i, from Latin that means *to hurt*). The nociceptors arise from cell bodies in either the dorsal root ganglia or the trigeminal ganglia and they extend their axons towards the skin with unspecialized nerve ending, that is why these terminals are called free nerve endings. On the other side, they extend their axons towards the spinal cord making connections with second order neurons. Figure 1.1 shows an experiment conducted to demonstrate that two different pathways are involved in the perception of noxious and non-noxious stimuli. Fig. 1.1(A), the experimental setup. An electrode is recording the neural activity of a non-nociceptive thermo-receptor and a nociceptor, and a heat stimulus is applied on the skin. Fig. 1.1(B), the discharge of these two neurons follows a different pattern when the temperature is increased. Fig. 1.1(C), the number of action potentials against stimulating temperature. The nociceptor starts discharging at around 45°C and from this threshold its response follows linearly the increase in temperature, while the non-nociceptive thermo-receptor has got a lower threshold and it saturates at lower temperature meaning that it cannot warn the brain about pain sensations. The nociceptors either lack of myelin or are thinly myelinated, while the somatosensory fibers are myelinated and thus faster. The somatosensory system is basically subdivided into $A\alpha$ fibers and $A\beta$ fibers with a

conduction velocity of about 80–120 m/s and 33–75 m/s respectively. Instead, the nociceptive system is subdivided into *A δ* fibers and *C* fibers.

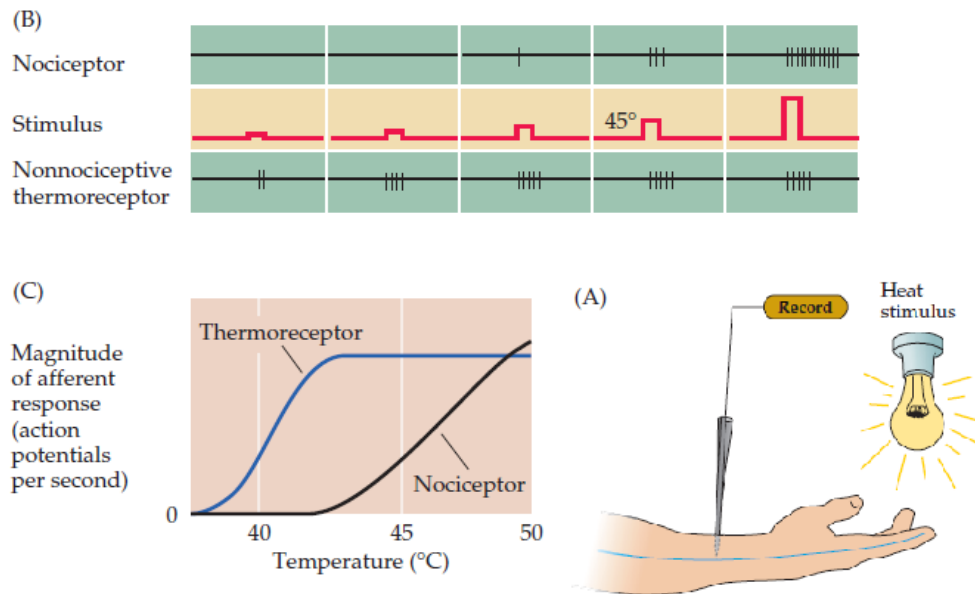


Fig. 1.1: An experiment for demonstrating that noxious and non-noxious sensations have two different pathways (A) The setup: a noxious and non-noxious receptor are recorded, heat is applied on the skin. (B) The discharge pattern of these two neurons following temperature increases. (C) The number of action potentials against stimulating temperature. [Pur+04]

1.2 The nociceptors

The nociceptors are subdivided into two groups since the nociceptive system conveys different pain sensations to the brain. These are thinly myelinated nociceptors (*A δ* fibers) and unmyelinated nociceptors (*C* fibers). *A δ* fibers are slightly faster than *C* fibers since they have thin myelin sheets on them, the former has a conduction velocity within a range of 3–30 m/s and the latter around 0.5–2.0 m/s. Therefore, the pain experienced when harmful stimuli are applied on the skin is perceived through different pain sensations. A first sharp and intense pain followed by a second delayed, longer-lasting and diffuse pain sensation, as depicted in figure 1.2. Within these subgroups the *C* fibers can be classified into 4 different types (type 1A: mechano-responsive nociceptors, CMR; type 1B: mechano-insensitive nociceptors, CMI; type 2: cold nociceptors; type 3: unknown function (presumed light touch nociceptors); type 4: sympathetic fibers [Geo+07]) and the *A δ* fibers into two types (mechanosensitive nociceptors; mechanothermally sensitive nociceptors [Pur+04]).

1.3 Nociceptive transduction

In the free endings terminals of these nociceptors there are some transducer channels that open their pores when are stimulated by chemical compounds as well mechanical and heat/cold stimuli. Among them we can find the transient receptor potential (TRP) that convey information about noxious temperatures as well as some chemicals. However, there are plenty of other channel sub-types that transduce information regarding noxious stimuli [Men10; Edg09] as shown in figure 1.3. In a peptidergic C nociceptor, among others there are the acid-sensitive ion channels (ASIC), receptors for growth factors (TrkA), G-protein-coupled receptors (GPCR) as well as a particular set of voltage-gated sodium channels (Na_v) and potassium (K^+) channels for action potential generation and propagation. It is worth noting that these ion channels can be the building block of some type of nociceptors such as the high threshold mechanoreceptors (HTMRs) that respond to noxious mechanical stimuli.

1.3.1 Transient receptor potential (TRP)

These is a very large group of polymodal receptors that can react to chemicals as well heat/cold and other stimuli both innocuous and noxious. In the subfamily of noxious heat temperature there are the TRPV1 and TRPV2 receptors. TRPV1 is found in the free nerve ending of C and *Aδ* fibers and it opens its pore when the temperature is higher than 45°C, however it is activated as well by capsaicin, a chemical found in red hot chili peppers [Dha+09], by acidic extracellular environments (pH 6.0 or less) and by basic intracellular environments (pH 7.8 or more) [MSM16]. However, every subclass of nociceptors express a specific type of receptors and lack of other ones, that is the reason why among others there are mechanosensitive and mechanoinsensitive nociceptors. That said, another receptor (TRPV2) is found only in *Aδ* fibers and it has a higher heat threshold (52°C).

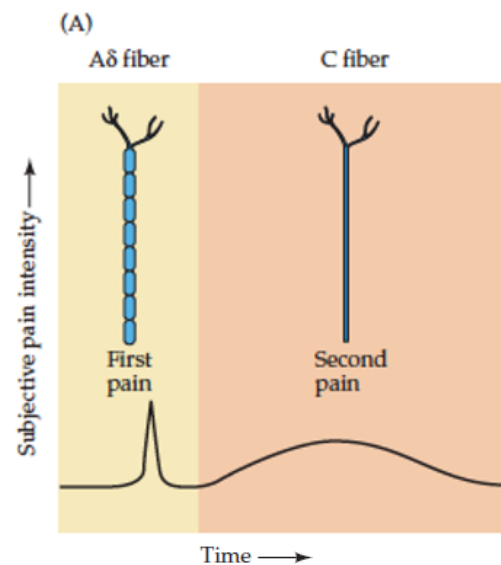


Fig. 1.2: The pain sensation experienced by the human body is subdivided into a first sharp and intense pain followed by a second more delayed and diffuse pain sensation. These are due to differences in the conduction velocity of the two types of nociceptors that arise from the dorsal root ganglia, namely *Aδ* fibers and *C* fibers [Pur+04]

Other types of TRP receptors are the TRPA1, the TRPM8 and the TRPM3. The former starts discharging below 15°C however it is not clear if it is involved in noxious cold sensing, most likely it is more a detector of irritant substances. The TRPM8 instead discharges below 28°C, however its current intensity increases down to 8°C, covering both innocuous cool and noxious cold temperatures [McK05]. Lastly, the TRPM3 is involved in heat sensing in thermosensory neurons [Dym+19]. Moreover, sometimes some of these transducers are polymodal and they are not only activated by chemicals and noxious heat but as well by noxious mechanical stimuli [Men10], like the TRPV4 that has a heat threshold around 42°C [PS06].

1.3.2 Acid-sensing ion channels (ASICs)

The acid-sensing ion channels (ASICs) are expressed in several tissues and they are excitatory cation channels gated by extracellular protons. In general ASIC1a is founded in muscles, joints and in the gastro-intestinal tract; ASIC2 in the gastrointestinal tract and in the heart; ASIC3 in muscle, joints, skin, gastro-intestinal tract and heart. ASIC3 is involved in acidic and inflammatory pain and, in the heart, together with ASIC2 in ischemic pain. ASIC1a conveys inflammatory pain and it participates in central sensitization (sec. 1.7.2), and in the gastro-intestinal tract together with ASIC3 and ASIC2 facilitates mechanoperception and/or mechanonociception. [Dev+10]

1.3.3 G-protein coupled receptors (GPCRs)

The G-protein coupled receptors are composed by seven trans-membrane domains and they detect extracellular molecules, that is the reason why nearly the 34% of drugs target these receptors. They actuate activating a intracellular signal cascade that regulate the excitability of the nociceptors. Depending on the ligand the signal cascade can involve different molecules and enzymes and can activate different receptor subunits (i.e. Gs, G_{q/11}, Gi, etc.). For instance once a epinephrene binds a GPCR receptor its intracellular conformation changes activating the Gs alpha subunit, temporarily switched off by guanosine diphosphate (GDP). The G-protein is now bind by another protein Guanosine-5'-triphosphate (GTP) that let the enzyme adenylate cyclase to interact with it. This subtracts a phosphorus to the GTP that becomes a GDP and turn off the Gs alpha subunit. Then the cascade activate an ATP molecule that with the energy subtracted by the enzyme generates cAMP that in turn bind with another enzyme, the so-called protein kinase A (pKA). The pKA enzyme interact with some ion channels by means of phosphorylation, changing the membrane permeability of these ions and thus their excitability [Ner17]. While, once the Gi alpha subunit is activated the enzyme adenylate cyclase is inhibited

and the excitability is downregulated. Moreover, the muscarinic acetylcholine can activate the $G_{q/11}$ alpha subunit. This G-protein activates a primary effector, the phospholipase (i.e. PLC_{β}). This enzyme hydrolyzes the PIP molecules yielding two second messengers (i.e. DAG and IP molecules). IP releases Ca^{2+} and DAG activates the protein kinase C (pKC). This drop in PIP levels can then affect some ion channels changing their excitability [KSJ91].

1.3.4 High threshold mechanoreceptors (HTMRs)

The high threshold mechanoreceptors are found in *C* and *A δ* fibers in both hairy and glabrous skin and they transduce noxious mechanical stimuli. These are slow adapting receptors, thus they can be called SA-HTMR as well. The receptive field of these nociceptors covers an area around 1-3 mm² [Rou+12]. *A δ -HTMR* fibers contact the second order neurons in lamina I and V, and *C-HTMR* fibers in the lamina II. This family of mechanoreceptors includes the TACAN, OSCA/TMEM6, TREK-1/TRAAK and the Piezo 2 channels.

1.3.5 Low threshold mechanoreceptors (LTMRs)

However, there is another subclass of transducers that respond to light mechanical stimulation, both in *C* and *A δ* fibers and this is associate with pleasant touches, social interactions and caress. These transducers are probably expressed in the type 3 of *C* fibers. Also, the receptive field of these nociceptors covers an area between 1-3 mm² [Rou+12]. This family includes the Piezo 2 channel.

1.3.6 Tropomyosin receptor kinase (TRK) and REarranged during Transfection (RET)

Three different types of Tropomyosin receptor kinase has been already discovered: Tropomyosin receptor kinase A (TrkA), Tropomyosin receptor kinase B (TrkB) and Tropomyosin receptor kinase C (TrkC). TrkA interacts with Nerve Growth Factors (NGF) and it is expressed in a subpopulation of nociceptors that are sensible to noxious heat or noxious mechanical forces. TrkB instead is bind by Neurotrophin-4 (NT-4) and Brain-Derived Neurotrophic Factors (BDNF), a growth factory that promotes synaptogenesis, the differentiation of new neurons and the support of existing neurons. It is expressed in low threshold mechanoreceptors. TrkC eventually is expressed in proprioceptors and it is bind by Neurotrophin-3 (NT-3), another neurotrophic factor. [Fri12] However, there exist another receptor that is included in the tyrosine kinase family, namely the RET receptor encoded by REarranged during

1.4 Action potential generation and propagation

When the transducers are in the open state a flux of ions pass through the cell membrane and a signal cascade is activated. For instance, TRP channels in their activated state allow an influx of sodium and calcium that generate the initiation of an action potential. As depicted in figure 1.4 the rising phase of an action potential is mediated by sodium channels. In particular, in a small-diameter dorsal root ganglia neuron a fast TTX-S (sensitive) current is generated by $\text{Na}_v1.3$, $\text{Na}_v1.6$ and $\text{Na}_v1.7$, a slow TTX-R (resistant) current by the $\text{Na}_v1.8$ and a persistent TTX-R current by the $\text{Na}_v1.9$. That is the reason why there are different sodium channels involved in the generation of the action potential rising phase. The $\text{Na}_v1.9$ is involved in the amplification of sub-threshold stimuli and it is the first one to be activated by the alteration of the cell membrane ions gradient. It has got a low activation threshold and a ultra-slow kinetics.

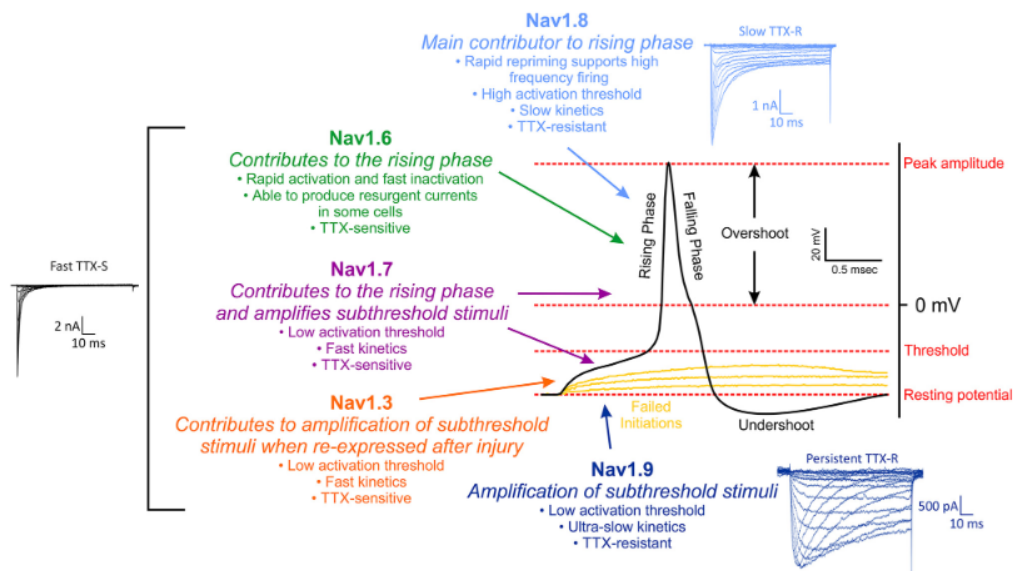


Fig. 1.4: Ion channels involved in the rising phase of an action potential. $\text{Na}_v1.9$ and $\text{Na}_v1.3$, involved in the amplification of sub-threshold stimuli. $\text{Na}_v1.7$ contributes to the rising phase as well as it helps $\text{Na}_v1.3$ and $\text{Na}_v1.9$ to amplify subthreshold stimuli. $\text{Na}_v1.6$ is the channel able to produce a resurgent current in some cells and with the help of $\text{Na}_v1.8$, it contributes to the rising phase of the action potential. [Ben+ 19]

The $\text{Na}_v1.3$ is involved in the amplification of sub-threshold stimuli as well however it is re-expressed after an injury and it has got a fast kinetics. The $\text{Na}_v1.7$ contributes to the rising phase as well as it helps $\text{Na}_v1.3$ and $\text{Na}_v1.9$ to amplify sub-threshold stimuli. It has got a low activation threshold and a fast kinetics. $\text{Na}_v1.6$ is the channel able to produce a resurgent current in some cells and since it is rapidly activated and fast inactivated it accounts mostly for giving to the action potential -with the help of $\text{Na}_v1.8$ - its characteristic spike-like shape. $\text{Na}_v1.8$ has got a slow

kinetics, high activation threshold and a rapid repriming support of high frequency firing. [Ben+19] The falling phase of an action potential is instead mediated by potassium channels that in nociceptors are expressed by voltage-gated (K_v), calcium(Ca^{2+})–activated (K_{Ca}), sodium(Na^+)–activated (K_{Na}) and 2-pore (K_{2p}) channels [Ben+19]. The K_{Ca} channel is activated by calcium ions that accumulate during repetitive neuronal firing. It is used as feedback channel for slowing down repetitive action potential firing. The K_{Na} is activated by sodium channels and it contributes to a long-lasting slow hyper-polarization following repetitive firing. The K_{2p} produces a leak current that regulate the resting membrane potential (RMP) of the nociceptors below the firing threshold. The K_v gathers a subclass of ion channels that likewise the sodium channels helps the propagation of the action potential during the falling phase: $K_v1.1$, $K_v1.4$, $K_v2.2$, $K_v3.4$, $K_v4.3$, $K_v7.2$, $K_v7.3$, $K_v7.5$. The $K_v1.1$ is responsible of the slowly inactivating and delayed-rectifier currents during action potential repolarization. The $K_v2.2$ regulate the membrane repolarization and the interspike hyperpolarization during repetitive firing. The $K_v3.4$ generates a rapidly inactivating current that accelerates repolarization. The $K_v1.4$ and the $K_v4.3$ regulate fast activation and inactivation and mediate A-type currents that limit the threshold, the duration and the firing frequency of the action potentials. Lastly, the K_v7 family ($K_v7.2$, $K_v7.3$ and $K_v7.5$) opens its pore when the membrane potential approach the RMP and express a low-threshold non-inactivating M current that stabilizes it, furthermore they regulate the accommodation and the threshold of the action potentials. After the activation of Na_v and K channels the Na^+/K^+ pump uses ATP energy to pump out and in ions in order to reestablish the initial conditions.

1.5 Nociceptive transmission

Once the action potential is generated it travels along the axon and if any fails occur it reaches the spinal cord where second order neurons take this information and send it towards the brain. This communication is mediated by some neurotransmitter, basically substance P, GCRP and glutamate for *C fibers* and only glutamate for *A δ fibers* [Yos+14]. However more upstream the system is analyzed more complicated it becomes. Indeed second order neurons make connections with more than one nociceptors making the propagation more complex than a simple transduction.

1.5.1 Spatial and temporal summation

The nociceptor needs only to probe the noxious stimuli and convert these perturbations into action potentials, however at the medula level there are other effects that build up like the temporal summation and spatial summation (figure 1.5). Regarding the spatial summation, if the pre-synaptic neurons discharge at the same time and

if some of them are connected to the same second order neuron their potential builds up increasing the likelihood of making the post-synaptic neurons discharge. The temporal summation is instead linked to a single pre-synaptic neuron. When it generates consecutive action potentials the post-synaptic potential builds up since the second order neuron do not have the time to reach a resting condition and likewise the spatial summation the likelihood of making the post-synaptic neuron firing an action potential increases.

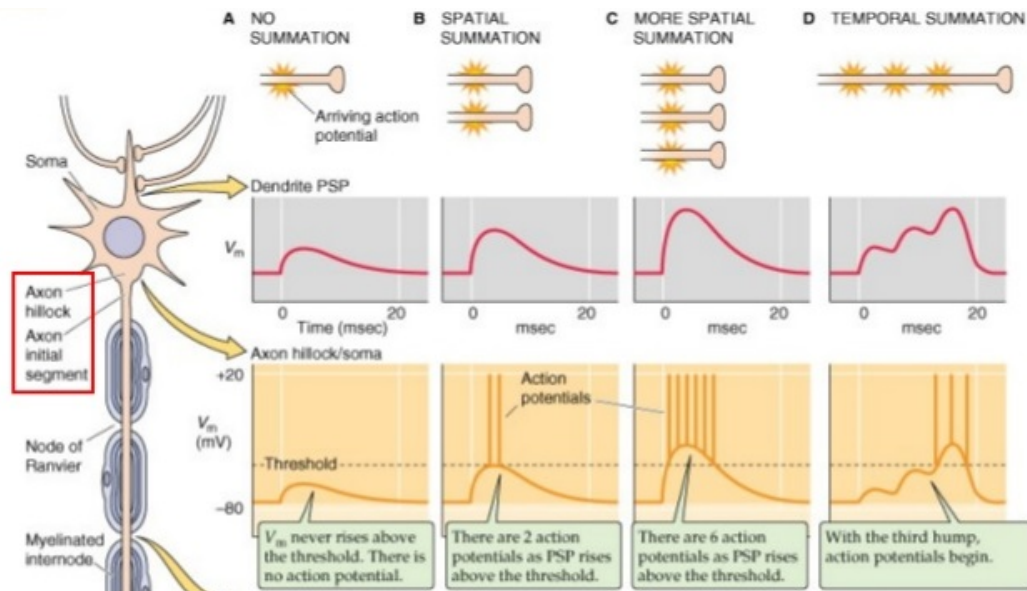


Fig. 1.5: Post synaptic potential. (A) No summation: a single action potential coming from a single pre-synaptic neuron is not enough for the second order neuron to fire, since the post-synaptic potential does not reach threshold. (B-C) Spatial summation: several pre-synaptic neurons fire at the same time and make connection with the same second order neuron increasing its likelihood to fire. (D) Temporal summation: the same pre-synaptic neuron consecutively fires building up the post synaptic potential [Sha]

1.5.2 Peripheral modulation of pain (Gate control theory)

As described before when some nociceptors are stimulated they in turn activate the second order neuron increasing its activity, in the so-called excitatory post synaptic potential. However there are some inhibitory effects that can lower its activity, and apart from some chemicals such as opioids and some drugs, the somatosensory system can decrease the likelihood of making the second-order neuron to fire a action potential. Indeed, as shown in figure 1.6 according to the gate control theory [Dic02] [MMSD15] the nociceptive fibers make connection to the second-order neuron both directly and indirectly. In the former case an excitatory synapse is generated, in the latter case they are connected to the second-order neuron through an inhibitory interneuron. The inhibitory interneuron receives the signal from the nociceptor through inhibitory synapses and they make connection to the second order neuron through the same synapses type. Mainly the interneuron releases a

inhibitory neurotransmitter such as GABA. Therefore when the nociceptor discharges it increases the activity of the post-synaptic neuron and meanwhile it lower the activity of the inhibitory neuron and a strong signal is sent to the thalamus. This is the unmodulated pain. However, some mechanoreceptor such as $A\beta$ fibers can make connection to the inhibitory interneuron through excitatory synapses. Hence, in this specific case when both fibers are excited a weaker signal is sent to the thalamus: the modulated pain. This is why when we hit a finger with a hammer after perceiving pain we start wiping our skin, in this way the strong signal sent to the brain is lowered by the mechanical stimulation.

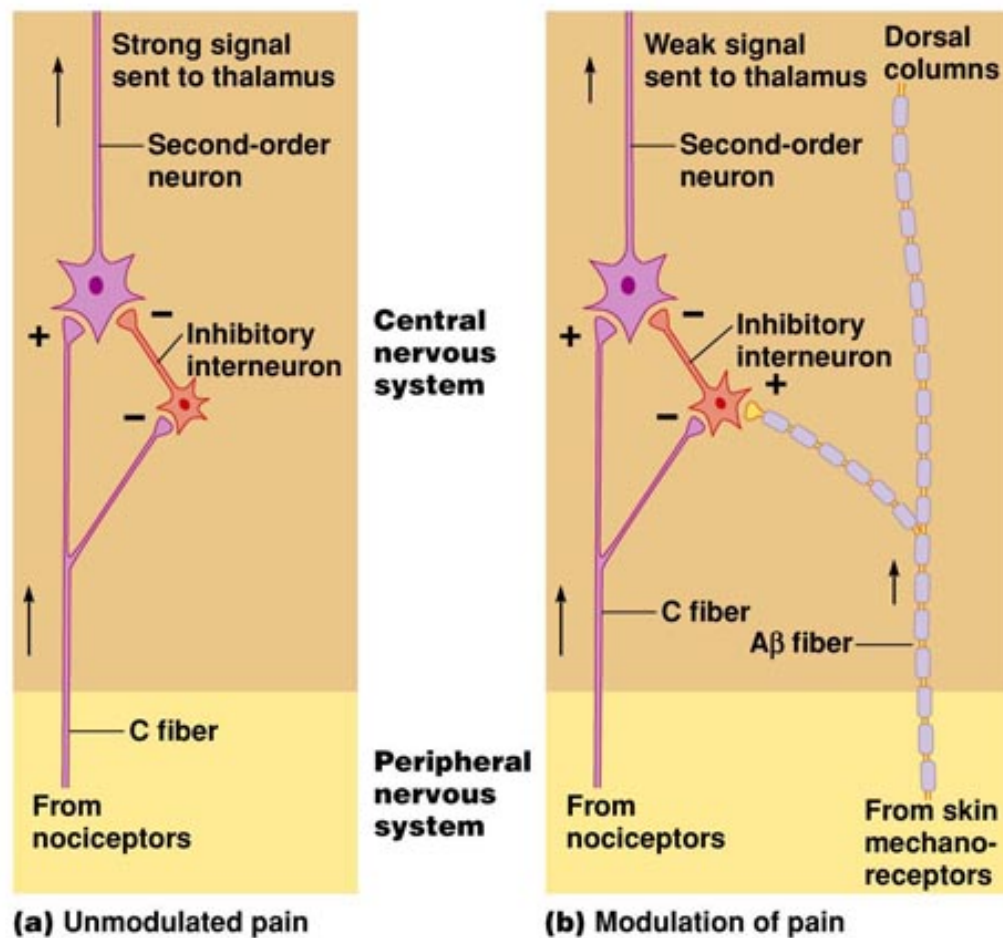


Fig. 1.6: Gate control theory. (A) Unmodulate pain. The nociceptor is connected through a excitatory synapses to the second-order neuron and through a inhibitory synapses to the inhibitory neuron. Therefore, when the nociceptor is excited it makes the second order neuron to discharge a strong signal towards the thalamus. (B) Modulated pain. Same principle of unmodulated pain with the exception of having a mechanoreceptors connected to the inhibitory neuron through an excitatory synapses. Thus when both the nociceptor and the mechanoreceptor are stimulated a weaker signal is sent to the brain. [Dic02] [MMSD15]

1.6 Central pain pathways

The transmission of pain signals towards the brain once the information reaches the medulla will split into two pathways, a sensory discriminative component and the affective-motivational component of pain as described in figure 1.7.

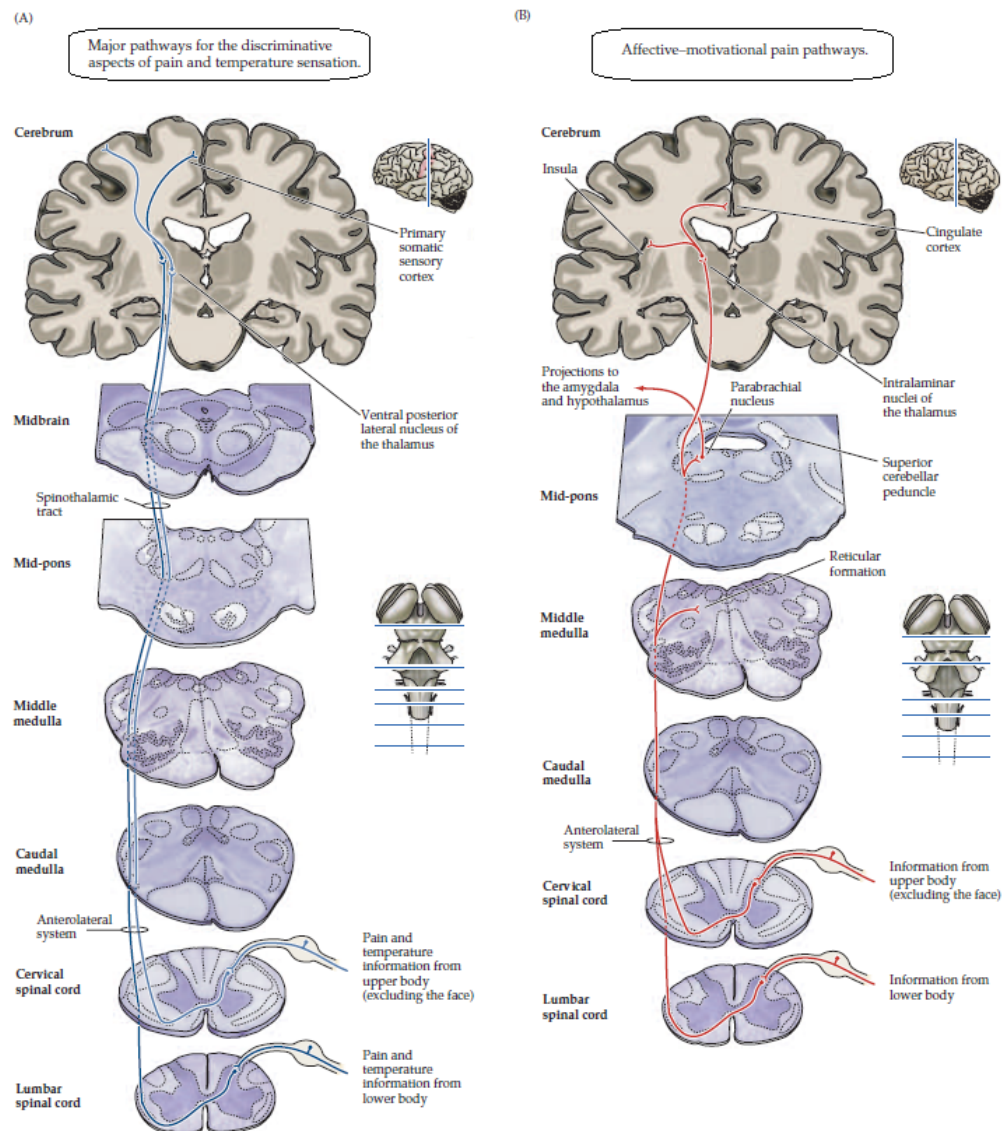


Fig. 1.7: Major pathways for the central transmission of pain and temperature. These pathways run along the spinothalamic (or anterolateral) system and they are centrally projected. (A) The sensory discriminative component. (B) The affective-motivational component. [Pur+04]

1.6.1 The sensory discriminative component

The sensory discriminative component underlies information regarding the intensity, location and quality of the noxious stimulus. The first order neuron enters the

dorsal horn through collateral branches, forming the dorsolateral tract of Lissauer. This tract is located in the tip of the posterior column, close to the entrance of the posterior nerve root and it runs up and down for one or two spinal cord segments and at every segment they penetrate the gray matter of the dorsal horn. Therefore first order neurons make connection with more than one second order neuron at the dorsal horn level along the Rexed's laminae. Then the second order neurons project their axons towards the brain in the so-called spinothalamic tract that runs in the anterior and lateral column of the contralateral half of the spinal cord, also defined as anterolateral system. However, it is worth pointing out that noxious information coming from the face follows a different tract. Pre-synaptic neurons originated from the trigeminal ganglia cells and from the facial nerves VII, IX and X enter the pons and they descend the medulla forming the spinal trigeminal tract. They split into the pars interpolaris and the pars caudalis, two subdivisions of the spinal trigeminal complex making connection with second-order neurons that then cross the medulla contralaterally and ascend towards the brain in the so-called trigeminothalamic tract. The spinothalamic and trigeminothalamic pathways target the ventral posterior nucleus of the thalamus, however information from the face convey towards the ventral posteromedial nucleus (VPM), and those coming from the body to the ventral posterolateral nucleus (VPL). Their axons extend then to the primary somatic sensory cortex.

1.6.2 The affective-motivational component

The affective-motivational component follows a similar pathway that run upward the anterolateral system but makes connection to the reticular formation of the midbrain, in the so-called parabrachial nucleus, and to the thalamic nuclei of the thalamus. The reticular formation has got projections to the amygdala and hypothalamus thus it underlies information regarding motivation and affect, and it is the source of some projections to the periaqueductal grey of the midbrain, that is involved in the descending pathway of pain. Instead, the intralaminar nuclei of the thalamus have got projections to areas in the frontal lobe, the insula and the cingulate cortex.

1.7 Sensitization

When an injury (e.g. cuts, scrapes and bruises) occurs the skin undergoes a series of structural changes that increase the intensity of noxious stimuli and the non-noxious stimuli are perceived as painful (e.g. painful sensation after a sunburn). The former sensitization is called hyperalgesia and the latter is the so-called allodynia, therefore both the peripheral receptors and the central projections are affected by an injury.

1.7.1 Peripheral sensitization

It is generated by a variety of substances that are released in the site of injury, the so-called inflammatory soup. Figure 1.8 shows this effects that it is basically mediated by the release of ATP, bradykinin, extracellular protons, histamine, prostaglandins, nucleotides, serotonin and nerve growth factor (NGF). These substances can increase the excitability of some channels and in turn that of nociceptors. TRPV1 is indeed directly sensitized by extracellular protons and lipid metabolites and indirectly by NGF and bradykinin.

Prostaglandins instead bind to G-protein-coupled receptors that enhanced the levels of cyclic AMP and it lower the threshold for firing an action potential through phosphorylation of subgroup of Na_v channels TTX-resistant. Furthermore the nociceptors release peptides, ATP and some neurotransmitters such as substance P and calcitonin-gene-related peptide (CGRP). This causes vasodilation, swelling and the release of histamine through mast cells as well as the increase of blood flow. These changes are aimed to prevent further damages and also to promote healing and protection against infection attracting white blood cells in the injured site. That is why the administration of some nonsteroidal anti-inflammatory drugs (NSAIDs) lowers the pain perceived by the patient, indeed they act by inhibiting the cyclooxygenase (COX), an enzyme involved in the biosynthesis of prostaglandins.

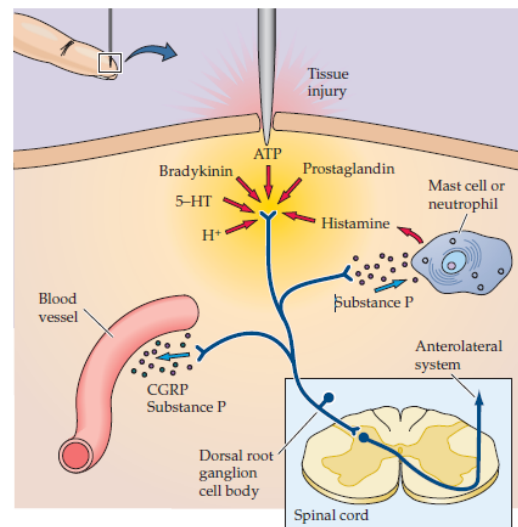


Fig. 1.8: Inflammatory soup following tissue injury. Some chemicals released by the nociceptors (e.g. Substance P, CGRP, etc..) and the body (e.g. ATP, histamine, prostaglandin, etc..) enhance the activity of nociceptors contributing to a temporary allodynia and hyperalgesia in the site of damage. This effect allows the body to heal and to avoid further damages. [Pur+04]

1.7.2 Central sensitization

It is triggered in the dorsal horn of the spinal cord and it is generated by high activity of nociceptors, such the one following injuries. The mechanisms underlining this process can be divided into a activity dependent sensitization that is mainly active during repetitive stimulation such as the so-called windup. The windup effect

(namely a temporal summation effect, sec. 1.5.1) is triggered by repetitive stimulation of the nociceptors and it results from the activation of voltage dependent L-type calcium channels and from the removal of some Mg^{2+} ions that were blocking the NMDA receptors. NMDA receptors bind with the excitatory neurotransmitter glutamate. Therefore an increased sensitivity of the post-synaptic neuron is generated. Moreover, there also exist a longer lasting effect that is due to the release of some substances by microglia that promote the transcription of COX-2 and prostaglandins directly in the dorsal horn.

1.7.3 Central modulation of pain

However, there is also a descending pain pathway that as its peripheral modulation (sec. 1.5.2) can modulate this unpleasant sensation by releasing some chemicals that can alter the intensity of pain perceived. However, in the past this led to further studies that brought the pain field into the psychosomatic one. Indeed the central modulation of pain can be also triggered by some mind states such as anxiety, stress, rewards and other psychological states and this is why the placebo effect is actually something real that is mediated by our brain. For instance, as been found by Henry Beecher [Bee56] some soldiers that had hardly injuries their limbs started feeling less pain than usual. And, the same can happen in the other way around. Regarding the physiological basis, the analgesic effect is due to the stimulation of some areas within the brain that project to the dorsal horn of the spinal cord and the spinal trigeminal nucleus. One of the most important regions that produce this analgesic effect is located in the periaqueductal gray of the midbrain, mediated by the parabrachial nucleus, the dorsal raphe, the locus coeruleus and the medullary reticular formation. These areas release several neurotransmitters such as noradrenaline, serotonin, dopamine, histamine and acetylcholine and they can either lower or enhance the pain sensation acting directly to the dorsal horn. The basic action is due to changes at the level of the synaptic terminals, excitatory and inhibitory interneurons, synaptic terminals of other descending pathways and acting directly to the projection neurons. Furthermore, some chemicals such as endogenous opioids (e.g. enkephalins, endorphins and dynorphins) underlie the modulation of pain perception as well. They can bind central areas such as the periaqueductal gray matter and peripheral areas at the dorsal horn level. In there, some enkephalin-containing circuit neurons once stimulated by some descending inputs (e.g. raphe nuclei) will release opioids that in turn interact with first order neuron synapses, lowering the post synaptic signal and thus their likelihood to fire. These are therefore the targets of some medical drugs responsible of pain relief.

1.8 Neuropathic pain

As described before the nociceptive system is very complex but it can effectively alert the brain about noxious stimuli. It is an alert system that is always seeking for dangerous situations. It is important for the survival of the human being as well as other species in a hostile environment as the one in which we live in. However, what if the system does not work properly such as in a chronic pain state, in which the physiological pain threshold is altered and therefore its perception? This can lead to a wide range of misinformation, making the pain system useless as an alert system. In this case the nociceptive pain turns into the so-called neuropathic pain, this is in effect a disease.

1.8.1 Diseases

The study and treatment of neuropathic pain have been and continue to be a major clinical challenge. Many causes are responsible for neuropathic pain: traumatic nerve injury, neuropathies associated with diabetes or cancer, genetic disorders, among others [Att11; For17; Fin+16; Sèn18]. The mechanisms underlying neuropathic pain are complex and involve central and peripheral pathophysiological mechanisms [Djo+06; FW10; Kle+12; Qui+10]. Among them, increased/decreased expression of ion channels, sensitization resulting in reduced thresholds and enhanced responses to suprathreshold stimuli of small-size nociceptive afferents and collateral sprouting of nociceptive C- fibers play an important role. Nevertheless, nociception not only concerns C-fibers but A δ -fibers as well (sec. 1.2). Both pathways are essential for the perception of pain and they should be considered as a whole in the development of pain relief compounds. Therefore, a better understanding of the complexity of pain syndromes and its quantification may help to provide a more effective management and treatment of chronic pain problems.

1.8.2 Diagnostic tools

Several tools for the assessment and quantification of pain have been developed. These include tests and questionnaires that depend entirely on the patient [GJ97; Jen06; Mai+10], and tests that measure and quantify electrophysiological responses [Kie+00; SBN10; Ser+12]. A special electrophysiological technique called microneurography has been successfully employed to reveal neural characteristics of the C-nociceptors activity in patients and animal models of neuropathic pain [Ser+12]. Moreover, recordings of afferent discharges of different types of C-fiber identified by a latency-based marking method have become an important tool to identify abnormalities in neural traffic of unmyelinated C-nociceptors. However,

current analysis tools must cope with limited ability of customization and restricted analyses capabilities that are suited only for a small subclass of nerve fibers. A logical next step is to update these automated methods for detection and quantification of the ongoing normal and abnormal spontaneous activity in nociceptors. Furthermore, this can be pushed forward aimed to quantify behaviors of nerve fibers that are not clearly understood yet such as A δ -fibers.

1.9 Microneurography

This technique has been established after the second world war in a time in which the analyses of cutaneous and propiceptive sense organs in mammals was a prominent branch of neuroscience. This has been done by direct recording from peripheral nerves or single afferents in the dorsal roots. Further studies suggested that human perception could be set at the level of primary afferents, thus the study of the peripheral nervous system started to be very promising in the understanding of human perception [Mou67; Tal+68]. In such a context, around the year 1965 the development of microneurography began, this term has been coined by Zotterman (1939), a physiology professor in Stockholm. And, it has been developed by two researchers, Karl-Erik Hagbarth and Åke Vallbo, at the Department of Clinical Neurophysiology of the Academic Hospital in Uppsala, Sweden. It consists in the impalement of a peripheral nerve with a tungsten needle electrode, several times larger than the nerve fibers. In such a way, the recording of single-unit nerve impulses in humans in myelinated and unmyelinated fibers has been achieved. [Val18]

1.9.1 Procedure

It is a simple technique but it needs a skillful manipulation of the recording electrode, since it is inserted percutaneously inside a nerve either in a limb or in the face and it is left to freely float in the flesh. Once a little cut has been performed on the skin the electrode needs to impale the nerve, and this is done by the researcher that needs to listen the sound coming from the electrode in order to understand if it already entered a nerve bundle. In human studies, the electrode adjustments are done by hand, in animal studies by means of a micromanipulator. However, due to the high friction between the flesh and the electrode shaft, big movements at the skin surface turn into small movement at the tip of the electrode. The searching of neural activity can be done through a loudspeaker and the stimulation can be done by means of a stimulating electrode or by wiping the skin in a more distal site. Anesthetics are not required since pain is only minor-to-moderate and short-lasting, and in this way the patient can collaborate in the searching of the nerve bundle. Temporary paresthesiae are common, however enduring sequelae never occur.

1.9.2 First attempts

Considering that the technique was born in the sixties computers were not used at that time, being too slow and bulky, thus most laboratories relied on analog technology. The electrode signal was displayed on a oscilloscope screen stored on analog tape by means of a Grass camera facing the oscilloscope. In such a context, Hagbarth started testing some needle electrodes in his own ulnar and median nerves [Val18]. He occasionally noticed a change in the background noise when stroking the skin, thinking that it could be of neural traffic origin rather than an electrical artifact. However, the signal was too small and demanding to obtain, thus he dropped the idea of pursuing its development. Fortunately, with the joining of Vallbo in the lab they started thinking about alternative approaches, and one of them was to use muscle spindles. This was of scientific interest at that time, in the study of the fusimotor system in natural movements. The fusimotor system (γ -system) avoids the overstretching of muscle fibers through a feedback system that sense the muscle stretching and if it is too high it activates its contraction through γ -motor neurons. They used an approach similar to that of a colleague of theirs with a juxtneural needle. They were trying to increase the signal-to-noise ratio through the technique of averaging, however they failed and they came back to the idea of an intraneural recording.

1.9.3 The electrode

Previous studies used the nerve splitting technique for the recordings, however it is a very invasive technique that fits well in animal studies but do not match in *in vivo* human recordings. This technique consists in the incision of the skin and a filament of dorsal root or nerve bundles is taken and placed on silver hook electrodes in a pool of paraffin oil. However, while such metal needle electrodes were commonly used in some experiments of central structures they were not used in peripheral nerve recordings. Therefore, they started testing some electrode materials and they ended up with the idea that tungsten was the best option. One advantage was the mechanical property of this material, it is indeed semi-flexible but at the same time non-brittle. Avoiding thus that the electrode breaks during the searching process of the nerve bundle leaving metal fragments in the flesh of the patient. Instead, other materials such as silver and platina-iridium are too soft and steel is too brittle. Furthermore, another challenge was how to fabricate the tip of the electrode and its coating in order to optimize the signal-to-noise ratio and its selectivity to recognize single-unit discharges but meanwhile avoiding its damage during the insertion through the skin. Insul-x coating did not stick very well to the tungsten electrode. Hostaflon was aimed to lower the friction with the flesh however this was not very advantageous in microneurography due to the manipulation by

hand. Glass-coated platina-iridium had excellent electrical properties, however they could leave fragments in the flesh and they very discharged. Therefore the epoxy coating has been selected, nevertheless it had a fundamental drawback when used in microneurographic recordings: it does not adhere very well with the tungsten electrode and once it is inserted the epoxy layer wears out and the impedance drops to $<500\text{ k}\Omega$ (measured with 1-KHz 20 mV sinusoid using an AC bridge). Thus, different approaches have been investigated, such as the change in the thickness of the coatings, varying in the baking time, or chemically roughing the electrode before coating. However, nowadays the electrode fabrication has not yet been improved and still tungsten electrodes with epoxy coatings are used in microneurographic recordings.

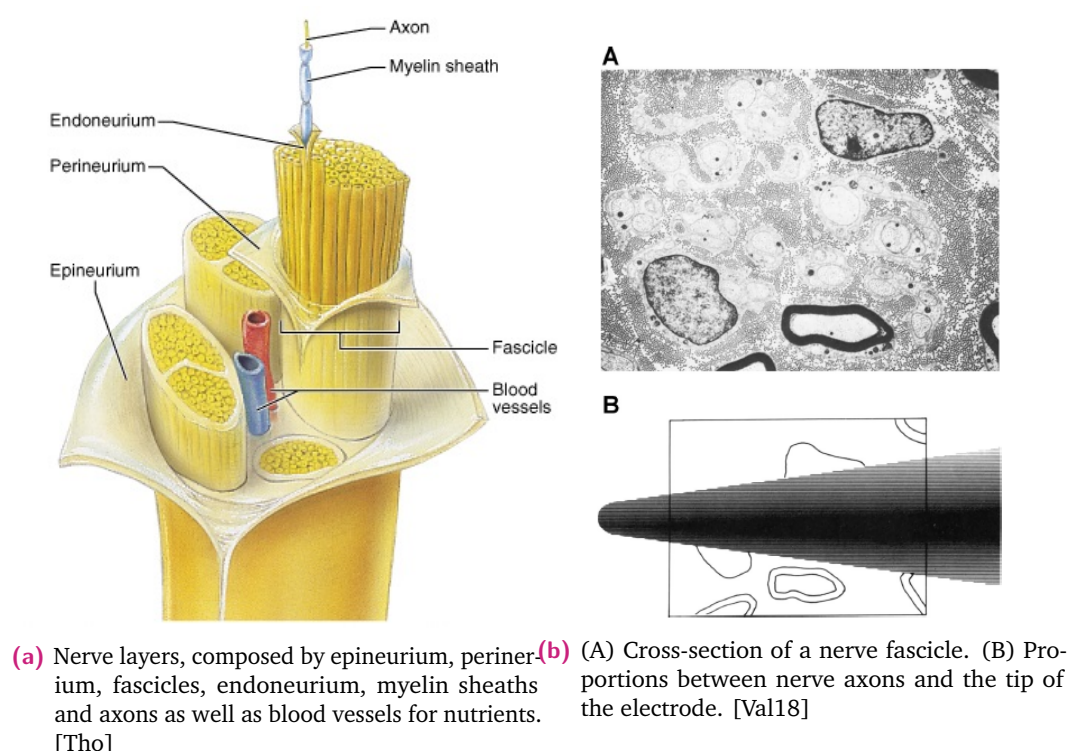


Fig. 1.9: Schematic view of a nerve and its comparison with the tip of the electrode used for microneurographic studies.

They then turned to animal recordings to understand how to proceed, mainly into exposed cat nerves. They figured out that the penetration of the perineurium of the nerve (figure 1.9a) is fundamental for the detection of neural activity. However, it is not achieved very easily since the electrode can pass through the nerve before actually impaling a single fascicle. This is due to the toughness of the perineurium made of a fibrous sheath and a very soft interconnecting tissue that cover it. Thus the electrode since it has got a rounded tip with a diameter of $3\text{--}5\text{ }\mu\text{m}$ has to hit the fascicle in the center of it otherwise it will roll and slip away. Figure 1.9b on top shows the cross-section of a nerve fascicle with some unmyelinated and myelinated fibers on it as well as two Schwann cell nuclei. On bottom, the shape of the tip

of the electrode compared with the nerve fascicle. It is clear that the size of the electrode is much bigger than that of the axons (after insertion the uncoated area is 30 μm long and the shaft 200 μm in diameter) thus single-unit discrimination turned out to be very challenging, and impossible for some colleagues of theirs. Indeed, extracellular currents produced by nerve fiber impulses is too small to give rise to measurable potential changes due to a low resistance in the extracellular space. Thus they started making other experiments regarding the fusimotor system, and after having improved their skills in the manipulation of the electrode and in the technique, they were able to record some neural activities that was that of a single-unit discrimination. Hence, the technique skill turned out to be very important in microneurographic recordings but showed that single-unit discrimination was possible.

1.9.4 Single unit discrimination of fiber impulses

Looking at figure 1.9b there was skepticism in the research community since it seemed that the metal part of the electrode might shortcut the signal coming from different axons. However, it turned out that the tip of the electrode placed in the flesh is not equivalent to a resistance but rather to a capacitance of almost 1 nF. This is due to the fact that the carriers in bodily fluids and metals are of different nature. Ions in the former and electrons in the latter, and they cannot cross the interface between the two (i.e. the surface of the electrode). Electrical charges from one side therefore attract or repulse the charges stored in the other side of the interface and the filling up of the capacitance -through theses charges- is seen by the amplifier as a signal amplitude.

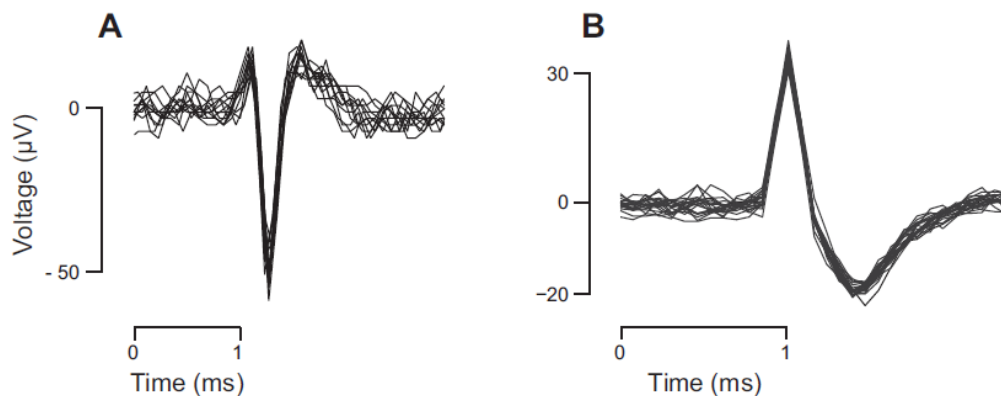


Fig. 1.10: Typical action potential (AP) shapes recorded during microneurographic studies. (A) Unmyelinated neuron AP, such as that of a *C fiber*. (B) Thinly myelinated neuron AP, such as that of a *A δ fiber*. [Val18]

The dimension of the tip is then only used to evaluate the capacitance at the interface. The shape of the nerve impulses is also very important in the fiber classification.

Indeed, as shown in figure 1.10 unmyelinated fibers have a triphasic complex with the biggest peak pointing downward, this is due to the probing by the electrode of the nerve inward current during action potential propagation. The myelinated fibers can also have a triphasic complex but if and only if the electrode is placed at a node of Ranvier, that is rare, thus in most of the cases since the electrode is located between two nodes of Ranvier it has got a biphasic complex. And moreover, it has a peak pointing upward, the opposite of the unmyelinated complex. This is due to either the sensing by the electrode of the outward transmembrane current through the myelin sheath or less probable the picking up of the intracellular action potential. Furthermore, the huge amplitude is most likely due to the local reduction in thickness of the myelin sheath due to the pressure employed by the recording electrode. However, as the experiment goes by the fiber wears out due to the electrode scratching and thus the downstream current flux slows down. This causes the downstream node to delay the propagation of the action potential and thus the biphasic complex starts to be quadriphasic, with two peaks on it. The two peaks then separate even more until after a certain amount of time the downstream node blocks and the quadriphasic phase comes back to the initial biphasic phase, as shown in figure 1.11

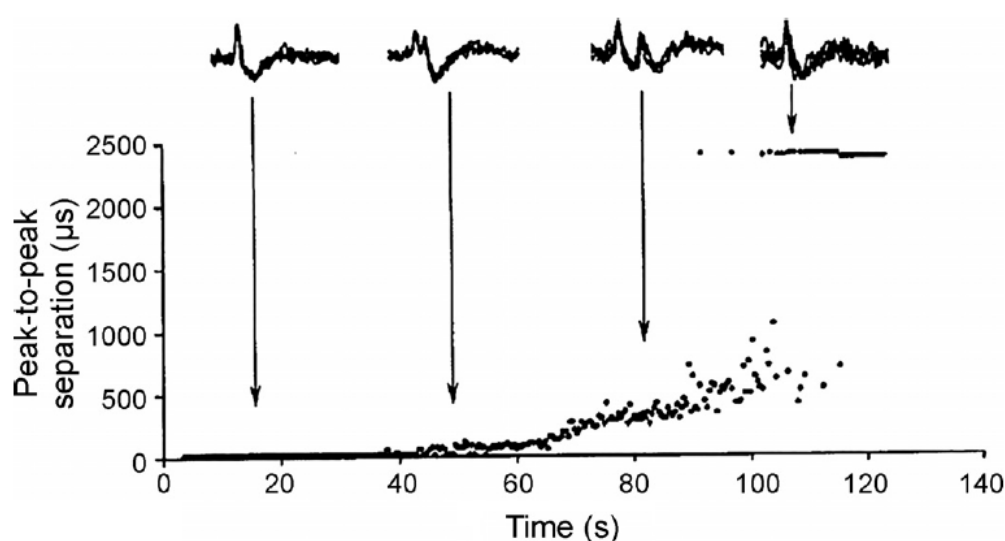


Fig. 1.11: Peak separation of a myelinated fiber during microneurographic studies. If the electrode is inserted between two nodes of Ranvier at time 0 the recorded action potential (AP) has got a biphasic shape. However, as the time goes by the downstream node due to the damage generated by the electrode starts slowing down and the upstream and downstream AP shapes are no longer synchronized. This generates a quadriphasic shape complex that starts to be more evident until the downstream node fails and the complex becomes again biphasic. [Val18]

It is worth pointing out that the big amplitude of the unmyelinated fibers ($\sim 30\text{-}50 \mu\text{V}$) cannot be explained in the same way of the myelinated fibers, it is most likely due to a longer stretch of the fiber in tight contact with the electrode rather than a single spot contact as it happens in multi-unit recordings that accounts of a \sim

15-20 μV amplitude. This allows single-unit fibers to stand out from the noise that accounts of a $\sim 20 \mu\text{V}$ peak-to-peak. Thus the insertion of the electrode as parallel as possible with the nerve is preferable than an insertion at a right angle.

1.9.5 Medical and ethical considerations

Once the technique has been improved and the possibility of recording single-unit afferents has been demonstrated, other questions raised. Among the possibility of irreparably damaging the nerve fibers due to the insertion of the electrode inside the nerve fascicle. They assumed that the longer the search period the larger the number of damaged and severed fibers. Therefore the question was if those damaged fibers were able to heal and recover and if additional side effects might rise, such as intraneural bleeding with consequent neural scars, bacterial or viral infections, or immunological reactions due to disintegration of myelin and axonal structures. To answer to all these questions animal recordings were needed and histological analyses to assess the degree of fiber degeneration and other intraneural changes required. However, they did not have the expertise for doing that and at that time the ethical committee system had not yet been established. Therefore, they used their own nerves to assess the presence of a long-lasting damage [Val18]. A common symptom was hypersensitivity to local pressure at the site of impalement and a firm pressure generated paresthesiae. These phenomena appeared couple of days after the experiment and lasted for few weeks after. Therefore, as general rule the impalement at the same recording site should not be performed more than once a month. Moreover, further studies by other research groups were pursued to quantify the nerve damage after nerve impalement, establishing that the technique may be considered safe as long as the researcher is performing it with recommended care and following all the procedures. Among others, the recording site must be picked away from a bone, since the hitting of such a anatomical structure by the electrode might hook its tip. A hooked tip may generate considerable nerve injuries.

Karl-Erik Hagbarth and Åke Vallbo kept doing research using the microneurographic technique in the following years but they were more focused on the muscular proprioceptive system, the cutaneous mechanoreceptive system, and the sympathetic efferent system to skin and muscles [HV68a; HV68b; HV69; VH68]. The cutaneous nociceptive system was instead largely studied by Torebjörk and Hallin [Val18; Tor70; TH76].

1.10 Human vs. rodent nociceptors

In previous studies, human nociceptors have been compared with rodent nociceptors. The goal was to assess similarities and differences among them. This is useful for studies in the field of pain since human subjects cannot afford the pain generated by such experiments. In the study performed by Rostock and his group [Ros+18], postmortem DRG neurons from 6 unrelated patients have been extracted and compared with 3-4 adult mice DRG tissue slices using dual-fluorescence *in situ* hybridization and immunohistochemistry. They placed a particular emphasis on the characterization of peptidergic nociceptive neurons (TRKA positive). Indeed, TRKA is a receptor with high affinity to nerve growth factors (NGF) that is fundamental for the development of the majority of sensory neurons. At a embryonic age E13, 80% of sensory neurons express TrkA and its absence means a loss of 70-80 % DRG neurons. Therefore, they investigated the expression of the neurotrophin receptors TrkA (Ntrk1) that is indeed linked to nociceptors (detection of painful stimuli such as heat or noxious mechanical forces), the TrkB (Ntrk2) linked to mechanoreceptors (low threshold mechanoreceptors responding to innocuous mechanical forces) and TrkC (Ntrk3) linked to proprioceptors (detection muscle spindle tension). Furthermore, including the receptor tyrosine kinase RET expressed in TrkA negative nociceptors (non-peptidergic) all the main subtypes are included. Moreover, in this study they analyzed some ion channels that are important in the mediation of nociception such as TRPV1 and some sodium channels $\text{Na}_v1.6$ - $\text{Na}_v1.9$. It is worth pointing out that DRG neurons are a heterogeneous population of cells that transmit sensor information towards the brain. Every DRG neuron has a particular molecular composition and the oldest and best characterized molecular markers are the TrkA, TrkB and TrkC receptors.

1.10.1 TrkB and TrkC against TrkA expression

Figure 1.12 shows the comparison between TrkB and TrkC receptors against TrkA in mice and human DRGs. This is a representative dual-cloro fluorescence *in situ* hybridization. The ratio of TrkB positive neurons against TrkA positive neurons in humans compared to that of mice has no significant difference (5.3 +/- 0.7% in humans, 4.8 +/- 1.7% in mice) as the ratio between TrkC against TrkA positive neurons (16.0 +/- 1.5% in humans, 10.8 +/- 1.2% in mice) with a p-value of 0.956 and 0.111 respectively. Additionally, they showed the relative total number of DRG neurons expressing TrkA compared to those expressing TrkB and TrkC with similar outcomes in humans and mice (human TrkB: 27.8 +/- 7.3%, mouse TrkB: 36.2 +/-13.5%, $p = 0.531$; human TrkC: 39.5 +/- 9.9%, mouse TrkC: 53.8 +/- 5.5%, $p = 0.295$). They concluded that only small groups of human DRG neurons express

TRKA together with either TRKB and TRKC. They also analyzed the cell area of these neurons concluding that both in humans and mice the majority of TRKA positive neurons have the smallest area size (300-700 μm^2 in humans, 100-300 μm^2 in mice) then TRKB have a larger cell area (a peak around 1200-1400 μm^2 in humans, 600 μm^2 in mice) and TRKC positive neurons are the biggest (a peak around 1600 μm^2 in humans, 600-800 μm^2 in mice). The only difference was that the human sensory neurons are shifted to a larger cell soma, approximately 1.5 to 3 times larger.

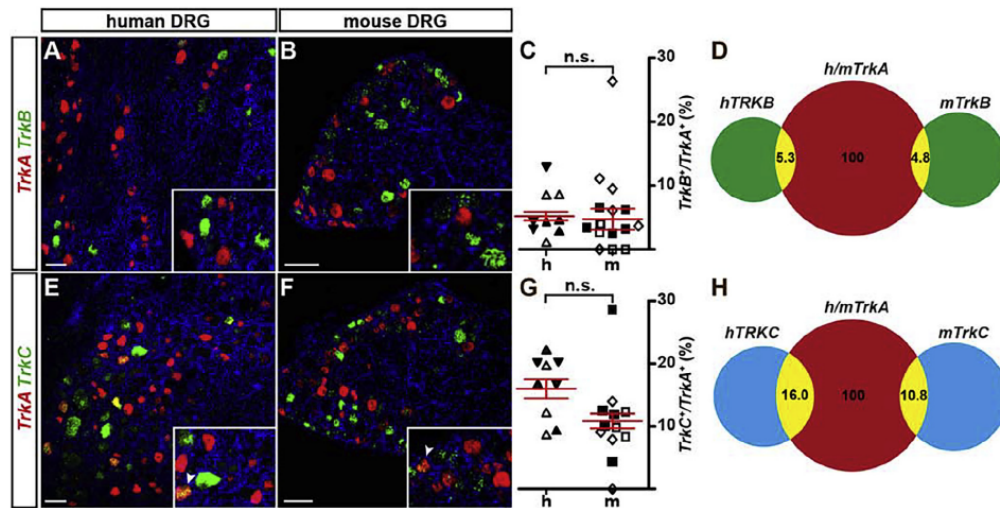


Fig. 1.12: Comparison of TrkB/TrkA and TrkC/TrkA double positive sensory neurons in mice and humans, in the dorsal root ganglia. Scale bar = 100 μm . The images (A,B,E,F) shows a representative dual-color fluorescence in situ hybridization for the detection of TrkA (in red) against TrkB (in green in A and B) and TrkC (in green in E and F). The insertion in (E, F) shows double-positive cells. (C) Quantification of double-positive TrkB cells against TrkA cells as scatter blots (mean \pm SEM). (G) Quantification of double-positive TrkC cells against TrkA cells represented as scatter blots (mean \pm SEM). No significant (n.s.) difference has been found. Differently oriented squares/triangles shaded or filled represents different subjects. (D,H) Venn diagrams showing the percentage of TrkB/TrkA (D) and TrkC/TrkA (H) from all TrkA expressing cells. [Ros+18]

1.10.2 TRPV1 against TrkA expression

As the comparison of TrkA-positive neurons against TrkB- and TrkC-ones, an analysis of the expression of TRPV1 against TrkA has been conducted (figure 1.13). In mice TRPV1 is expressed in 22-38% of all sensory neurons, in both peptidergic and non-peptidergic nociceptors. They applied the same technique as described before assessing that the ratio TRPV1/TrkA is equal to 35.4 \pm 0.6% in mice against 54.2 \pm 2.9% in humans. There is then a significant difference between humans and mice with a p-value < 0.001 . It is worth pointing out that the TRPA1 receptor is also coexpressed in a subpopulation of TRPV1 positive sensory neurons.

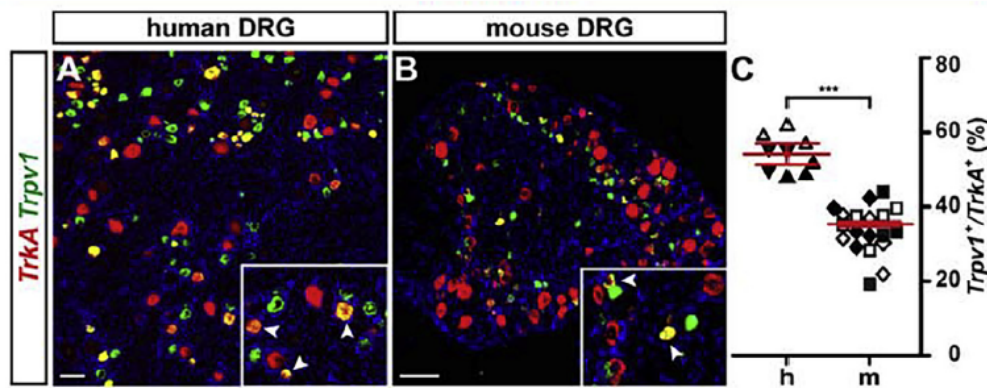


Fig. 1.13: Comparison of TRPV1/TrkA double positive sensory neurons in mice and humans, in the dorsal root ganglia. Scale bar = 100 μ m. The images (A,B) shows a representative dual-cloro fluorescence in situ hybridization for the detection of TrkA (in red) against TRPV1 (in green). The insertion in (A, B) shows double-positive cells. (C) Quantification of double-positive TRPV1 cells against TrkA cells. Significant difference has been found ($p = 0.0003$). Differently oriented squares/triangles shaded or filled represents different subjects. [Ros+18]

1.10.3 RET against TrkA expression

During the development of the peripheral nervous system TrkA positive cells undergo to transition changes and they divide into two groups. The first group keeps expressing the TrkA receptor, however some of them downregulate the TrkA expression and upregulate the tyrosine receptor kinase RET (a receptor for glial-derived neurotrophic factor, GDNF) becoming then TrkA negative neurons and in turn non-peptidergic neurons.

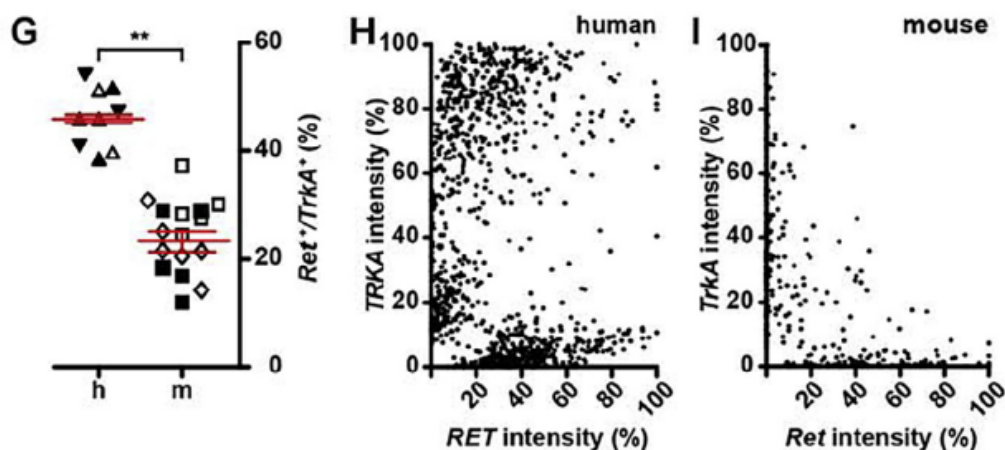


Fig. 1.14: Comparison of RET/TrkA double positive sensory neurons in mice and humans, in the dorsal root ganglia. (G) Quantification of double-positive RET cells against TrkA cells. Significant difference has been found ($p = 0.002$). Differently oriented squares/triangles shaded or filled represents different subjects. (H,I) Analysis of the relative RET and TrkA transcript expression levels in humans (H) and mice (I), evaluated through fluorescent intensities. In (H) a large group of RET/TrkA double-positive neurons is detectable, but it is not in mice DRGs [Ros+18]

However, there is also another subfamily that co-express both TrkA and RET receptors. Therefore a similar analysis as the two described before (sec. 1.10.1, 1.10.2) must be conducted as well. They showed that in human DRG neurons the $45.9 \pm 0.7\%$ of TRKA-positive neurons co-express RET, and the $23.2 \pm 1.8\%$ of TRKA-positive neurons in mice (figure 1.14). This suggest that a TRKA/RET population of sensory neurons exist in humans DRGs and it is almost the double in size with respect to that of mice DRGs ($p = 0.002$). In mice, this population has been associated with neurons that convey itch information towards central centers.

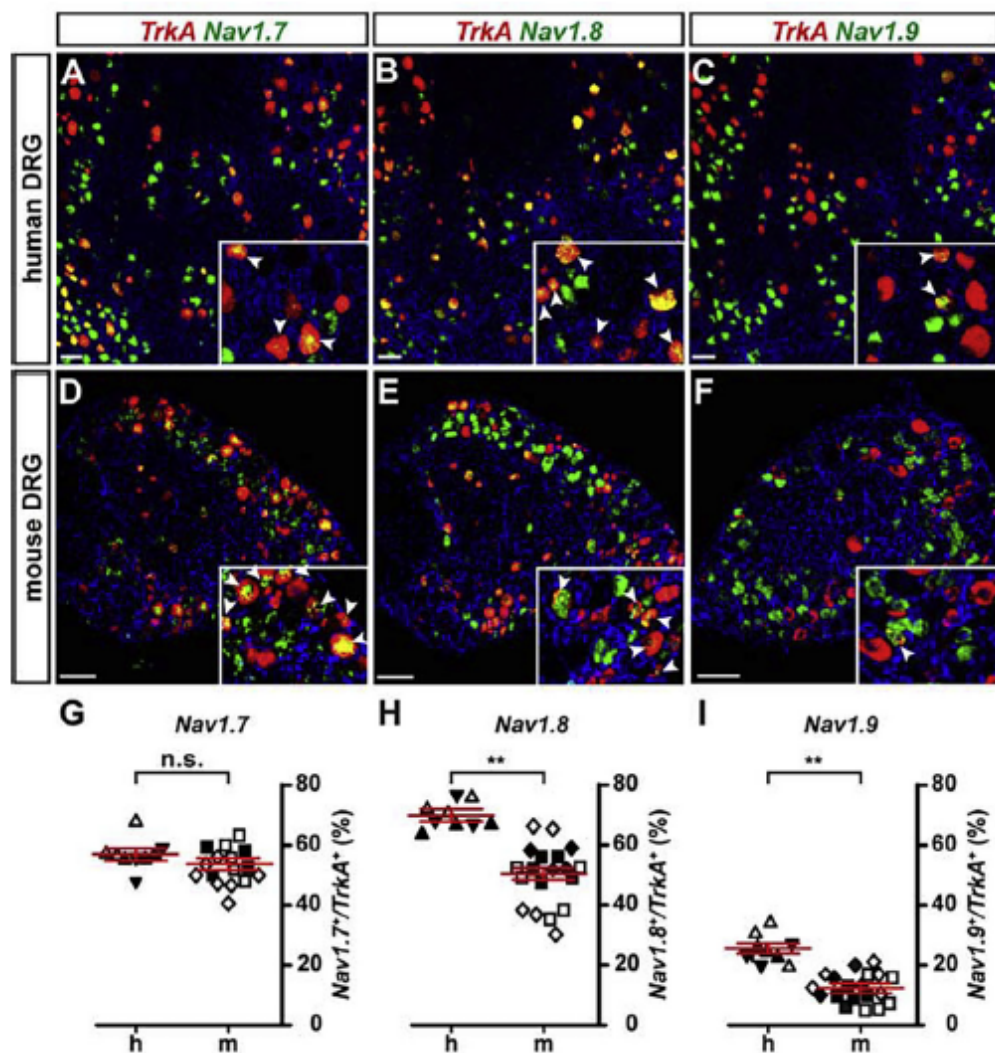


Fig. 1.15: Comparison of $\text{Nav}1.6\text{-Nav}1.9/\text{TrkA}$ double positive sensory neurons in mice and humans, in the dorsal root ganglia. (G) Quantification of double-positive RET cells against TrkA cells. Significant difference has been found ($p = 0.002$). Differently oriented squares/triangles shaded or filled represents different subjects. (H,I) Analysis of the relative RET and TrkA transcript expression levels in humans (H) and mice (I), evaluated through fluorescent intensities. In (H) a large group of RET/TrkA double-positive neurons is detectable, but it is not in mice DRGs [Ros+18]

1.10.4 $\text{Na}_v1.6$ - $\text{Na}_v1.9$ against TrkA expression

Some mutations in sodium channels may generate devastating pain disorders. Mutations of $\text{Na}_v1.7$ may cause congenital insensitivity to pain (CIP), a disease that cause to the affected patients to not feel any pain at all. Other mutations of the same sodium channel generate syndromes such as the small fiber neuropathy (SFN), paroxysmal extreme pain disorder (PEPD) and the inherited primary erithromelalgia (IEM). Also mutations affecting $\text{Na}_v1.8$ and $\text{Na}_v1.9$ can cause diseases, such as SFN and pain insensitivity or familial episodic pain respectively. These channels are indeed the target of new analgesic drugs. Thus similarities and differences between humans and mice must be studied such that preclinical studies may be conducted before clinical ones. They found that $42.9 \pm 2.7\%$ of TrkA-positive neurons co-express $\text{Na}_v1.6$ in humans and $35.2 \pm 5.9\%$ in mice, with no significant difference ($p = 0.204$) among them. Also, the ratio of $\text{Na}_v1.7$ in humans was $53.8 \pm 2.0\%$, and $57.0 \pm 2.1\%$ in mice, with no significant difference ($p = 0.281$). There was instead significant differences in the expression of $\text{Na}_v1.8$ ($p = 0.009$) and $\text{Na}_v1.9$ ($p = 0.003$). The ratio of $\text{Na}_v1.8$ in humans was $69.8 \pm 2.0\%$, and $50.6 \pm 2.0\%$ in mice, and that of $\text{Na}_v1.9$ in humans was $25.6 \pm 1.7\%$, and $12.4 \pm 1.6\%$ in mice (figure 1.15). Therefore the co-expression of $\text{Na}_v1.6$ and $\text{Na}_v1.7$ is almost similar in humans and mice however there are some differences in the expression of the channels $\text{Na}_v1.8$ and $\text{Na}_v1.9$, meaning that this can imply some functional consequences in the transmission of pain signals and other somatosensory information.

1.10.5 Overall view

Translational medicine has been exploited in the last decades to perform experiments in animals before applying new drugs and procedures to human patients, even more in the field of pain due to its unpleasantness. However, even if animal models are helpful for drug discovery and development they cannot mimic exactly the human body. Thus, studies concerning differences and similarities between the two have been conducted, and new approaches discovered (i.e. the generation of sensory neurons through human induced pluripotent stem cell-technology or human embryonic stem cells). Regarding the analysis conducted by the C. Rostock group [Ros+18] there are no significant differences in the expression of TrkB, TrkC, $\text{Na}_v1.6$ and $\text{Na}_v1.7$ against TrkA comparing humans with mice, the only difference is the size of TrkB and TrkC expressing neurons that is bigger in humans. The other way around, there are instead differences in the expression of Ret, TRPV1, $\text{Na}_v1.8$ and $\text{Na}_v1.9$ against TrkA.

1.11 Software used in microneurographic recordings

For microneurographic studies a software already available in the market has been used so far by researchers. It includes several modules for other studies such as nerve excitability, muscle excitability and cortical excitability [†]. It is indicated for studies in which the response of the nerve under investigation varies slowly with time. The raw data is stored after the recording is over and it can be used to retrieve information in the post-processing analysis. It is composed of two software, the QTracS and QTracP, both of them written in visual basic 6.0. The first one is used for simulation purposes and the latter for post processing analyses. QTrac is a multi-channel software with up to 20 between inputs and outputs, and different stimulation parameters can be tuned. QTrac can be operated through a command windows or by running scripts. QTrac can be used with PCs running Windows XP, Vista, 7, 8 or 10. Instead, to be able to run the software in a Mac a Windows emulator must be used, such as Parallels. It can be interfaced with some data acquisition card/units, mainly National Instruments PCI (i.e. PCI-6221M), PCMCIA (i.e. DAQCard-6062E) and USB units (i.e. USB-6221, USB-6251 and USB-6341) and two Cambridge Electronic Design USB units (i.e. Micro-1401 and Power-1401). However, USB units are slower than PCI boards, thus the latter is more indicated when a fast data processing is required. The stimulation is done through one of the two 16-bit analogue channels outputs of the PCI NI device. The recording is performed at the same time of the stimulation and the software allows to record up to 32k samples per second through one of the 16-bit A/D inputs. The response waveform can be sampled by any amplifier with an output in the range $\pm 10V$. The raw response can be filtered out with a high pass, low pass, mains frequency or a smooth filter, and other calculation can be applied (e.g. differentiation, rectification, subtraction, etc...). Furthermore, a raster plot (sec. method 3) can be populated for microneurographic studies with the picking of up to 60 points above a threshold that is applied on the raw data.

However, if a more user-friendly software is needed, faster fibers want to be analyzed (e.g. A δ -fibers) and cutting-edge analyses should be used, then an enhanced software not yet available in the market must be built. That is the main reason of these project. The developed software is meant for the study and analysis of slow and fast

[†]

https://www.digitimer.com/wp-content/uploads/2020/07/QtracW_Operators_Manual.pdf

fibers as well as a more intuitive use of the software along with advanced analyses performed on the raw data.

1.12 The work done

Previous paragraphs contain literature review providing a brief description of the nociceptive system such as the role of different nociceptors and the signal processing mediated by them. The following chapters instead show the work done within this project and they have the following subdivision.

The chapter "Methods" (ch. 3) shows programming techniques used for the development of the software and some data analysis performed on its outcomes useful for research outputs.

The chapter "Results" (ch. 4) contains graphs and plots associated with the Spiike software, as well as its layout and some recordings. It is also shown a statistical analysis with a real case study performed in a couple of patients.

The chapter "Discussion" (ch. 5) shows some comments concerning the Spiike software and how it can be exploited by the community for further recordings and analysis.

The chapter "Conclusions" (ch. 6) contains the comparison between the Spiike software and the Qtrac software, with its advantages against the latter.



Objectives

The main goal of this project is to develop advanced techniques and tools for a better recording, analysis and understanding of microneurographic signals obtained from peripheral nerves, in naïve and preclinical models of pain, which could also be used in human patients. Specific objectives are:

- To establish models, stimulation paradigms, electrophysiological readouts and developing analytical tools for detection and signal analysis.
- To characterize peripheral nerve fibers discharge through spike recognition, spike sorting and pattern analysis, packaged in a user-friendly software tool.
- To validate automated readouts by comparison with previous established methods.
- To extend the analysis to human microneurographic recordings.



Methods

3.1 Introduction

” *The whole [scientific] process resembles biological evolution. A problem is like an ecological niche, and a theory is like a gene or a species which is being tested for viability in that niche.*

— **David Deutsch**

The Fabric of Reality: The Science of Parallel
Universes—and Its Implications

The experimental approach is composed by stimulation, animal models, recording, software (machine learning and data analysis) and discoveries (figure 3.1). This software is mainly intended for preclinical studies, but it can be extended to clinical investigations as well. Therefore, in the following there will be description of how to perform the microneurography (sec. 1.9) in animal models.

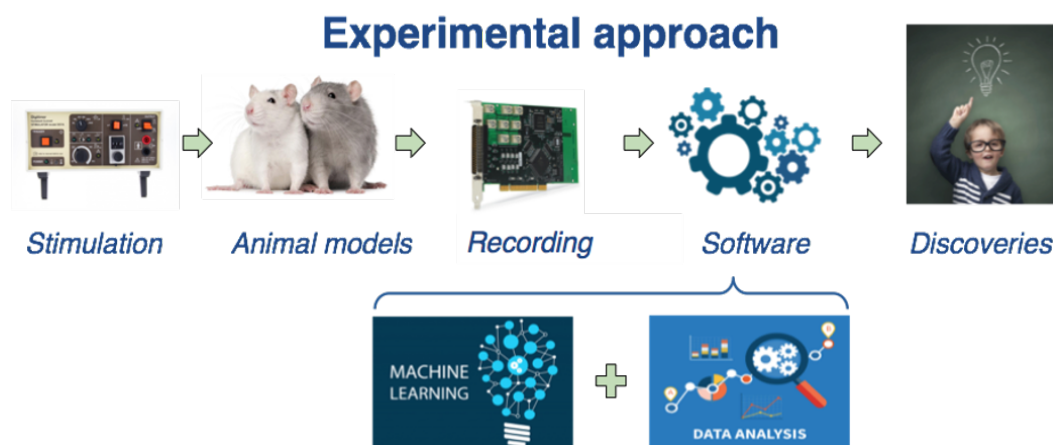


Fig. 3.1: The experimental approach of this study is composed by a stimulation module, animal models, recording module, software development (machine learning and data analysis capabilities) that may led to some discoveries.

As shown in figure 3.2 the setup for a microneurography recording is composed by stimulation, amplification, control and acquisition modules. The stimulation module includes a high voltage current stimulator (i.e. Digitimer DS7a). The amplification module gathers an audio monitor (i.e. Grass AM10), an animal model (i.e. mice or rats), a electrode, a micromanipulator (i.e. Tritech MM-3), an amplifier (i.e. Neuro Amp EX) and a 50/60 Hz noise eliminator (i.e. Hum Bug). Eventually, the signal is sent to the control and acquisition module that not only control the stimulator through a trigger signal but also acquire the neural activity by means of data acquisition board (DAQ) devices (BNC-2110, PCI 6221 and PowerLab). The BNC-2110 device is connected to the PCI-6221 through a dedicated cable, the former takes the BNC signal coming from the HumBug and the latter digitized it to the HDD of the computer making it available for the Spiike software. The PowerLab is another DAQ that works in synergy with the LabChart software and it is used in parallel with Spiike.

3.2 Stimulation paradigms

A pulse train is used to stimulate the fiber under investigation. The stimulus is delivered to their receptive field and it can be tuned to make different subgroups fire [Ond+16]. In this experiment the stimulating electrode is directly connected to the paw of the animal and the receptive field is searched listening at the discharge of the neurons. Upon discharge, the action potentials will travel along their axon towards the central nervous system. The time that they need to reach the recording site as well as their responsiveness to different stimuli is characteristic of each fiber population and it can be used as a classification technique in normal and abnormal nociceptors.

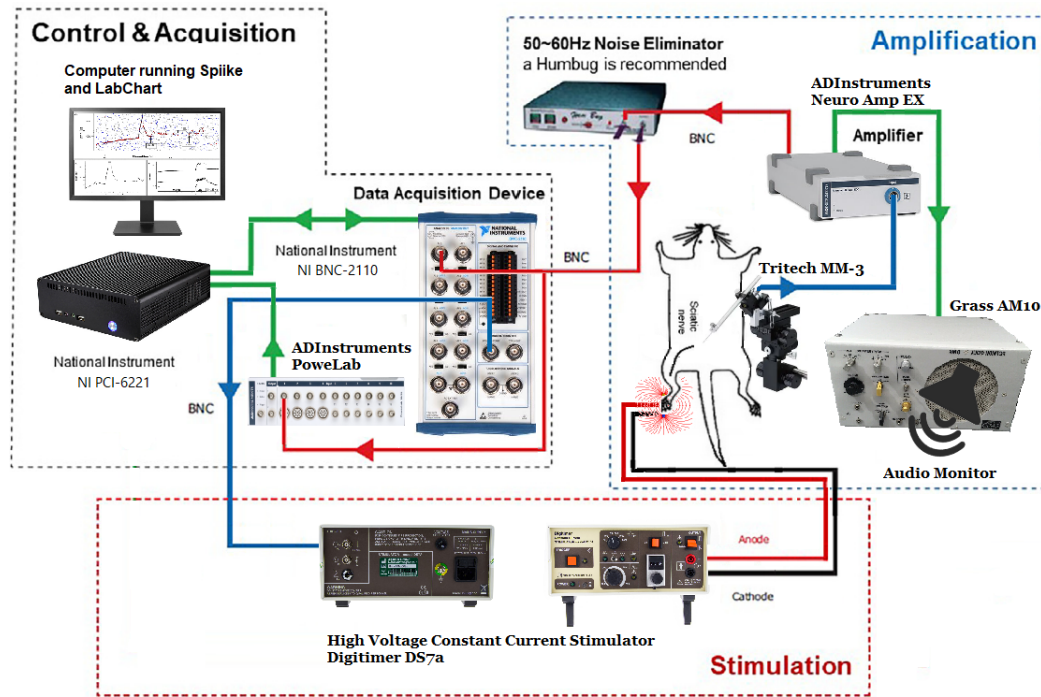


Fig. 3.2: Setup for a microneurography recording (adapted from [Kie+20])

3.2.1 High voltage constant current stimulator - Digitimer[®] DS7a

A stimulator made by Digitimer[®] (mod. DS7a) has been used for these studies [Ds7]. This is a high voltage constant current stimulator with a pulse duration that can be tuned, from $50\mu s$ up to 2ms. The constant output current at 400V is 100mA. It has got a flexible TTL compatible trigger that can be driven by a data acquisition board or activated by the user through a front panel push button. This is a human-proof device with a MDD CE certification and FDA clearance for medical devices. Therefore, it can be used for both preclinical and clinical studies. The stimulus is triggered by a Data Acquisition Board made by National Instruments (mod. PCI 6221) and its intensity is regulated in such a way that neural activity is seen with the minimum amount of current delivered. This is required to avoid both damaging the skin of the animal and the stimulation of too many fibers. If a lot of fibers are excited they will overlap during the recording, making the analysis very challenging.

3.2.2 DAQ for control NI - National Instruments[®] PCI 6221 and BNC-2110

A Data Acquisition Board (DAQ) is used to both control the stimulator DS7a and acquire the signal of the recording electrode. The board is the National Instruments[®]

PCI 6221 [Daqa]. It has to be plugged into the motherboard of the computer and an external device must be connected to this module. Since the external port is universal different type of devices can be connected, however for the matter of this project the National Instruments[®] BNC-2110 [Bnc] has been used. As controlling purposes it is worth pointing out that it has a 2 analog output channels that can be used for the generation of whatever signal, and 24 pin I/O channels for the generation of digital waveforms. To have a wide range of functionalities and possibilities Spiike software has been developed looking not only at the hardware available at the time for animal recordings, but at future experiments as well. Therefore, even if the Digitimer DS7a receives a trigger signal for the releasing of the signal that is basically a pulse train other functions has been added as well in the SPIike software (i.e.). However, the DS7a cannot be used as signal follower (the output is equal to the input in shape), therefore other devices should be used for this purpose. In the DS7a the 2 analog outputs have a DAC resolution of about 16 bits with a maximum update rate of 833 kS/s if used individually, otherwise it drops to 740 kS/s per channel. The timing accuracy is 50 ppm of sample rate, with a timing resolution of about 50 ns. The output range is ± 10 V, the output impedance is 0.2Ω with an output current drive equal to ± 5 mA and a slew rate of $15 \text{ V}/\mu\text{s}$. These are outstanding specifications that can be used for the purpose of this project, namely as mentioned before the stimulation of thinly myelinated nociceptors (*A δ fibers*) and unmyelinated nociceptors (*C fibers*) (sec. 1.2)

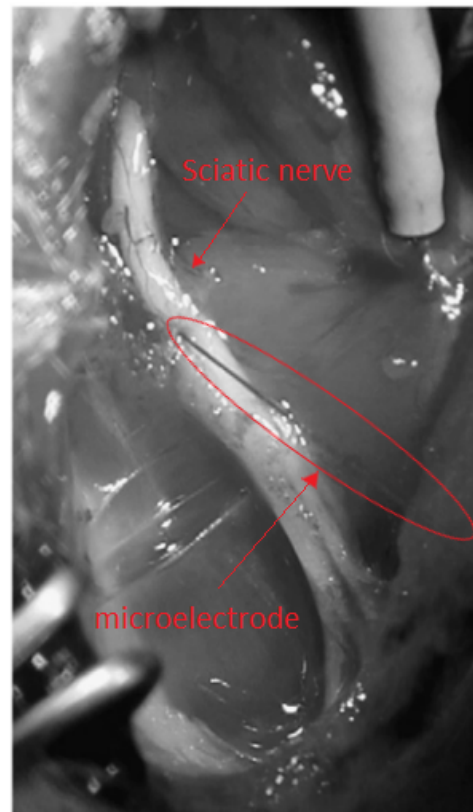
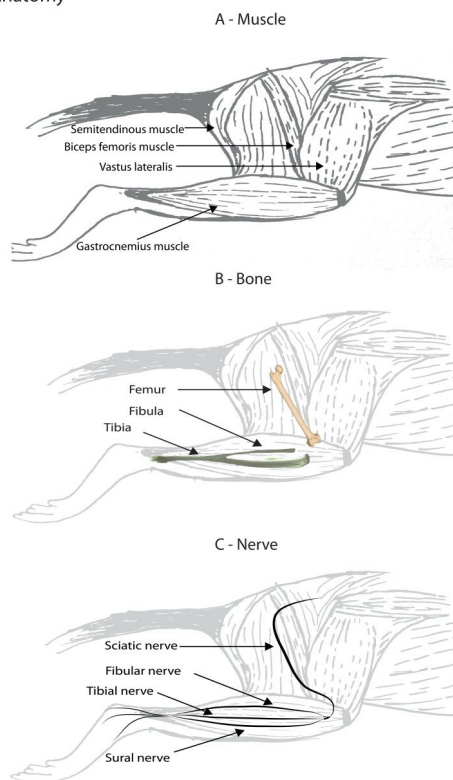
3.3 Animal models

The experimental procedure follows the recommendations of the European Union for the care and use of laboratory animals and were approved by the CEEAH (Committee for Ethics on Experimental Animal and Human Research). The animal (i.e. rats, mice) is anesthetized through an intraperitoneal injection according to its weight [ψ] and properly shaved around the electrode insertion sites. During the trial, vital signs (i.e. core temperature, skin temperature, and heart rate) are checked and kept within an acceptable range. If the animal shows any recover from the anesthesia half of the initial dose [ψ] must be injected. For assessing the functionality of the software wild type mice have been used, however knock-out and knock-in mice models can be employed as well. Once the anesthesia has kicked in, the animal must be places on a homeothermic blanket to keep its core temperature within a wanted range. After that some tools must be used to expose the nerve fascicle. Therefore, with the animal faced down the researcher must look for its keen (the right or the left

[ψ] 60mg/Kg Ketamine + 0,5mg/Kg Medetomidine in rats

leg can be used arbitrarily) once it has been located a cut on the skin is done with a scalpel. Then with curved surgical forceps the joint between the biceps femoris (BF) and vastus lateralis (VL) must be separated looking for the sciatic nerve underneath them (figure 3.3a). Once this is done sternberg retractors are placed to keep the cut opened exposing the sciatic nerve. Then the epineurium and perineurium of the sciatic nerve are cutted with a surgical scissor to avoid damaging the electrode during the insertion. The insertion is carried out with the help of a micromanipulator. Eventually, once the electrode is properly inserted (figure 3.3b) the palpation of the paw will generate neural discharges that can be listened through the audio monitor.

Anatomy



- (a) Anatomy of a rat hindlimb. The sciatic nerve is localized right below the biceps femoris muscle and the vastus lateralis, pretty close to the femur of the animal. [Nij+13]
- (b) Image of a microneurography recording with the microelectrode inserted inside the sciatic nerve of a rat. (adapted from [SBN10])

Fig. 3.3

3.3.1 Homeothermic blanket system - Harvard Apparatus[®]

The homeothermic blanket system allows to keep the temperature of the animal within an acceptable level, usually 37 degrees Celsius.[Hom] The device is composed by a rectal probe for the measurement of the core temperature, a blanket for heating and a control unit. It is a feedback system that check in real time the core temperature of the animal and according to that tune the blanket heater for keeping the core

temperature at the desired level. The control temperature can be set through a rotary encoder between 20°C and 50°C, therefore it can be used for other application or models as well. The flexible probe is a thermistor enclosed in a bed of epoxy resin at the top of a flexible hollow plastic tube.

3.4 Microneurography recording

The stimulation site is located on the hind paw of the animal and the recording site on the thigh. The recording electrode is inserted into the sciatic nerve with the help of a micromanipulator. Palpation of the hind paw sole, on the same electrode side, evokes differences in the recorded signal if the electrode is properly inserted in the fiber receptive field. It is worth noting that bigger distances can improve the quality of the recordings (plots with more clear fiber populations). Thus, rats are preferred to mice. The electronic setup is composed by an electrode with its amplifier ADInstruments[®] Neuro Amp EX, a noise eliminator Digitimer[®] Hum Bug, and two Data Acquisition Boards. One board (National Instruments[®] PCI 6221) is used for the recording through the SPIke software and the other one (AD instruments[®] PowerLab unit) for the recording through the LabChart environment. It is a good practice to record the same signal in parallel to check the functionality of the software and also to have a backup unit in case the software fails.

3.4.1 Electrode - FHC[®] Microelectrode Neurography

The electrode is made by FHC and it is suited for microneurography recordings. [Fhca] The selected electrode is sold with the catalog number UNA35F1U [Fhcb] meaning a nominal impedance of about $1\text{M} \pm 0.2\text{M}$, a shaft diameter of about 200 μm with 35mm of electrode length. These parameters can be changed according to the catalog provided by FHC[®] [Fhcb], more specifically the electrode length, the shank diameter, the impedance and the termination pin. Basically the most important parameters are the nominal impedance and the shank diameter. The former is important for a good single-unit discrimination and for a good signal-to-noise ratio, while the latter will determine the damage caused to the nerve but also the resistance to electrode damages during insertion like bending or cracks as well as the number of fiber fascicles in contact with the electrode. It is worth noting that when the electrode is inserted inside the nerve fascicle -due to friction- the coating will wear out decreasing its impedance. Thus, the nominal impedance of the electrode must be chosen a little bit higher than the desired one. Moreover, after few insertions due to this problem the impedance will drop to a very low value decreasing the quality of the recordings, namely after 3-4 experiments the electrode must be discharged or when a low SNR is detected.

3.4.2 Micromanipulator - Tritech Research[®] MM-3

The micromanipulator Tritech Research[®] MM-3 [Mic] is used to lower the electrode with precision inside the nerve. In human patients is not required since the fascicle is searched through repetitive insertion of the electrode percutaneously in the foot of the patient, however in preclinical studies the skin of the animal is opened and the nerve exposed, therefore the electrode must be inserted vertically (or even better with a little angle to maximize the number of touched fibers) and hold it in the same position during the whole experiment. Moreover, due to the small dimension of the nerve the electrode needs to be moved with good precision and little movements. For this purpose a micromanipulator is used and it allows the user to fulfill all these requirements.

3.4.3 Headstage - ADInstruments[®] MLT185 Neuro Amp EX Headstage

The electrode is then connected to one of the 3-pins connector of a headstage (ADInstruments[®] MLT185 Neuro Amp EX Headstage) [Adi]. The other two pins are used for the reference electrode that is a normal electrode inserted into the flesh of the animal pretty close to the active electrode and the second one is the ground electrode that is placed far from this two in the flesh of the animal as well. The headstage is then connected to the Amplifier Neuro Amp EX.

3.4.4 Amplifier - ADInstruments[®] Neuro Amp EX

The headstage is connected directly to the amplifier, the ADInstruments[®] Neuro Amp EX[Adn]. It allows the recording of extracellular action potentials from single-unit neurons or a group of them. The amplifier is connected through a I²C connection to the DAQ Powerlab, and thanks to this and the LabChart software the user can change several parameters such as the filter (i.e. low-pass, high-pass and mains). The built-in amplifier is a low-noise, high-gain and differential amplifier. Furthermore, the differential input AC is fully electrically isolated to guarantee the subject safety, with an isolated ground connection. The input socket, that is connected to the headstage, is composed by 5 pins, that provide 7.5V supply lines for the headstage powering, a protected ground and some differential input lines. The rear panel -a part from the aforementioned I²C socket that provided also the power to the amplifier- is composed by a BNC signal output that is connected to the Hum Bug for noise elimination purposes, and an audio output for the connection to the audio monitor.

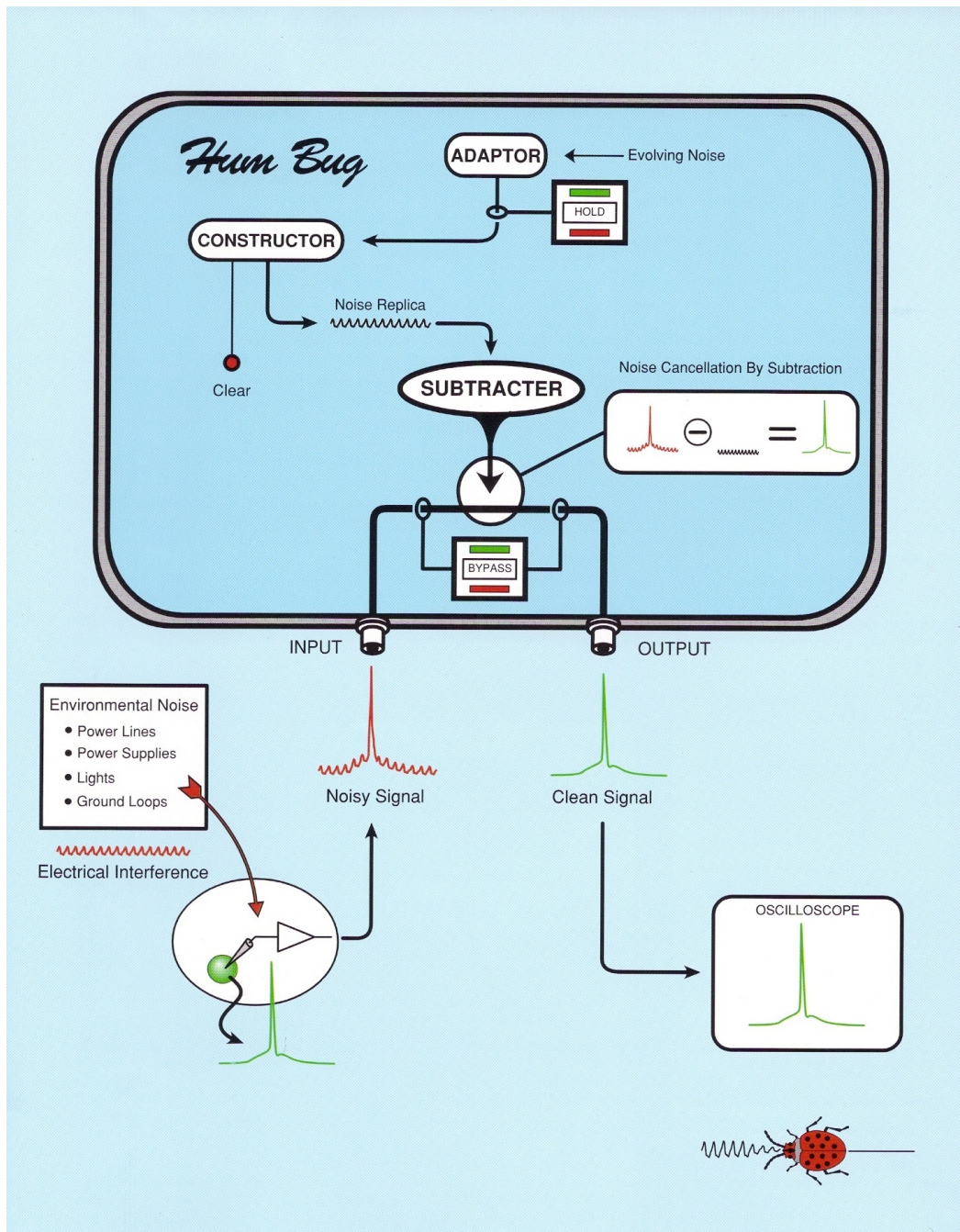


Fig. 3.4: Functional elements of a Digitimer Hum Bug. [Hum]

3.4.5 Audio Monitor - Natus® Grass AM10

The audio monitor Natus® Grass AM10 comes with two input channels (one of them can be used as voltage controlled oscillator (VCO)), a volume knob, a -6dB filter with its high pass filter that can be tuned from 10 up to 1000 Hz and a low pass filter with a changeable cutoff frequency from .1 up to 10 kHz. It also includes an amplifier (tunable with a low, medium and high setting) and a squelch with a noise clipper, that is used to suppress the background noise. As rule of thumbs, as every kind of mixer or audio monitor, it is recommendable to keep the knobs in their

resting position, namely vertically and little adjustments must be carried out to look for the wanted signal.

3.4.6 Noise Eliminator - Digitimer[®] Hum Bug

The noise eliminator HumBug [Hum] is used to cancel out the noise coming from the environment such as the 50/60Hz power line noise and other interferences without altering the frequency characteristic of the coming signal. The interferences can come from the light bulbs, fluorescent lamps and other electrical equipments (figure 3.4). This noise is associated with ground loops and an inadequate shielding. However, even with a good shielding the noise will remain, so the Hum Bug is a must for these kind of applications. Clearly some precautions can be taken as well since the de-noising is not perfect neither thus the use of a Faraday cage is highly recommended. The advantage of the Hum Bug is that it does not filter the coming signal, however as shown in figure 3.4 it generates a replica of the noise and subtracts it to the input signal. It then generates ideally a noise free signal at the output of the system without altering the biological input that may have some 50/60Hz components.

3.4.7 DAQ for acquisition NI - National Instruments[®] PCI 6221 and BNC-2110

The output of the Hum Bug is connected to the Data Acquisition board National Instruments[®] PCI 6221 through the BNC-2110 terminal. This is the same DAQ used for the control of the stimulator however in this case it is used for the recording of the neural signal. It has 8 differential or 16 single ended analog inputs, with a sample rate up to 250kS/s and outstanding parameters (e.g. -for the Analog Input Channels- CMRR=92dB, Timing accuracy=50 ppm of sample rate, ADC resolution=16 bits, Crosstalk at 100kHz equal to -75dB for adjacent channels). This is more than enough for the recording of faster fiber such as *A δ fibers*, one of the objectives of this project. Furthermore, this board is compatible with the MATLAB software used for the development of the Spiike software.

3.4.8 DAQ ADI - ADInstruments[®] PowerLab

The output of the hum bug is also connected to the Powerlab through a BNC cable. The Powerlab [Pow] unit is a DAQ as well but it is controlled through the LabChart software provided by the same company ADInstruments[®]. The powerlab has 16 BNC connectors in its 16/35 version, and 4 alternative DIN pod connectors for recording

external signals. It has got indicators to check if the device is working properly, a trigger channel that be controlled by an external signal and 2 analog outputs. For the purpose of this project one input BNC channel is used for recording (the output of the humbug) and two other channels for the recording of ECG and EEG signals for monitoring the vital signs of the animal. Moreover, a infrared thermometer can be used to the check the temperature of the paw and the core temperature of the homeothermic blanket can be recorded as well. It is important to check the temperature since nociceptor latency can change according to that and some fiber can also discharge if the temperature is too high or too low. It is worth pointing out that the analog inputs receive external signals up to $\pm 10V$. Every channel has a independent programmable gain amplifier, filtering AC/DC coupling that can be set through the LabChart software. Moreover external signals can be as low as the μV without the need of an external amplifier. The rear panel has a power socket, a I²C socket for the communication with the Neuro Amp EX and a USB port for sending and receiving data from the computer. The input impedance of the BNC channels is around $1\text{ M}\Omega \parallel 100\text{ pF}$, with a sample rate up to 200 kHz using one or two inputs, and a ADC resolution of about 16 bits.

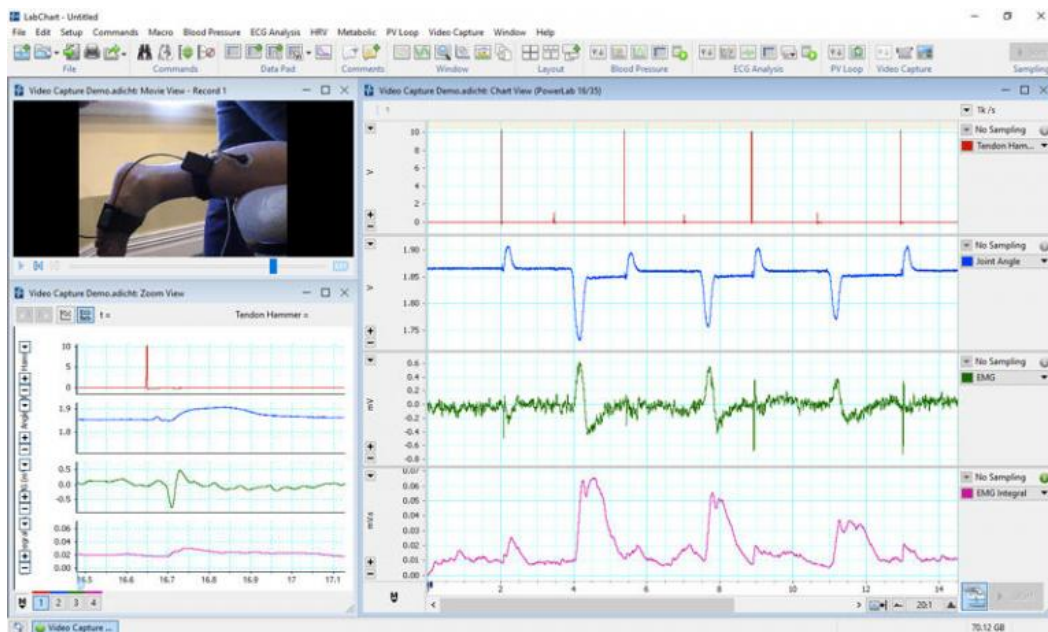


Fig. 3.5: Labchart software. [Laba]

3.4.9 DAQ ADI - ADInstruments[®] LabChart

The ADInstruments[®] PowerLab is controlled and data collected through its own software called LabChart (figure 3.5)[Labb]. It allows the user to change all the parameters that are tunable with the Neuro Amp Ex and the PowerLab. It can be run in Windows as well as Mac operating systems. When a new document has been generated some parameters of the input amplifier must be set, namely the input range, the filter and the sampling rate. And if a Neuro Amp EX is connected to the

device -as our case- also its range, low pass and high pass filter must be tuned to get the wanted signal and suppress any noise that could affect the recording. Then the whole experiment can be recorded through this software and the signal can be retrieved afterwards for making some analysis on them. However this software is not meant for microneurographic studies, and only a free-running signal can be recorded. Therefore another software must be used as well.

3.5 Software development

Spiike, the developed software, stores the acquired signal and with proper elaborations extract patterns from the experimental data. Raw data must be analyzed, and useless information must be eliminated for making hidden information able to pop up from the noise. Spiike software can be divided into 2 main modules: the tool able to record and store information and the tool able to analyze this data. Both are essential for the purposes of this project and they have been written in Matlab[®] language.

3.5.1 Matlab

Matlab[®] is a software that is provided with an integrated development interface (IDE) that is basically a 'text editor' with its integrated compiler that compile the code written in its own programming language, namely M language. Figure 3.6 shows this IDE. It is composed by four windows that are used for scripts and developing purposes. There is a *command window* on the bottom that displays outputs and errors generated by the compiler and it can be also used for inputs. It is basically the same as a script when used for writing code, however in a script the code stays there in the command window is eliminated once the enter button is pressed and the code runs. Therefore another window, called *editor* is used for programming. In this window all the scripts are written and they can be opened and closed to check a limited portion of the whole software. Once few lines are written is a good practice to save the scripts in the folder in which the software is located and where all the scripts and functions are stored. This folder can be shown by the *folder view*, where the scripts are saved as m-files and the developer can navigate through the subfolders and new folders and scripts can be created. On the top instead there is the *toolbar* in which icons for saving the written scripts, opening a project, running the compiler, inserting a breakpoint, running a toolbox and several more functions can be found. Eventually, the *workspace window* shows all the data and the functions generated once the software is run. In there matrices, variables, strings, functions and objects and everything also can be found, checked and changed.

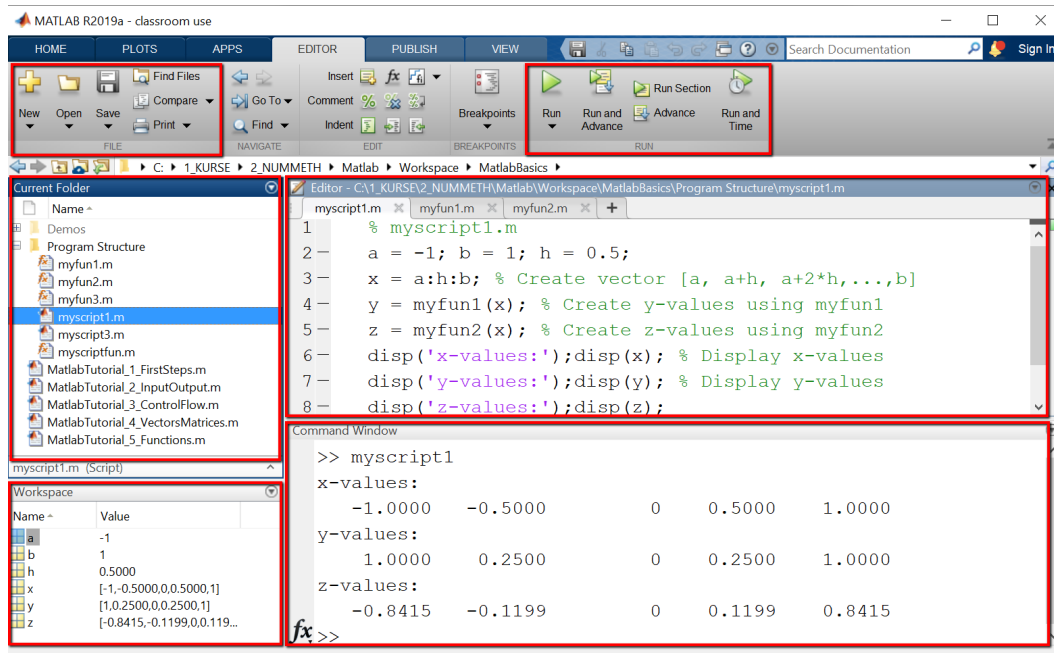


Fig. 3.6: Matlab IDE. It is composed by four windows. A command window that shows commands and output as well as it can be used for inserting some inputs. A workspace window that displays functions and variables of the running scripts. A folder view that shows all the saved scripts and subfolders. A editor window that displays the content of the scripts, and allows the user to change it. [Mat]

This is actually the default disposition of the different window panels, however their positions can be changed and some of them even close. It depends on the preferences of the developer and how he is used to code.

3.5.2 Compiler

The compiler is just a software that reads the human-readable code and convert it into a machine-readable code, namely a binary code made of 0s and 1s. Therefore the compiler converts a high-level programming language into a lower level language. The high-level programming language populate a text file that is the so-called source code. The compiler is taking this source code and through several steps converts it into a machine code. Basically, as shown on figure 3.7 it consists of a lexical analysis, syntax analysis, semantic analysis, IR generation, IR optimization, code generation, optimization. The lexical analysis converts the source code into tokens.[Coma] Every written word is considered as a token and the white spaces are ignored by the compiler as well as the comments. It also creates the symbol table and generates errors. Then the tokens are read by the parser that performs the syntax analysis and the actions are dictated by the token order [Comb]. It also updates the symbol table entries and generates errors if there exist. Then, in the semantic analysis the symbols are interpreted as well as their types and how they are related to each other.

This step is helpful to understand if the syntax structure makes any sense. In these phase the compiler can come up with an error as well. [Sem]

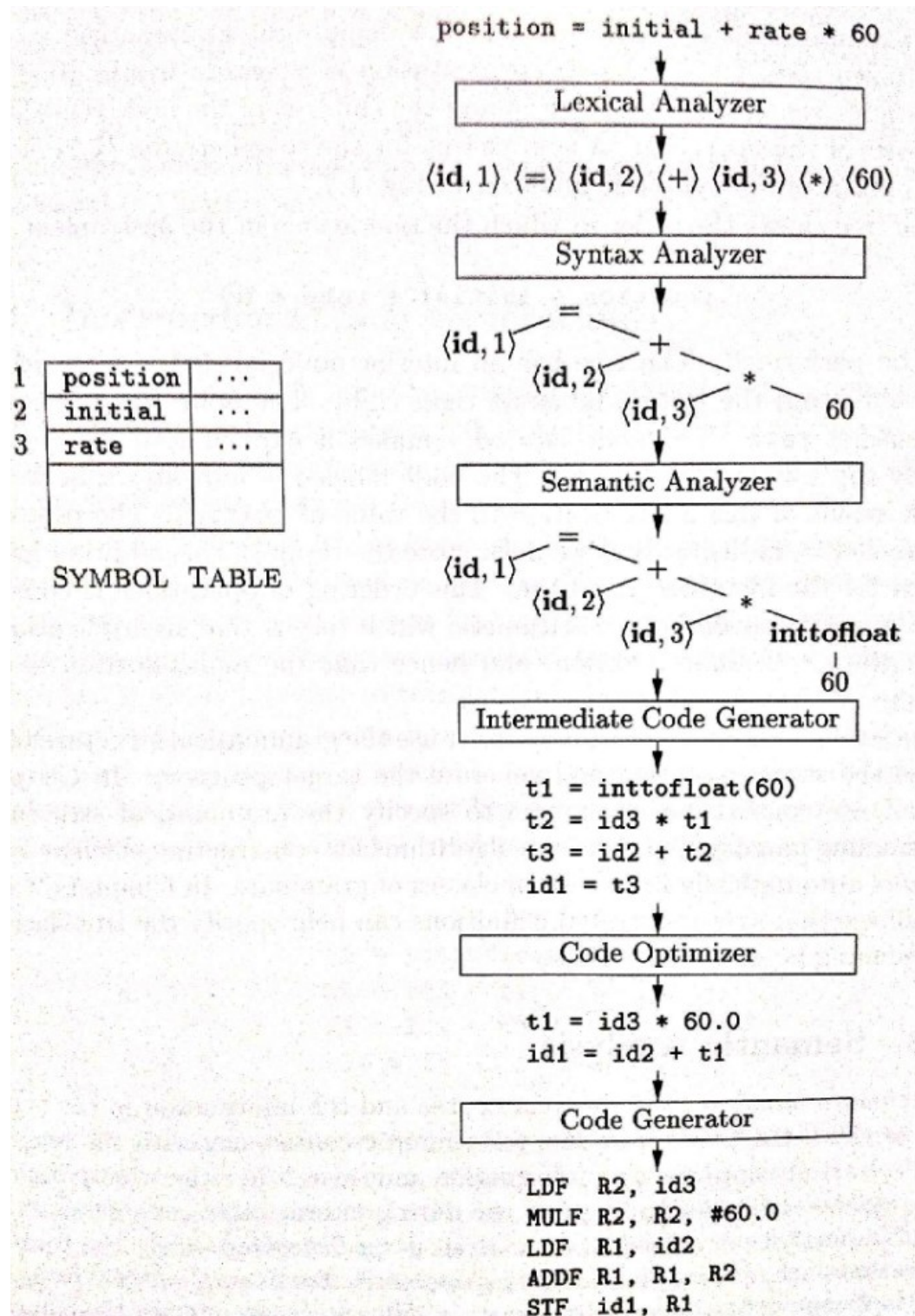


Fig. 3.7: The flowchart of a compiler, from the source code to a machine code readable from the hardware. [Coma]

Once the code has been checked the following step is to convert the information into a representation that is much closer to the machine code. This is just an intermediate

step, that is the reason why it is called intermediate representation (IR). The IR code is generated through a walk-through process starting from the leaf nodes and going all the way up to the tree root. [Irg]. The next step is the optimization of the IR code. Basically, the code is modified in a way that the algorithm needs less memory and/or it runs faster. The optimizer can be set from basic to aggressive, the latter will generate a better optimization however longer compilation times are needed. [Irg]. The last step is the code generation, namely the IR code is converted into a machine code. The machine code varies among processors and architectures and it is composed by binary code and it is not readable by humans since composed by 0s and 1s. In order to be readable every command is represented through assembly code, that is the lowest level programming language. The assembly code since it is strictly linked to the hardware varies among processors and the architectures as well. In such a way higher-level programming languages (e.g. M, C, C++, Java, etc..) can be used by a developer for modeling his ideas and through the compiler these ideas can be converted into a lower-level programming language readable by the hardware.

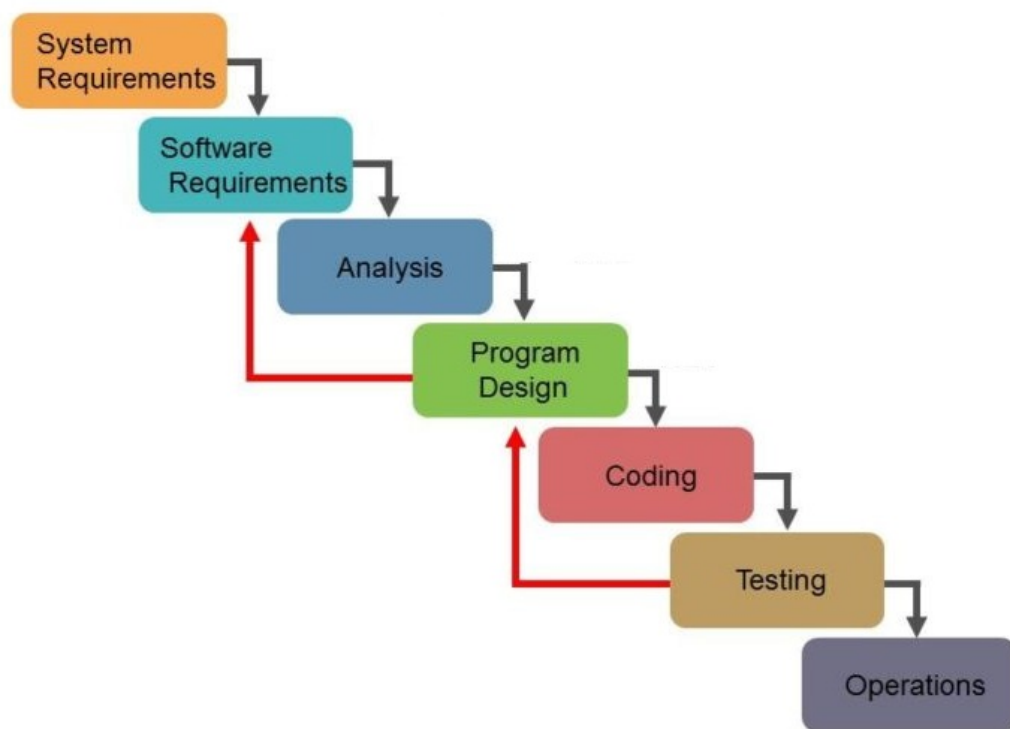


Fig. 3.8: Basic waterfall model for software development [Dev]

3.5.3 Waterfall model

The development of a software requires an iterative process that converts an idea into a tangible software. It is not a straightforward process. Most of the time it requires forward and backward steps, that allow the generation of a final product

reliable and free of errors. Figure 3.8 shows the steps to be followed for the making of a software starting from scratch. The first step is to analyze the system such as the hardware and the analogical equipment to assess bottlenecks and if there is room for the development. If it does not fulfill the requirements a more powerful system should be used. Also the architecture of the system is crucial. For instance, will the software be run in a windows operating system or Mac OS? Or even both? All these assessments should be done before that the software development can start. In this specific case a Data Acquisition Board has been used for the acquiring of the neural signal and the stimulation of the neurons receptive field. Therefore its speed must be checked a priori. The PCI 6221 (sec. 3.2.2) is actually fast enough to cope with design constraints such as stimulation of faster fibers (e.g. A δ -fibers) and a sampling rate of at least 40kS/s.

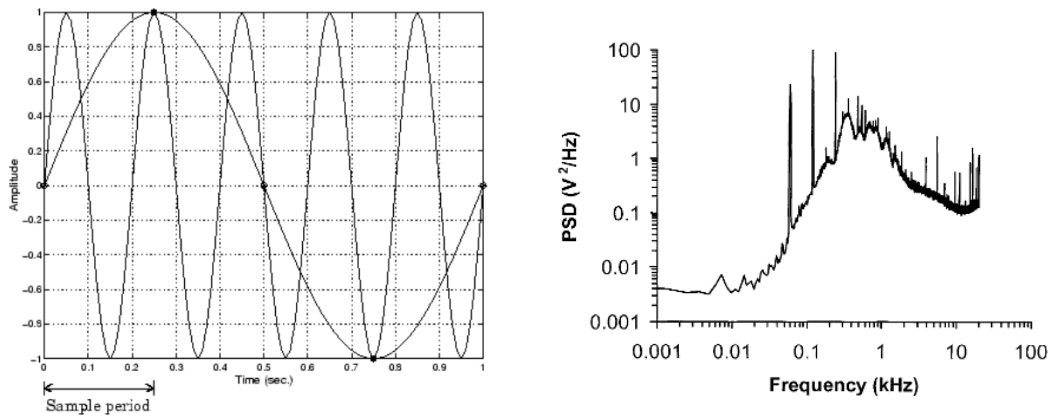
3.6 System and software requirements

This includes all the requirements for the hardware as well as the software needed for the correct functioning of the whole system. Software requirements can be everything related with the operating system as well as the software under development, such as sample rate or computational power.

3.6.1 Sample rate and aliasing

Every time a continuous signal is sampled some information are lost, however the higher the sample rate the lower the information lost. The drawback is that higher sample rate means more computational power needed and more space in the memory of the system. On the other way around if the sample rate is too low artificial information can be generated, this is the so-called aliasing. Therefore a trade-off must be reached. Aliasing can appear when the sampling frequency is lower than the double of the Nyquist frequency, this is the last frequency component of a signal. As shown in figure 3.9a the real signal is a sinusoidal waveform with a period equal to 0.2 sec. This means that in the Fourier domain this is a delta function at frequency $\pm \frac{1}{0.2}\text{Hz} = 5\text{ Hz}$, namely the last frequency component of the signal. The sampling rate is instead 0.25 sec, that in frequency is equivalent to $\frac{1}{0.25}\text{Hz} = 4\text{Hz}$, that is the sampling frequency. Since the sampling frequency is lower than the double of the last component of the signal, namely 10 Hz, aliasing occurs. Therefore, as shown in the figure the dots are actually the time points at which the signal is sampled and as you can see a sinusoidal signal with period 1 sec appears (this waveform is generated if a DAC is applied at the output of the system coupled with a RC filter since a condenser smooths the signal, otherwise a triangular waveform will appear, in any case both of them do not resemble the real signal). The sinusoidal function with a

frequency of 5Hz is then replaced with another one with a frequency of 1Hz due to aliasing. For the purpose of this project, since spike shape analysis is carried out, a high enough sampling rate must be chosen. Thus, as described in previous studies ‘In electrical recording, higher sampling rates (e.g. 10–40kHz) are often necessary to distinguish neurons based on spike shapes when each electrode monitors multiple neurons.’[Mag+13]. This is confirmed looking at the power density spectra of a microneurography neurogram shown in other previous studies [Die+03] (figure 3.9b). In this figure, it can be seen that the power of the signal is concentrated between 500Hz and 5-6 KHz, and doing some comparisons it has been shown that the average total squared error with a sampling frequency of 5KHz generates an error equal to 98 ± 28 , @10KHz the error is 0.02 ± 0.00 and @20KHz the error is 0.00 ± 0.00 . Therefore even a sampling frequency of about 20KHz should be enough for spike sorting, however if the system can cope with higher sampling rate is a good practice to increase it a little bit to have room for errors, therefore for the purpose of this project 40kS/s has been picked as the optimal sampling rate.



(a) Aliasing problem due to low sampling rate. (b) Power spectra of a microneurography neurogram. [Die+03]

Fig. 3.9

3.6.2 Data acquisition toolbox

Matlab comes with basic functions, thus for more complex projects additional toolboxes are needed. In this specific case the Data Acquisition Toolbox is required. It allows the Matlab IDE to communicate with the NI Data Acquisition Board. In such a way some signals such as a trigger for starting or stopping the data acquisition or the deletion of the queue can be inserted inside the software and with dedicated buttons the user can tell to the board what to do. As shown in figure 3.10 a data acquisition system can be subdivided into sensors, actuators, signal conditioning, acquisition hardware, computer and software. The acquisition hardware is the board that is able to record the physical phenomena coming from the environment and to activate the actuators for generate some sort of physical signals. In the

former, the board is converting an analogical signal into a digital signal and the other way around when is driving the actuator. Sensors and actuators are then transducers that convert input energy into output energy of another form. For instance a microphone converts sound energy into electrical energy, a loudspeaker instead transform a electrical energy into sound energy, and so on so forth. In this case the micro-electrode is the sensor since it is converting ions charges into electrical charges that can flow through the cable connected to the amplifier, the signal conditioning hardware. Indeed in this project the electrical signal generated by neural discharges is too low for being recorded directly by the DAQ, therefore the signal must be amplified through the Neuro Amp EX, and then the noise must be eliminated with the help of the Hum Bug. Successively the acquisition hardware communicates with the computer through bus lines dedicated exclusively to it and the installed drivers allow the operating system to identify and control the board. The developed software uses these installed drivers for doing the same work of the operating system, namely to control the data acquisition board. The computer is then the interface between the DAQ and the software, providing to the board a processor, a system clock and a hard disk drive for storing data.

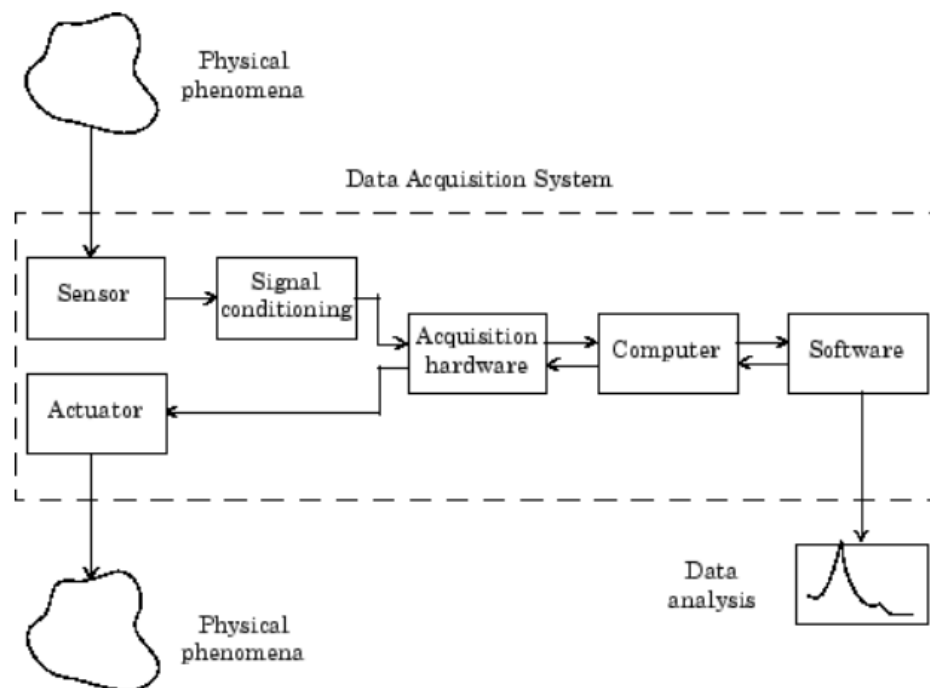


Fig. 3.10: A data acquisition system. [Daqb]

In order to transfer data from the acquisition hardware to the system a buffer is used. This board implements a FIFO (First-In First-Out) buffer. Therefore the data are collected in the buffer and the computer is taking step by step these data starting from the first one that have been recorded. Hence the communication between the board and the processor must be fast enough to cope with the acquisition rate

of the board. In number, with a sample rate of about 40kS/s the computer must read, delete and store in its own hard disk drive 40'000 samples every second. It seems a huge number but nowadays computer can manage this speed with no problems. Therefore the requirements of having at least a sample rate of 40kS/s for the recording of fast fibers can be fulfilled with a sufficient powerful computer (e.g. Intel Core processors and at least 4/8 Gb of RAM) and with the NI PCI 6221. It is worth noting that the computer while the board is recording is doing other operations, such as processing the video sent to the monitor or receiving information from the mouse, and the same is doing the DAQ therefore these operations must be stopped temporarily allowing the system to record the data. With this purpose in mind, interrupts or direct memory access (DMA) routines are used to allow the communication between computer and board. This is used to know when one of them is busy and when is instead able to send or receive data. More specifically, the DAQ after a certain number of acquired samples is generating an interrupt request signal (IRQ) saying to the computer that is ready for sending data through the bus.

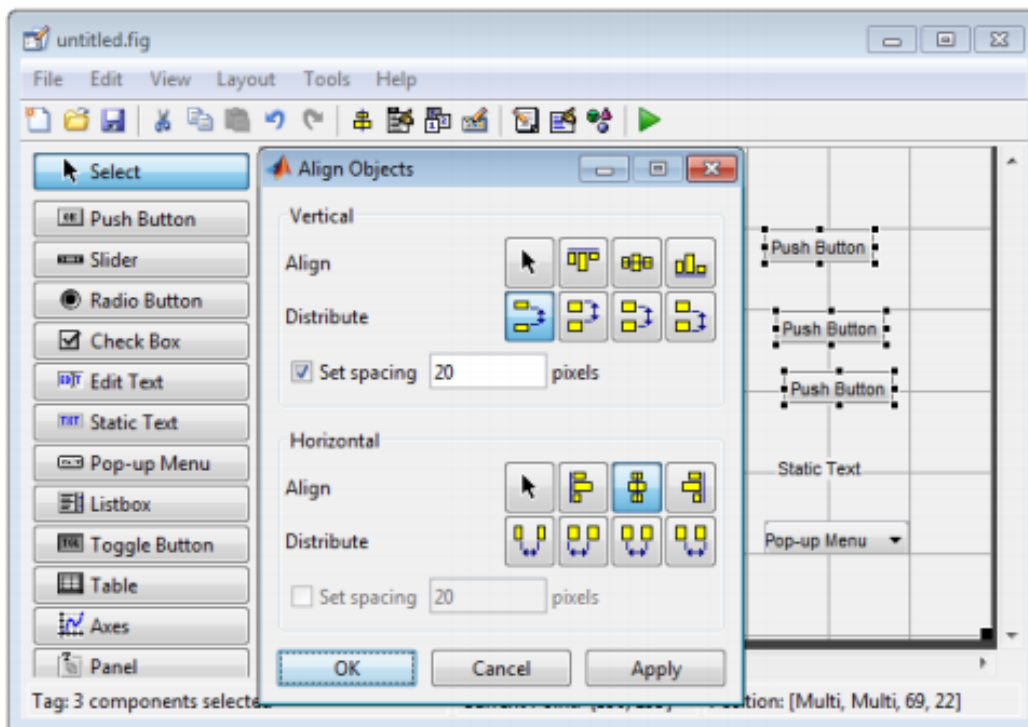


Fig. 3.11: Guide layout for the design of a GUI. [Gui]

Then once the computer receives the IRQ it stops the CPU processes (e.g. video processing) and runs a special interrupt handler routine that saves the current machine registers, and then sets them to get access to the board. The data are transferred to the system memory and then the CPU restores the previous registers and returns to the interrupted process. However, in this specific case even if the communication is very fast there are a lot of steps to be processed for accomplish the transfer therefore when the sampling rate is higher than 5kS/s the direct memory

access (DMA) is preferred. In the DMA protocol there is no interaction between board and CPU. The board is communicating with the system DMA controller that takes data from the FIFO buffer and moves them directly into memory pointing to the next open memory location. It is worth pointing out that the SPiike recording module needs a DAQ board to work, however if temporarily a DAQ board is not available a simulated device can be added through the NI-DAQmx software.

3.6.3 Guide

Another software requirement was the implementation of a graphical user interface (GUI) that needed to be user-friendly. For this purpose the Matlab GUIDE utility has been used. GUIDE allows the creation of a graphical display that contains controls, called components. These components allow the user to perform several tasks avoiding the use of a script or a command line. Therefore the user can interact with the software even if he does not have any programming skills, widening in such a way the pool of researchers that can have access to the software. The GUI components can include toolbars, menus, push buttons. Figure 3.11 shows the guide layout editor for the design of a new GUI. On the left panel some components such graphs, checkboxes, text boxes can be added to the layout, building in this way the software in the way the developer has thought about that.

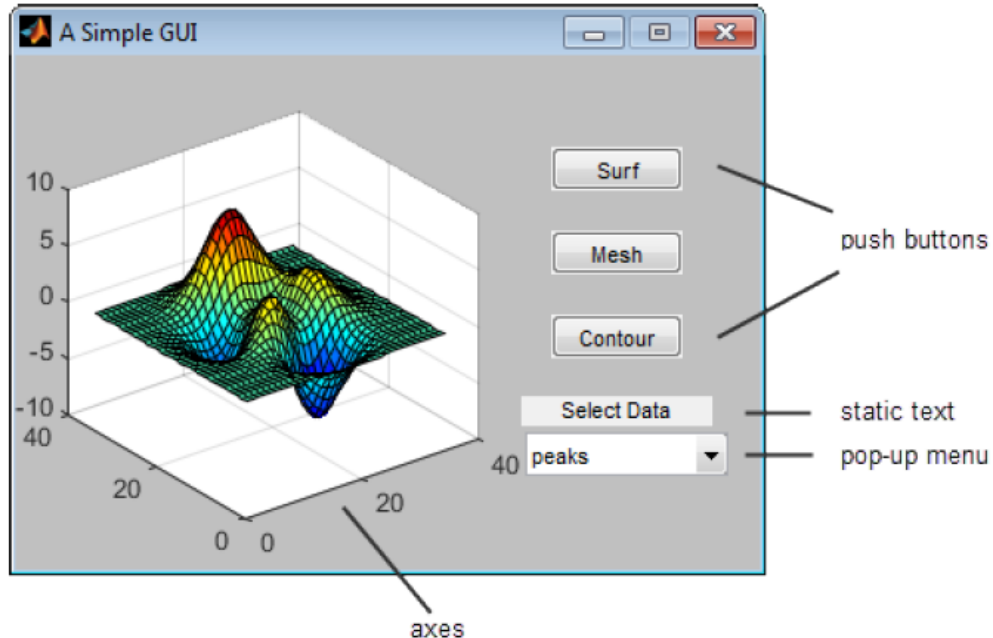


Fig. 3.12: Guide graphical user interface example. [Gui]

Figure 3.12 shows an example of a simple GUI built through the GUIDE utility. The user can interact with the implemented buttons and some parameters can be changed directly through this window without the need to write tedious commands

in the command line interface. Moreover a toolbar and a menu can be implemented as well in the upper part of the window allowing a more immersive interaction with the software. The GUI works by means of callback functions, namely every button has one or more functions that interrupt whatever the software is doing, they then call a routine function that interact with the software and in turn to the code wrote by the developer. That way pressing a button means to actually perform a sequence of actions to import data, export data or simple change some parameters within the software. This kind of programming is referred as event-driven programming and the callback function are asynchronous, this means that hitting a button instantaneously trigger an event. On the contrary, synchronous functions needs to request the execution and the software has to acknowledge them. However, since the software may be busy when the button is pressed this is not acceptable since there would be a delay that would mess up with the correct execution of the software.

3.7 Analysis and program design

In this part the software and and system requirements are analyzed and a draft of the software is created. The program design is nevertheless a iterative process, since during the design some problems in the requirements can be noticed or simply they cannot be fulfil as previously thought with the available technology. During this phase also the menu, toolbar and all the pop-up menus as well as the plots need to be designed before start writing the actual code. However, if every variable has been considered properly the iterations are few and the coding phase can start.

3.7.1 Spike design

SPiike software consists of two modules, one for the recording and one for the post recording analysis. In such a way the two modules do not require a lot of computational power for their functioning, being actually two separate software. Both of them have been designed in such a way that two graphs are shown on the main window of the program, and some tools like a pan a zoom in, zoom out icons can be activated for the interaction with those graphs. In the upper part a raw data, or filtered input data signal is inserted and in the lower part a raster plot useful for the characterization of the fiber type as well as to asses their healthiness. Furthermore in the menu bar basic functions like saving and closing of the program are inserted as well as other tabs to change parameters such as filter types and cutoff frequencies. In the analysis module, moreover a routine GUI for spike sorting and additional analysis such as the instantaneous firing rate evaluation and the fibers activity has been integrated as well. Moreover, the possibility of importing LabChart data is a must of the analysis module since it allows the researchers to extend the

analysis to human patients. Lastly, to speed up the recording as well as the analysis script functions can be used. They can be written through a basic text editor or recorded during the use of the software and they can be called back once required.

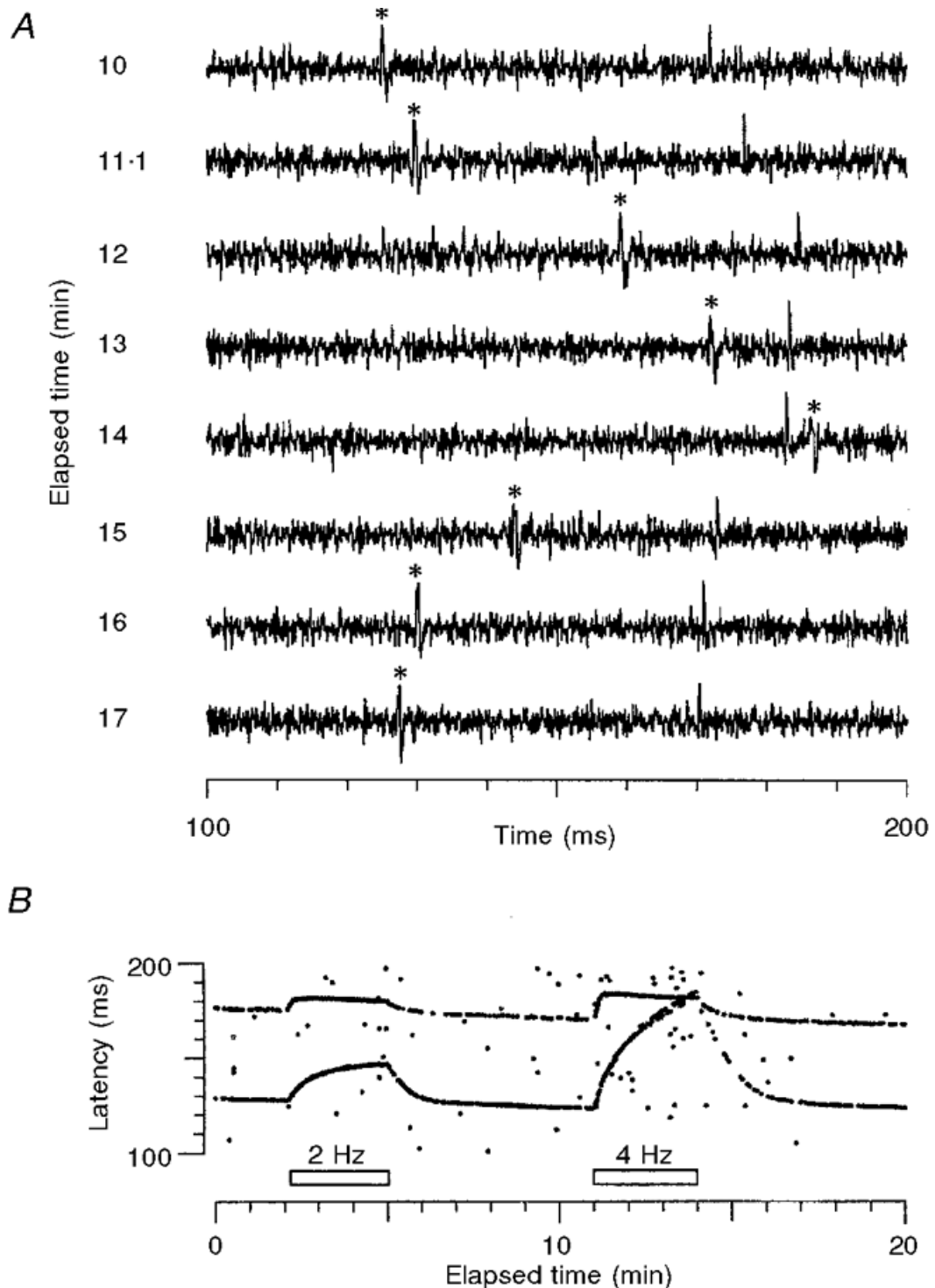


Fig. 3.13: Raster plot extraction. (A) Sweep traces with two action potentials on it. They are first increasing their latency and they then recover back. (B) A raster plot extracted putting a horizontal threshold on all the traces above and plotting a dot only when the signal is exceeding this value. On it two horizontal thin-like lines are shown, those correspond to the two neurons that were discharging in the graph above. [Ser+99]

3.8 Recording module - Spiike

The acquiring tool makes researchers capable of recording all the information they need. To this end, the SPiike software has been developed. It accounts of a graphical user interface (GUI) that allow users to change recording parameters (i.e. spike detection threshold, cut-off filter frequencies, sampling frequency, stimulation frequency, etc.) and visualize all the acquired data. The SPiike software is user-friendly and several plots such as a raster plot, a raw signal and a filtered signal graphs make the recording of nerve fiber discharges as easy as possible.

3.8.1 Raster plot

It displays information about neural discharges. It mainly consists in plotting fiber latencies against sweeps. Every time a single pulse is delivered (the sweep) neurons discharge sending action potentials centrally along their axons. The velocity of these action potentials is fixed -upon same stimulation parameters- thus the time (the latency) they need to reach the recording electrode can be recorded and it varies among fiber types. If the signal exceeds a threshold a dot is placed on the raster plot. Namely, a dot means that the tool has recognized an action potential with a high likelihood. Every sweep will draw a vertical trace composed by dots at different latencies, evaluated from the stimulus pulse (y-axis). The elapsed time, time from the beginning of the recording, is displayed on the x-axis.

As shown in figure 3.13 in the upper plot there are the sweeps at the minutes 10, 11, 12, 13, 14, 15, 16 and 17 of the elapsed time. These are the neural signals that the recording electrode is receiving. Looking at the trace at the minute 10 of the elapsed time two action potentials can be localized, at the time 125ms of the x-axis and another one at the time 170ms. The same happens in the second trace and so on and so forth for all the other traces. The only difference is that firstly the action potentials are moving towards the right (their latency is increasing) and they then recover back to the initial position. This is due to changes in the stimulation frequency that generate a very characteristic morphology according to the fiber type, in the so-called activity dependent slowing. Summarizing, inserting a horizontal line in all the traces and plotting all the points above this threshold a raster plot is generated (figure 3.13, (B)). On the graph below the x-axis is swept with the y-axis and the other way around, and only when the signal overcomes the aforementioned threshold a dot is inserted. This means that the raster plot is a binary representations of the neural activity and ideally only the action potentials are represented in there. Actually, sometimes noise can exceed threshold randomly and random dots are placed on the raster plot.

3.8.2 Activity-dependent slowing and marking technique

This is a well-established technique [Ser+99] that can provide a powerful tool for the analysis of the neural traffic. It is used extensively throughout the whole project. If the stimulation frequency of the fibers under investigation is kept constant their latency will not change. However, consequently to either a shift in frequency or the use of marking methods (e.g. stimulation through metal rods, heat, ice cubes, etc.) their latency can change, and this is characteristic of the fiber type. The same effect has been seen during diseases (spontaneous ectopic discharges [Ser+12]), thus this technique can also be exploited for diagnostic purposes. Usually, a baseline stimulation frequency of about 0.25Hz is used to probe C-fibers. Increasing the frequency to 2Hz discharges with greater latency should be noticed. Decreasing again the frequency to the baseline of 0.25Hz a recovery will be noticed. The fibers will then reach asymptotically their new baseline latency. Through this technique 4 C-fiber fiber types have been already found [Geo+07]: type 1A (mechano-responsive nociceptors; CMR), 1B (mechano-insensitive nociceptors; CMI), 2 (cold fibers), 3 (unknown function), 4 (sympathetic fibers). New stimulation protocols for probing other fiber types (e.g. A δ -fibers) are now available in the last version of the SPiike software. As shown in 3.16 two different type of fibers are recorded

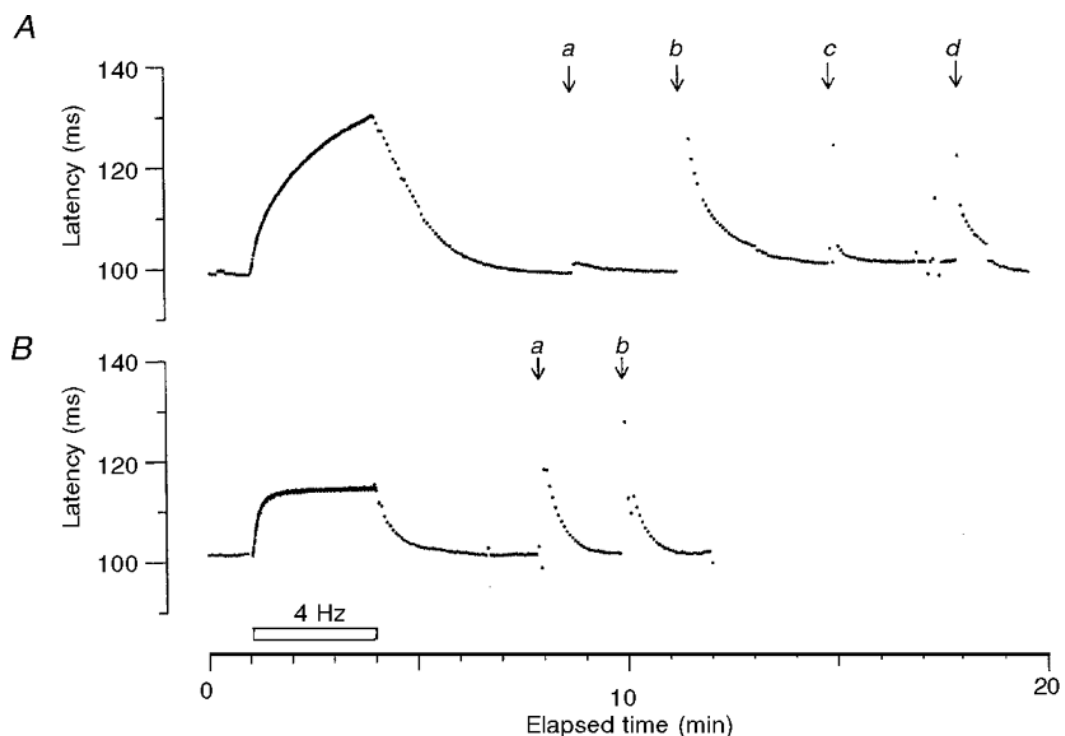


Fig. 3.14: Activity dependent slowing and marking technique. [Ser+99] (A) A type 1 fiber is shown, its latency increases during the 4Hz stimulation and it recovers to the baseline when the stimulation frequency comes back to 0.25Hz, this phenomenon is called activity dependent slowing. Then 4 natural stimuli are applied in the so-called marking technique, at a) by a metal rod (ca 25 °C), at b) by ice, at c) by Von Frey hair (24 bar) and at d) by heating to 48 °C for 5 s. (B) A type 2 unit is shown on it instead and its ADS is totally different with respect to the type 1 fiber, moreover at a) and b) a metal rod (ca 25 °C) is applied.

3.8.3 Recovery cycle

The activity-dependent slowing and the marking technique are very useful for characterizing the fiber type. However, in all those cases in which some doubts may arise and the functionality of the fiber should be assessed with more precision the recovery cycle protocol can be used. It consists in a baseline stimulation at a fixed frequency stimulation (the unconditioned stimulus) and a varying conditioned stimulus that sweep by sweep approaches the fixed pulse. Figure 3.15 shows the working principle of this conditioned stimulation. The stimulus pattern has a test pulse (i.e. unconditioned stimulus) and a varying conditioned pulse that starts at a latency of about 200ms and through sweep reaches eventually the 2ms of the interstimulus interval (ISI). Also a variation with 2 conditioned stimuli separated by 25 ms can be used [Geo+07]. However, the 2 conditioned stimuli stimulation is rarely used in actual microneurography recordings, the recovery cycle can be assessed with good precision through only one conditioned stimulus. This is an intrinsic effect of the fibers that after stimulation follows oscillatory changes in their excitability, with refractive periods (subnormality) that lower their likelihood to generate another action potential and excited phases (supernormality) in which the likelihood of discharging action potentials increases. In the figure 3.15 the subnormality is represented by the upward peak at the ISI range from 20ms to 200 ms, while the supernormality is represented by the downward peak at a ISI range from 2ms to 20ms. Moreover the part of the curve that is at ISI below 2ms represents the relative refractory periods (RRP).

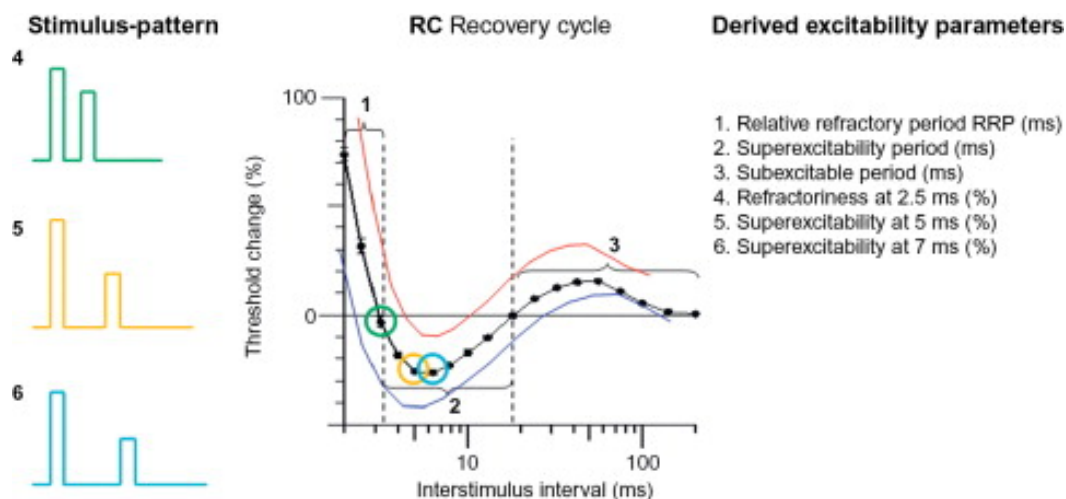


Fig. 3.15: Working principle of the recovery cycle. [KK13]

All of these parameters are intrinsic of every fiber type and they can change due to injuries and/or neuropathies, therefore they can be used in all these cases in which the healthiness of the fiber should be checked. Statistics can be applied on them to see the effect of some drugs to relief pain and to treat some diseases affecting the peripheral nervous system. SPIike software includes a feature that can activate this

stimulation protocol. Moreover, the software is reading an excel file for setting the ISI to use at each sweep, meaning that it can be changed if another protocol must be implemented. This gives researchers some freedom for trying new stimulation protocols that have not been tested yet.

3.8.4 Stimulation frequency up to 1kHz - A δ fibers

SPiike is also able to stimulate and record Adelta fibers. Being this an important leap in the understanding of the peripheral nervous system, and an innovative feature that no software has got yet. Basically, the software uses the same protocols as C-fibers, however with an increased frequency, the key point of Adelta fiber recordings. Software packages already available in the market are limited to 8/10Hz. This is still useful for the C-fibers, since their conduction velocity is quite low. However, SPiike software can increase its stimulation frequency up to 1000Hz and insights on faster fibers (e.g. A, B, etc...) can be obtained.

3.9 Analysis module - SPiike

Moreover, another SPiike module for the analysis of these datasets is used to extract information linked to nerve fibers. This second SPiike module provides outcomes useful for research purposes. Current microneurographic software packages allow users to visualize the recorded data and to perform additional tasks. The goal of this project is to implement more advanced techniques for the extraction of information.

3.9.1 Analysis module

The analysis module shows the same structure of the stimulation and recording module. Namely, the software is composed by a GUI like the recording module, that can be easily handled by the user and as mentioned before basic functions such as zooming, and saving are available. However, some features are exclusively implemented in this module (e.g. PCA, fiber ADS analysis, etc..). First, all the outcomes showed during stimulation and recording can be retrieved thanks to the availability of raw data. However, some parameters can be changed in order to highlight fibers of interest. In order to do so, filter parameters and peaks threshold can be tuned as wish. This will affect the entire raster plot, thus fibers barely shown during the stimulation might be easily visualized in the post-processing analysis.

3.9.2 Unsupervised machine learning algorithm, 1^o step - Principal component analysis (PCA)

The principal component analysis is a technique that has been used for decades with the aim of resolving exploratory data analysis and for making predictive models. Furthermore, it is usually used for dimensionality reduction, it projects indeed each data point in another lower-dimensionality space preserving the variance within data. Most of the time this manipulation increases algorithms outcomes lowering the computational time required to complete the task.

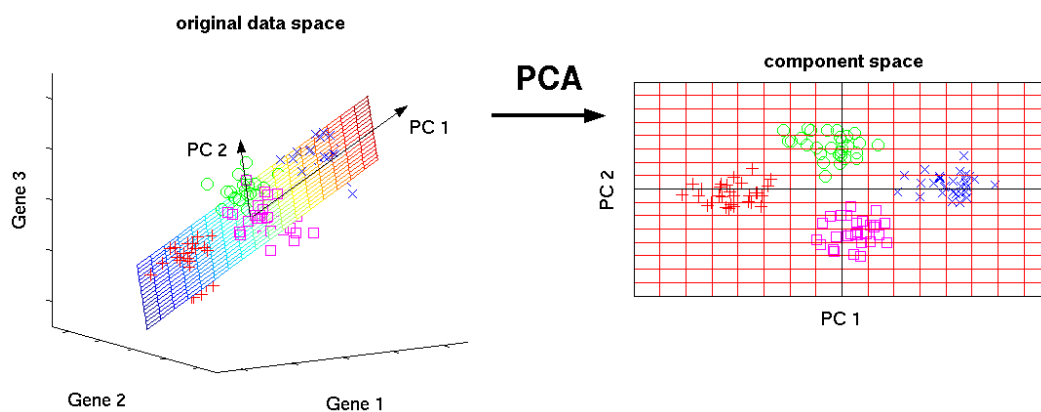


Fig. 3.16: Working principle of a principal component analysis (PCA). [Sch]

Figure 3.16 shows the working principle of a PCA algorithm. On the left, a 3-dimensional space. Every data entry is composed by 3 variables (i.e. gene 1, gene 2 and gene 3) and they can be represented in this 3-dimensional space with every gene composing each axis. The original data space can be composed by whatever variable type. For instance, for the purpose of this project they can be the width of the action potential, its rising phase, falling phase, its area, the amplitude of the upward peak and so on so forth. The original data space can include a very huge number of variables and thus dimensions. To this space a PCA algorithm is then applied. It looks at the data variance and generates a different space, the so-called component space, with a different orientation and position aimed to maximize the separation among data. In figure 3.16 for instance, in the original data space there are 4 clusters that can be represented in a 2 dimensional component space projecting the data entries into a 2 dimensional plane orientated in a way that the separation among data is maximized. On the right, the final representation is shown. As you can see the first principal component accounts for the largest possible variance, and the second principal component for the second largest possible variance, and so on. This means that in a large dataset with a lot of variables, few principal components are more than enough for analysis purposes, that is why it is called dimensionality reduction. However, it is worth pointing out that the number of principal components are equal to the number of initial variables, but only few of them are generally used.

The animation 3.9.2 shows the generation of the first principal component. As mentioned before the one with the largest possible variance. The data entries are the blues dots. The algorithm first of all is calculating the origin of the principal components, basically the centroid of the data entries (eq. 3.1), that corresponds to the statistical notion of arithmetic mean or average point.

$$G_j = \sum_{i=1}^N \frac{x_{ij}}{N} \quad (3.1)$$

(where G_j is the j-th component of the centroid (e.g. x,y and z axes), x_{ij} is the j-th component of the i-th data point and N the number of data points.)

Once this is evaluated the algorithm is drawing a line that pass through the origin and revolves around it, evaluating at every step the average of the squared distances from the projected points (red dots) to the origin. The algorithm keeps going until it is maximized, or saying in another words the average distance from the data entries (blue dots) and the projected points (red dots) is minimized. In this specific case, once the revolving line approach the purple lines the largest possible variance is reached and the algorithm stops. It then calculates the second principal component, taking into account that the second axis must pass through the origin and be perpendicular (i.e. uncorrelated) to the first principal component. Once the number of principal components match the number of variable the algorithm ends and further algorithms can be applied in the transformed space, such as the k-means clustering algorithm.

3.9.3 Unsupervised machine learning algorithm, 2^o step - K means clustering

Once the PCA has been applied to the data entries the K-means algorithm is generally used for clustering purposes. It takes as input the modified data space and through several iterations it assigns to each cluster a group. It works generally better if the clusters do not superimpose and if they are well characterized, otherwise more complicated algorithms that sometimes needs more computational time should be used. The animation 3.9.3 shows the working principle of this algorithm. The only input required to the user is the number of clusters that the algorithm must look for.

$$SST = \sum_{i=1}^N \left(\sqrt{\sum_{j=1}^D (x_{ij} - \hat{G}_j)^2} \right)^2 \quad (3.2)$$

(where \hat{G}_j is the j-th component of the estimated centroid (e.g. x,y and z axes), D the dimensionality of the space, x_{ij} is the j-th component of the i-th data point and N the number of data points.)

[Animated K-means clustering working principle. \[Kme\]](#)

Consequently, the algorithm chooses random points as the number inserted by the user that are considered as centroids (estimation of eq. 3.1, with notation \hat{G}_j) of each cluster, in this specific example it is four. Then it calculates the sum of squares (eq. 3.2) within each cluster, namely the sum of square of all the distances among the data points of each cluster from the centroid. Afterwards, the algorithm

changes the position of the centroid trying to minimize the sum of squares. The process is iterated until the sum of squares stays stable, in this specific case after 6/7 interactions. At this point the \hat{G}_j converge to G_j but sometimes it could take longer and even not converge. It depends on the clusters, so it is a good practice to check the PCA components before applying the K-means clustering algorithm. If the clusters are not well separated a different algorithm can be used (e.g. t-SNE, Linear discriminant analysis (LDA), Generalized discriminant analysis (GDA), etc..). However, for action potentials analyses the pairing of PCA and K-mean clustering once the sample rate is high enough and the signal to noise ratio is acceptable generates good outcomes.

3.9.4 Fiber ADS analysis

Another feature of SPiike software is the possibility of performing a quick analysis on the ADS shape and estimating thus the type of C-fiber the software is recording. To this aim, a function has been added to the pop-up menu, allowing the user to call it all the time he wants. The feature is asking to the user to click in different points of the ADS shape. It is worth recalling that the ADS is performed stimulating the fibers at 0.25Hz, than for 3 minutes the stimulus is shut down, after that there is another 0.25Hz stimulation, followed by 2Hz stimulation for other 3 minutes, and eventually the last 0.25Hz stimulation for 6 minutes. Thus, the first entry by the user is the last 0.25Hz discharge before the pause, the second one is the first discharge after the pause, the third one the last discharge before the 2Hz stimulation and eventually the asymptotic recovery of the last 0.25Hz stimulation. In such a way, parameters such as the the latency changes in percentage after the 0Hz, the 0.25Hz and 2Hz stimulation are shown. Furthermore, the recovery after 30 seconds of the 2Hz stimulation and the 50% recovery are displayed, as well as the conduction velocity of the fiber and the possible fiber type. These data can be also saved on a Excel data-sheet and used afterwards for statistical analysis.

3.9.5 LabChart recordings

SPiike is also able to analyze LabChart recordings, indeed the analysis module has been properly designed to import -among others- this type of file format. LabChart records free-running signals, therefore signal conditioning is needed. Once the LabChart archive is properly processed, it can be imported to SPiike. SPiike will then perform all the steps to automatically visualize the original recording, plotting the same graphs as QTrac (an already available software that can be easily found in the market). For the extraction of information from the raster plot of an analysis performed on human patients' recordings, as inclusion criteria two thresholds -low

and high- have been applied. This allow the software to pick as action potentials all the spikes that lay within the two thresholds. The low threshold spanned within 2-3 times the standard deviation (5-7.5uV) of the filtered signal. The standard deviation has been evaluated during the baseline stimulation at 0,25 Hz. The low threshold is used to prevent the collection of false positives coming from the noise, which usually accounts for a 2.5uV. [Lew98] The high threshold has been fixed to 50uV to avoid picking spikes due to other neural activities, such as muscular discharges, having that a C-fibers signal does not exceed 30-50uV [Val18]. To avoid over-counting the number of spikes due to the action potential tails that might exceed the low threshold an additional criterion has been used alongside the time domain. A window of 2,49ms width has been exploited, within which only one spike can lie (the maximum spike width is lower than 2,49ms [Ser+99]).

3.9.6 Fibers activity

Upon constant electrical stimulation the fibers discharge just once a sweep. However, when the frequency is changed or natural stimuli are applied, the C-fibers undergo to a transitional state in which more than an action potential is delivered. In this analysis, the response of the patient to these natural stimuli ("marking" technique) and his background neural activity has been evaluated. The SPIike tool looks at the network level instead of the fiber level, grouping all the discharging neurons together. Indeed, the stimulation of several receptive fields produces discharges of the peripheral neural network that are perceived by the patient as pain.

3.9.7 Instantaneous firing rate (IFR)

The instantaneous firing rate is evaluated considering the inter-spike interval within two action potentials. Since at the synaptic level the temporal and spatial summation play an important role in the pain perception experienced by the subject, this is a quantitative way to define the amount of pain reaching the central nervous system. The IFR is calculated by the inverse of $t_2 - t_1$, where t is the time at which an action potential occurs.

3.10 Coding

The coding is the part in which the design and all the other requirements analyzed before take form. M language is pretty similar to other programming languages such as C and C++ language. Therefore, with basic programming skills M language can be learned pretty fast. It is a good practice in big projects like this one to code

in a modular way, namely to generate a script for every basic task the software is suppose to implement. Afterwards, all the modules are put together for the creation of the final product. However, to have more security against hacking and to keep the modularity it is good to use a object-oriented programming. Namely in a script all the data and functions of an object are defined and in another script all the functions are implemented. These functions are used to get access to the data stored in the object and also to do several operations on them. Figure 3.17 shows how it works. Namely a generic class prototype is created. In this specific case there are three private variables (i.e. manufacturer, operating_system, cost), one public variable (i.e. model), a constructor and a method. The private ones can be accessed and manipulated only by the methods within the class, the public ones instead even directly from the outside. In this example when the object is generated the constructor is called automatically and all the input variables (i.e. man, o, m and c) are used to assign the proper value to the variables of the class. Afterwards once the object is generated (e.g. the iPhone) the only way to change the private variables is to use methods that can change their values. In this case a getModel() method is implemented in such a way that from an external script the variable model can be displayed. However, this is a public variable so without this function the model can be changed and displayed as well, however the other variables needs a method to do so.

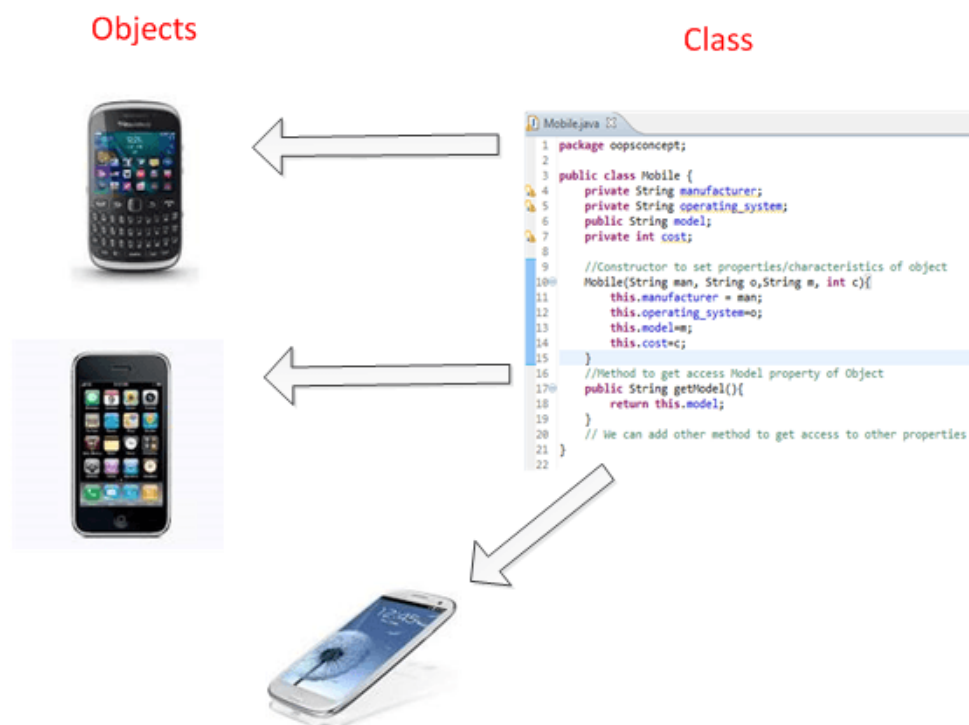


Fig. 3.17: Object-oriented programming. [Oop]

The OOP is very useful for creating a modular subdivision of the code, helping the developer to find bugs and errors during testing. Furthermore, since to have a direct

access to stored values within a variable is sometimes difficult or even impossible and the public variables are not directly stored in the main script hack attempts are deterred. In programming languages such as C++ the OOP is easy since linkers can be used to get access to the same object from different scripts. However, in Matlab is a little bit more tricky since linker are not implemented, however passing the object from one script to the other can solve the problem. However, C++ has not been used since for GUI purposes as well as for the interaction with a DAQ system and for visualization capabilities Matlab is a very powerful environment.

3.11 Testing

Once the software has been written it has to be tested. This is an iterative process, it starts after that the first line of code has been written. However not every single line is checked instantaneously, for speeding up the process several line of code or even functions must be written before starting the testing process. It is worth pointing out that there are two different type of errors, a syntax and a logic error. The first one can be checked with more frequency since it only needs the running of the compiler. The compiler will check the code and make some operations on it for the its conversion into a machine language, as described before (sec. 3.5.2). During all these steps some errors can come out. When this happens the compiler stops the compilation process and displays in the command window of the IDE the type of error and at which line it can be found. This can be solved by eye, and most of the time it is just a missing coma or parenthesis, a prohibited operations between data or even a misspelled word. These are the easiest errors to find since the command window is telling you at which line the error is found. It is worth noting that the error is not always localized exactly at the indicated line, sometimes it can be some lines before or after. However, in general it is located near the marked error line. Then once the syntax errors are solved the compiler can resolve the code and generates a machine code that is used for running the software. However, even if the software can be run it does not mean that it also work properly. For instance you can write a code for making a sum operation and once the software is run and you give as input $2 + 2$ it outputs 6. The result is wrong because there are some errors in the algorithm that do not allow the software to work properly. To solve the problem, most of the time the developer can use a breakpoint and run the code line by line. A breakpoint is just a mark that tell the compiler to stop compiling at that point giving to the developer the possibility of following the compilation line by line. He can thus check the data in order to assess the right functionality of the software. However, at which line a breakpoint must be put then? It depends on the error, if we know that a sum operations is not working properly we must check for a line that is making that operation. Sometimes is easy to find it, sometimes it is very

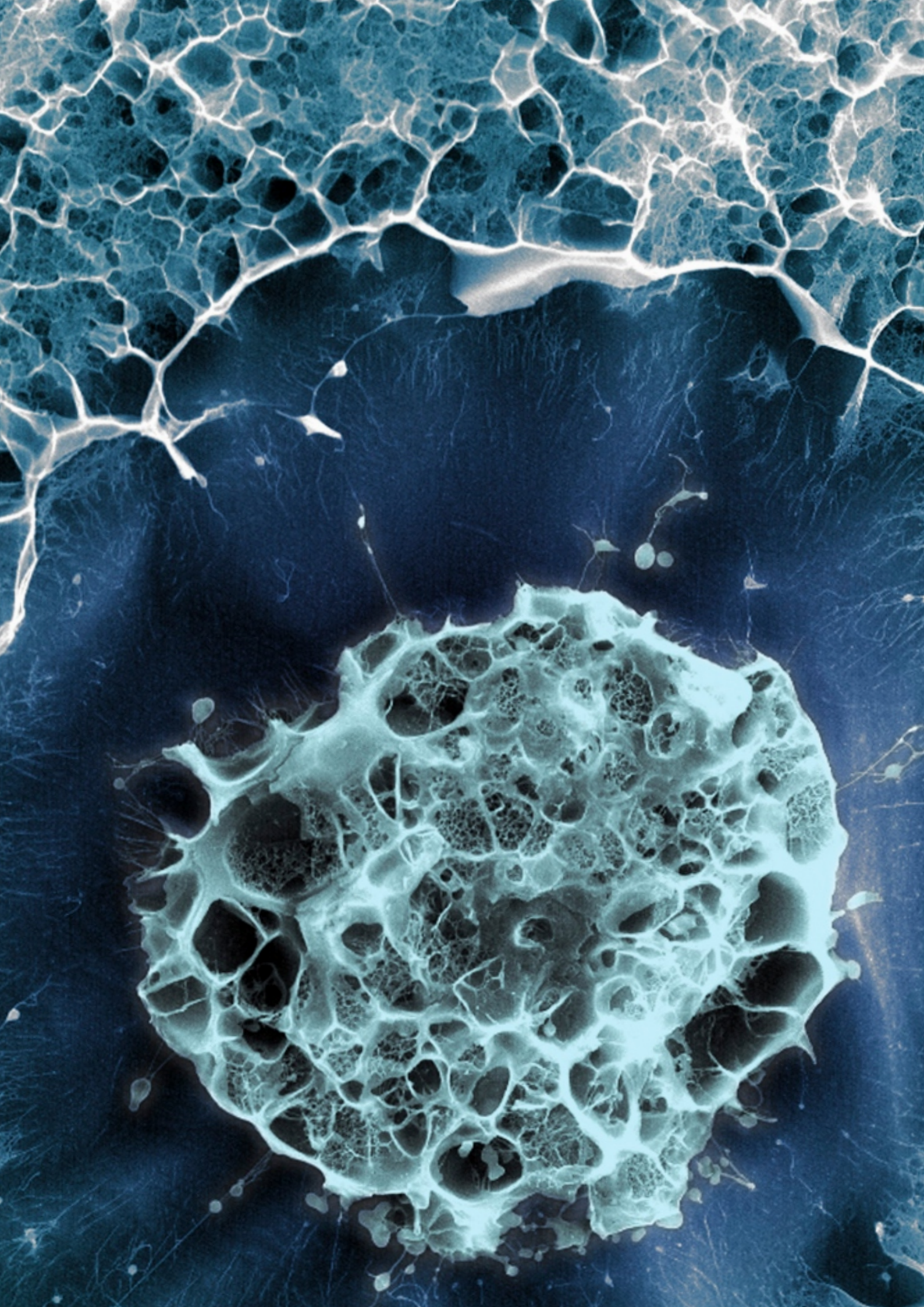
challenging. Basically a breakpoint can be put even near the guessed line error and more than one breakpoint can be used. However, when the code is kind of small the error can be found easily, the problem is when the software starts to become bigger and several functions are added to the software. This is way in big projects the modular coding is preferred, but still sometimes is very tricky to find errors, even if the code is well written. The intrinsic problem is that in big projects a data variable can be accessed from different functions and changed in different line of the code. Sometimes is just a small error but to find it several lines and functions must be checked, and once the problem is solved other logic error can comes out. As rule of thumbs the analysis and design phase must be used to keep the project as simple as possible in a way that logic problems can be found and solved easily. Actually not only $2+2$ can be wrong but also $2+3$ while $3+4$ be alright, therefore sometimes a string of characters or number are used as input to check the functionality. Once all the logic issues are fixed and the outcomes are in congruence with the estimated output the function can be considered as bug-free.

3.12 Operations and maintenance

As mentioned before some inputs are used to check the functionality of the software. However, only a subset of the whole possible inputs can be used during testing otherwise the time needed for coding would take ages. Therefore sometimes even if the algorithm works properly with the subset of inputs used by the developer it can happen that during the use by the users some bugs will pop up. For this reason the software must be checked through time and updates must be released. Some updates fix bugs or security problems within the software. A bug is an error in the algorithm that generates wrong outcomes, and sometimes they can even interact with other functions bringing the software to crash. The name is due to the first computer ever made, that was analogical and there was literally a trapped insect in the gears of the machine bringing the system to stop working properly. This happens in 1945, after that the computer technology evolved and now is everything digital but the name is still used for errors in software technology. That is why the first releases are generally beta version of the software, meaning that bugs can be found and the users are highly recommended to report those to the developers in order that the error can be fixed and a stable version of the software can be released. Furthermore, updates not only fix bugs but they can also add new functionality or even eliminate some functions that are no longer considered important for the use of the software. Therefore the communication between users and developers is very crucial for the stability of the system and a feedback can help the developers to understand what is missing in the software and what is redundant.

3.13 Discoveries

Once the software is ready it can be given to the scientific community for research purposes and the outcomes can be used for helping researcher to solve problems linked to the peripheral nervous system. As mentioned before Spiike software not only can be used for stimulating slow conducting fibers such as (*C fibers*) but also (*A δ fibers*) that is a new unexplored world in terms of microneurography. Therefore experiments that were impossible before become nowadays a new front line in the neuroscience research. New discoveries will follow give to the patients cutting edges drugs that can relief pain and mitigated other diseases concerning the peripheral nervous system.



Stem cell

[<http://www.nature.com/news/2016-in-pictures-the-best-science-images-of-the-year-1.21156>]

Results

“Your brain - every brain - is a work in progress. It is 'plastic.' From the day we're born to the day we die, it continuously revises and remodels, improving or slowly declining, as a function of how we use it.

— Michael Merzenich

SPiike software has been developed with the aim of enhancing the knowledge of the peripheral nervous system. In the past huge progresses in this field has been made, however the whole picture of this complex system is not clear yet. In this chapter the functionalities and potentialities of the SPiike software are revealed and some interesting results are shown.

4.1 SPiike software

Software packages able to process the neuronal traffic of peripheral nervous system need to be implemented. This has been done considering all the tasks separately: a tool able to record and stimulate fibers of interest, a tool able to analyze the acquired data.

4.1.1 Graphical user interface

The developed tool SPiike (Figure 4.1) is provided with a Graphical User Interface (GUI). In such a way, all the tedious steps necessary in the past to properly set up all

the recording parameters can be easily accessed by means of a toolbar and a menu bar.

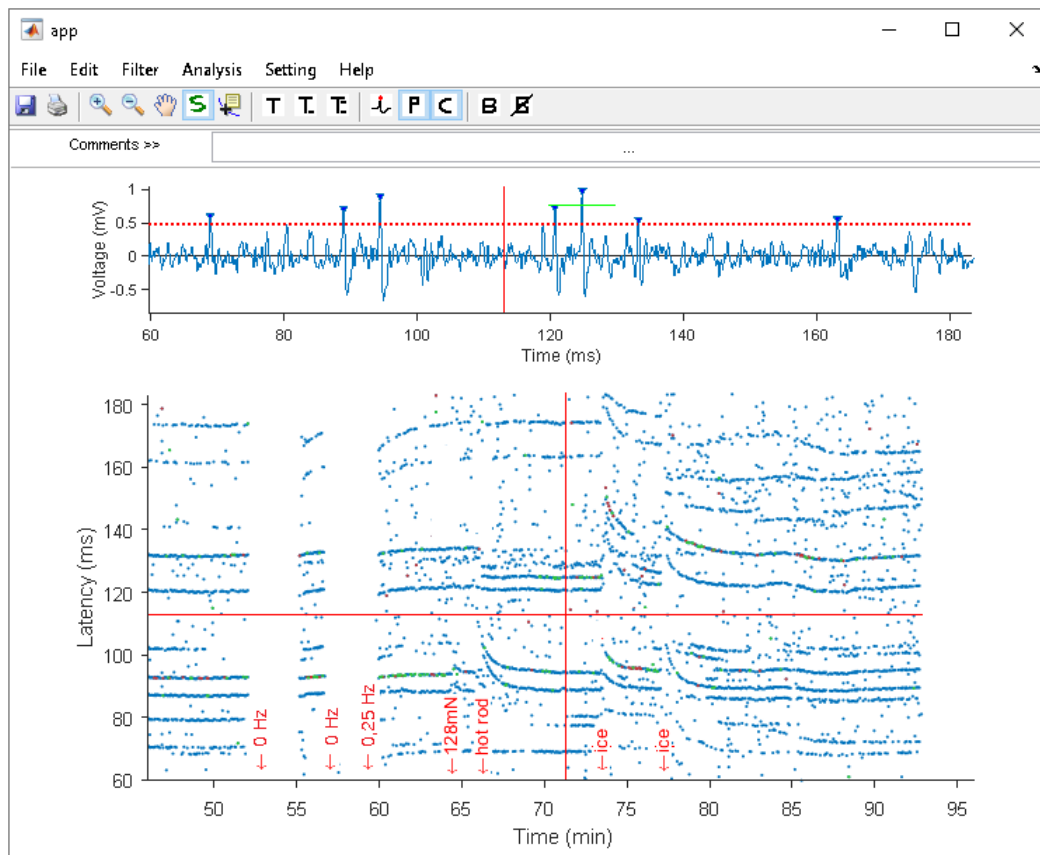


Fig. 4.1: SPiike software analysis module - Graphical User Interface (GUI). On the top, a graph showing the filtered data recorded by the recording electrode. On the bottom, the raster plot of the fibers under investigation, 9 fibers are shown on it and the marking technique has been applied. After 128mN, hot rod and ice application an exponential decay of some fiber latency can be noticed, meaning that the fibers reacted to the stimulation.

Furthermore, shortcuts (hot keys) and prompt commands have been implemented. The users can exploit these features to speed up the recording. Moreover, navigating through the menu bar, usual tabs (i.e. file, edit, etc.) can be found. Hence, even basic functions (e.g. saving data, editing plots, zooming in and out, and closing windows, etc.) are available. It is worth pointing out that additional tabs are the added value of this software. These tabs contain useful features that can be exploited during stimulation as well recording. Cutting edge algorithms have been used for reliable and fast results. The raw data is saved in the hard disk drive and the software can open LabChart recordings (for validation purposes and analysis of human subjects) as well as archives generated by the developed recording module. A filter is applied to the raw data in order to filter out unwanted information, such as background noise and spurious discharges. This band-pass filter is a Butterworth filter, and it can

be tuned changing the cutoff frequencies and its order. If required, the filter can be cut off in order to display the raw data. Another cutting-edge filter (wavelet-based [WGB08]) has been implemented as well. It is worth pointing out that the developed software is based on the Matlab IDE (Integrated development environment), and it can work within this platform or independently in its stand-alone version. Important neuronal parameters can be extracted from the raster plot. For instance, the fiber subclass can be easily figured out considering their activity-dependent slowing (ADS) [Ser+99] and using the marking technique as shown in figure 4.1 and explained in the last chapter (sec. 3.8.2).

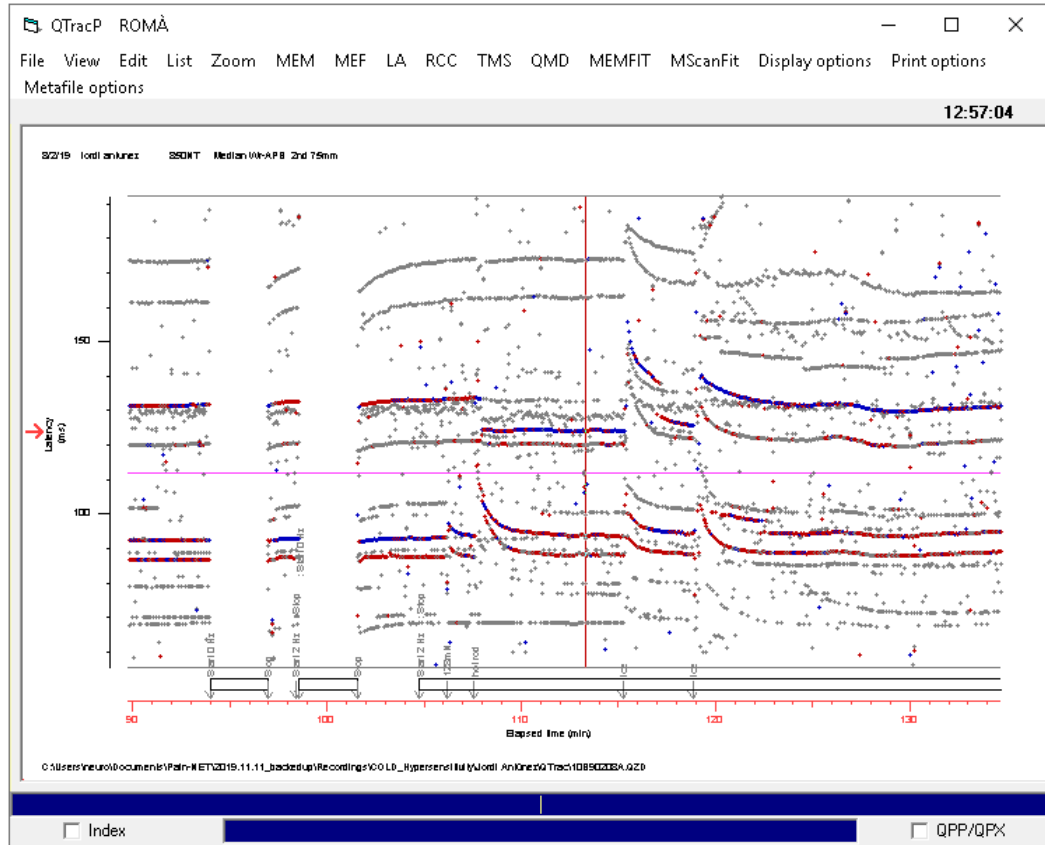


Fig. 4.2: QTrac software, with the same pattern discharge of the SPiike software (figure 4.1)

4.1.2 Standalone application

SPiike software has been designed in such a way that it will be given to the community in its standalone version. This means that it can be installed in the personal computer without the need of using neither the code written in Matlab nor to have an expertise in programming languages. The only requirement is to have a powerful computer, as explained in the previous chapter (sec. 3.6) and to have enough space in the hard disk drive (almost 1Gb, approximately 800Mb for the Matlab runtime

and less than 10Mb for the SPiike software). During the installation (figure 4.3) if not downloaded yet a Matlab runtime must be downloaded and installed. However, this is free of charge and none license need to be bought.

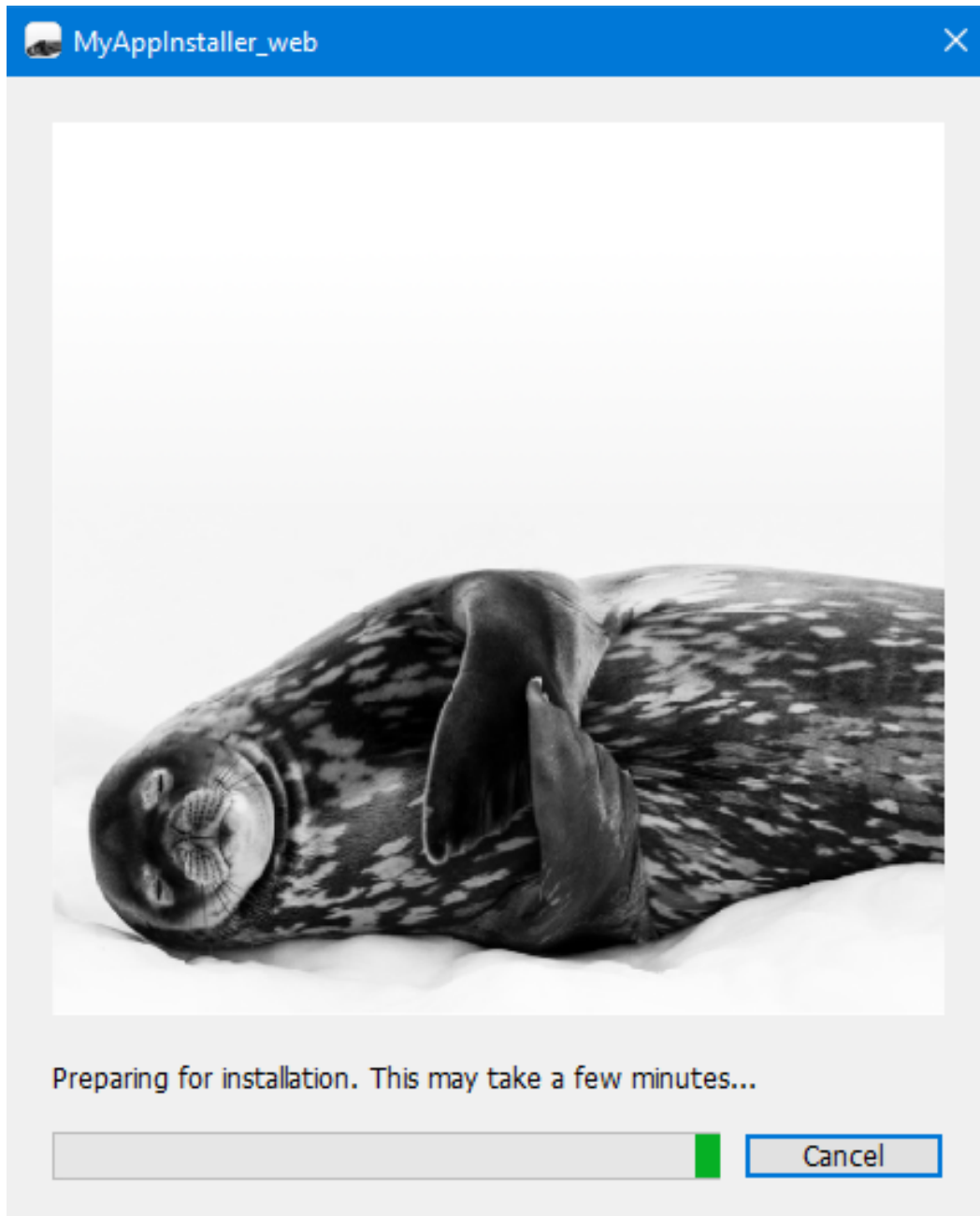


Fig. 4.3: Installation of the standalone SPiike software

Once the software has been installed in the device it can be opened as a normal program and all the GUIs and functionality explained in this chapter can be used.

4.1.3 Comparison with another software

SPiike software has been developed with the same basic functions of another software that can be purchased in the market, the Qtrac software. However, additional functions have been added to SPiike. As shown in figure 4.1, the SPiike software resembles the behavior of the QTrac software (figure 4.2). For this comparison the LabChart archive of a recording performed in a human patient and recorded simultaneously with QTrac has been imported into SPiike.

Therefore, the recording and analysis of slow conducting fibers such as (*C fibers*) can be done through the SPiike software in the same way it has been done in the past, however faster fibers (e.g. *A δ fibers*) can be now characterized as well.

4.2 SPiike, recording module

The recording module of SPiike software allows the users to stimulate peripheral nervous fibers and to record their neural discharges. In the following section a brief description of its capability will be described.

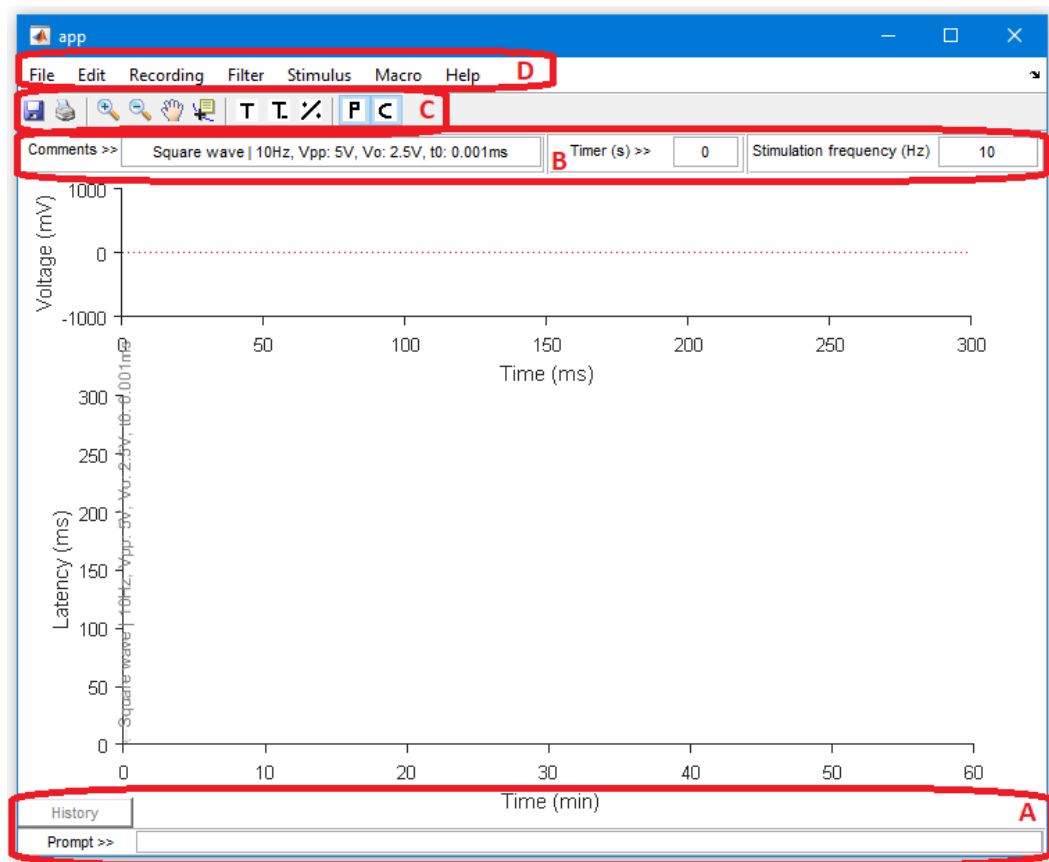


Fig. 4.4: Graphical user interface of SPiike recording module.

4.2.1 Menu and toolbar - SPiike recording module

The graphical use interface of the SPiike recording module is depicted in figure 4.4. It resembles that of the analysis module (figure 4.1) but with some differences. It is composed by a prompt command (box A) that can be used to stimulate, record and change some settings without navigating through the menu and toolbar. It also allows the user to check commands previous inserted by means of the history button. Moreover, in the upper part (box B) some comments can be added to the raster plot simple writing down the wanted comments and hitting the enter key, moreover when the stimulus is changed in there information about the waveform are displayed and a comment with this information is inserted in the raster plot. On it a clock is also showed that is useful when a protocol is used. A protocol indeed allows the user to automatize some recording steps such as ADS and recovery cycle stimulation. On the right the stimulation frequency is shown and it can also be changed writing the frequency of interest. Box C shows the toolbar. It is composed by the following icons: Save as, Print preview, Zoom in, Zoom out, Pan, Data cursor, Raster parameters, Threshold position, Latency change, Peaks location, Comments displayed. The data cursor option can be used to check in the graph the X and Y position of the displayed data thus the exact punctual value in the raster plot can be extract without the need of zooming in on that point. The raster parameters icon is used to change the dots size and their colors in the raster plot, as shown in figure 4.6.

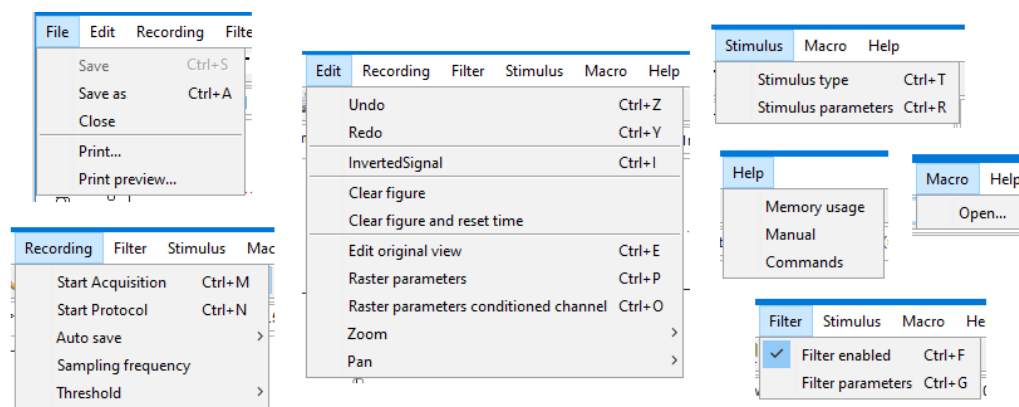


Fig. 4.5: Tabs of the menu bar.

The threshold position option is instead used for changing the position of the low and high thresholds in the filtered plot and the number of points to display per sweep in the raster plot. The latency change icon can be used for a quick analysis of the fibers under investigation giving as output the latency change from the fiber baseline in percentage. The peaks location option if it is selected shows what the algorithm is picking as action potential and if there are a lot of action potential it can be turned off for improving the signal visualization. The last icon, namely the

comment displayed option, allows to shown and hide the comments in the raster plot. Sometimes they can make the visualization a bit messy so this option is very useful in all these cases. Lastly, the box D of figure 4.5 shows the content of the menu tabs. Starting from the beginning the File tab includes the following options: Save, Save as, Close, Print and Print preview. The print option allows the user to print what it is shown on the graphical user interface at that moment. It can be done through a printer as well as the image can be saved as PDF document. The save as option is used when the archive has not been saved yet and it can be used for saving the recording, making it available for the SPiike analysis module. The Edit tab is instead useful for improving the visualization of the filtered plot and the raster plot. It is composed by the Undo and Redo options for going back to a previous visualization setting or for going forward once the undo option has been hit. The inverted signal button allows to invert the filtered signal, if the polarity of the neural signal is not correct as well as when the recording is meant for the stimulation of A δ fibers instead of C fibers, since they have a different polarity.

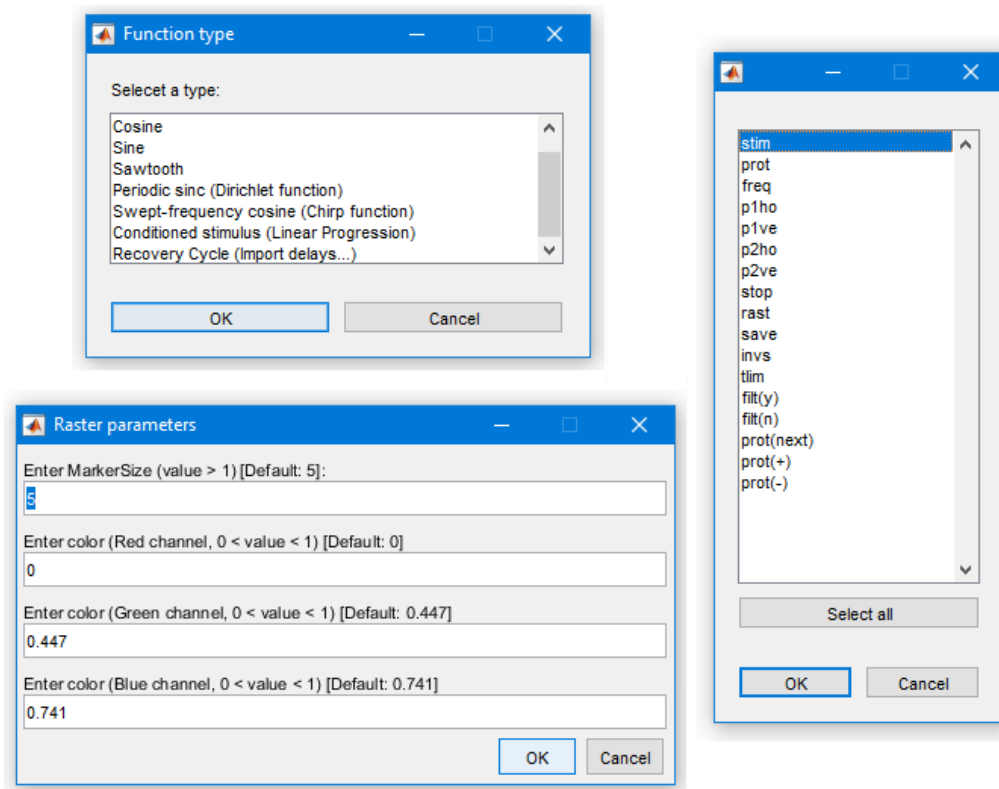


Fig. 4.6: Setting of some menu bar options.

The clear figure option is instead used to clear the raster plot, indeed sometimes when SPiike has been recording for a lot of time due to the high number of data processed the performance of the software can decrease. This is then useful for clearing the dots shown in the raster plot without affecting in any case the archive

that will be saved for analysis purposes. Furthermore, the clear figure option can be called along with the reset time option, indeed the former does not reset the elapsed time and the next sweep will be displayed at the same elapsed time, however sometimes this is not required. The Edit original view option allows the user to set the X and Y axis intervals once a double click is used on a plot. This can be done in the filtered plot as well as in the raster plot. The raster parameters is meant to change the dot size as well as their color, as shown in figure 4.6. The following one, the raster parameters conditioned channel is instead used for changing the visualization of the conditioned channel in the raster plot when the recovery cycle protocol is called. Indeed, as a reminder, the recovery cycle uses a conditioned and a unconditioned stimulus for the stimulation of the neural fibers, thus the fibers react twice during this stimulus being a sort of double stimulation. This is why two channels are shown on the raster plot. Lastly, the Zoom and Pan options allow the user to change the function of the zoom in, zoom out and pan into a unconstrained, horizontal or vertical mode.

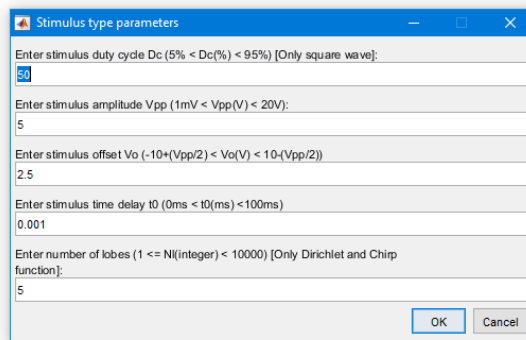


Fig. 4.7: Stimulus type parameters.

The recording tab includes instead the Start acquisition option for starting the stimulation and acquisition of the neural signal. Followed by the start protocol option that is used to read an external excel file for the automatization of the stimulation such as the ADS protocol. Nevertheless the excel file can be edited thus other protocols with different stimulation frequency can be used as well, this is pretty useful if other fiber types need to be stimulated such as $A\delta$ fibers. The auto save button can be used for setting the time after which the software is automatically saving the data and to disable this function if not needed. It is worth pointing out that this function allows the creation of a backup after a certain elapsed time and it can be used to recover hours of experiment if the app crashes. However, in order to avoid charging the software with a lot of tasks is a good practice to leave the setting of the auto saving option as default, namely 5 minutes. Furthermore, also the sampling frequency can be changed however as explained before it is recommended to keep it a 40kS/s. It can be decreased if the computational system does not cope

with the high amount of data to be stored, such as old personal computers. Or, it can be increased if a different type of experiment is designed. It can be lowered down to 10kS/s and increased up to 100Ks/s. Then, the threshold option is used to change the location of the thresholds in the raster plot and the number of dots per sweep that must be displayed in the raster plot, in the same way of the toolbar icon.

The following tab allows the setting of the filter and its activation. In here the usual Butterworth filter can be evoked with its parameters (filter order, low cut-off and high cut-off frequency). Default values for this filter are a third filter order, 300Hz for the low cut-off filter and 2kHz for the high cut-off filter. Furthermore a cutting edge filter has been added as well, a wavelet-based filter that should improved the filtering of the data. This is a beta option, thus the Butterworth filter is preferred for more reliable results but in all those case in which it does not work the wavelet-based filter can be used. The stimulus option is composed by a button that allows the selection of the stimulus type, as shown in figure 4.6. A square wave, cosine, sine, sawtooth, dirichlet or a chirp function can be selected as stimulus waveform as well as a linear progression of a conditioned stimulus and the usual recovery cycle through the importing of the delays from an external editable excel file. Moreover the stimulus parameters option as shown in figure 4.7 allows the setting of the stimulus duty cycle (i.e. Dc; only available for the square waveform), the stimulus amplitude peak-to-peak (i.e. Vpp), the stimulus offset (Vo), the stimulus delay starting from the onset of the sweep (i.e. t0) and the number of the lobes when the Dirichlet and the Chirp functions are selected. Moreover, since during the experiment some commands are used to speed up the recording and they can be retrieved through the history button, they can be saved into a text file and recalled thorough the Macro tab. This is pretty useful if several trials should follow the same recording procedure.

Lastly, the Help tab can be used for checking the memory usage and take some actions as troubleshooting when the memory is saturated such as clearing the raster plot or killing some background program that are saturating the RAM of the personal computer. Also the manual can be recalled through this option and a list of commands that can be inserted in the prompt command and written in the excel file can be displayed. As shown in figure 4.6, this commands are the following: stim for starting the stimulation, prot for the opening of the protocol document, freq for changing the stimulation frequency, p1ho for editing the original view of the filtered plot along the X-axis, likewise the p1ve for the Y-axis of the filtered plot, p2ho for the X-axis of the raster plot and p2ve for the Y-axis of the raster plot, stop is used for stopping the recording, raster for changing the raster parameters, save for saving the recording, invs for inverting the filtered signal, tlim for the filter plot thresholds, filt(y) for enabling the filter, filt(n) for disabling the filter, prot(next) to skip a line in the excel file of the protocol, prot(+) to add more time in one step of the protocol and prot(-) to subtract a certain time to the protocol.

4.2.2 Basic recording technique - *C fibers*

The usual recording is done stimulating the paw of the animal and recording the neural signal from its sciatic nerve, as described in the section 3.3. This allows the researcher to assess the healthiness of the fibers that are being stimulated as well as their type. SPiike software is able to stimulate this type of fibers since the stimulation frequency spans from 0Hz to 1000Hz, with possible frequency changes down to 0.01 Hz. The filter moreover can be set to clean the noisy data and allow the perfect visualization of C fibers action potentials. The filtered signal threshold can be then lowered or increased to improve the visualization of these fibers in the raster plot.

4.2.3 Improved recording technique - *A δ fibers* insights

However, *A δ fibers* can be now stimulated as well. For this recording a innovated recording technique has been implemented. The drawback at that time was that only mice were available thus to increase the distance between stimulating and recording electrode a new technique has been used. The usual recording done through the sciatic nerve of the rat has been replaced by a tail recording to improve the distance between the two electrodes. Furthermore, the recording electrode has been inserted directly in the cauda equina of the mouse to avoid the effects of second order neurons, otherwise a recording directly from the medulla would have shown such effects (e.g. wind-up).

4.2.4 ADS stimulation of C-fibers

As shown in figure 4.8 four types of C-fibers have been characterized so far, through the ADS stimulation. ADS works letting the fibers to recover for 3 minutes with no stimulation at all, afterwards a 3 (or 6) minutes stimulation at 0.25Hz is applied, followed by 3 minutes at 2Hz and another 6 minutes at 0.25Hz. In such a way the fibers can be characterized. SPiike software can read an excel file containing all these time of stimulation and frequencies. This is useful for C-fibers characterization as well as *A δ -fibers* since the time and the frequency of stimulation can be set as a wish through the excel spreadsheet.

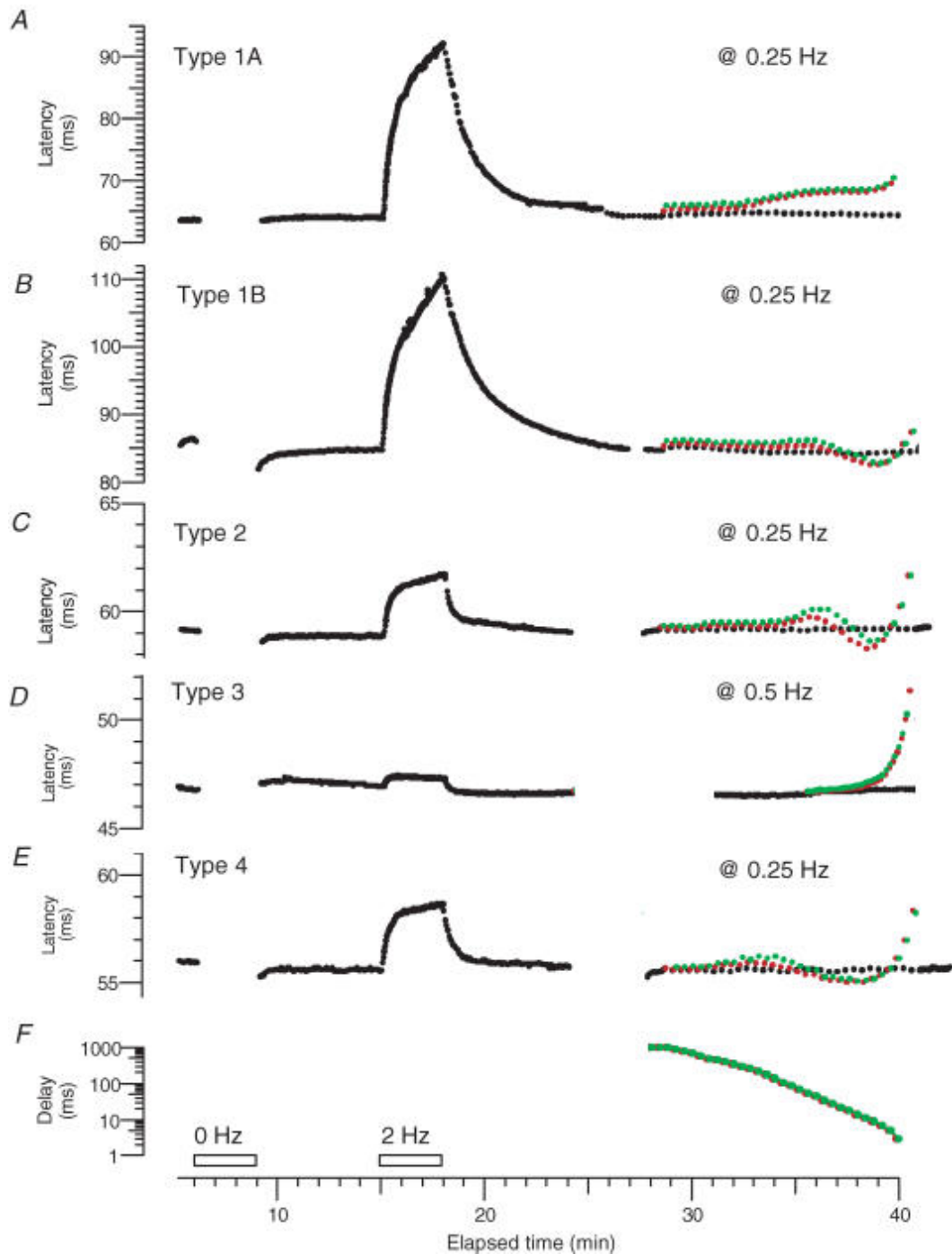


Fig. 4.8: Activity-dependent slowing of C fibers innervating rat skin [Geo+07]. The figure shows the activity-dependent slowing of C fibers innervating rat skin. This is also used as a comparison for the figure 4.9 in which faster fibers ($A\delta$ -fibers) have got the same ADS behavior, meaning that with SPiike software faster fibers can be recorded and analyzed as well.

4.2.5 ADS stimulation of A δ -fibers

Spiike as described before can then stimulate A δ -fibers as well. Initial trials have been already done and they showed promising results, such as an ADS behavior of A δ -fibers, comparable with that of C-fibers. Unluckily the sample size is quite small thus in order to have a statistical significance these outcomes should be checked through control groups and more trials. These results once verified may lead to improvements of our knowledge on peripheral nervous system properties.

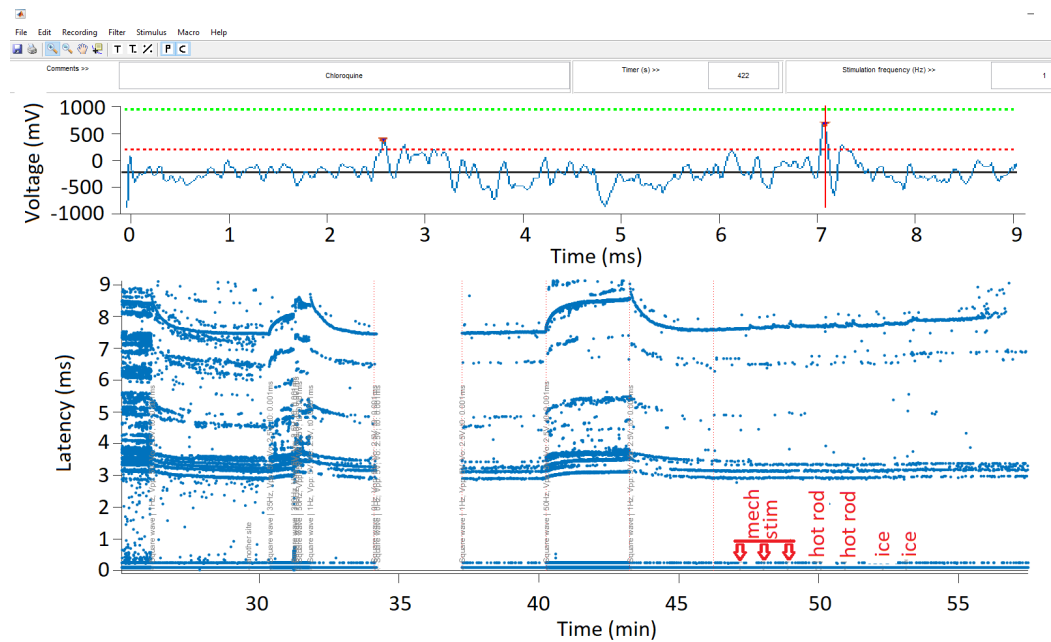


Fig. 4.9: Adelta fibers showing an activity-dependent slowing such as C fibers. In the raster plot, on top at a latency of 8ms an A δ -fiber shows activity-dependent slowing and a response to different stimuli (mechanical stimulation, hot rod and ice application). On the bottom, other A δ -fibers do not respond to the marking stimulation however they have got an ADS with his characteristic exponential decay slowing.

Figure 4.9 shows one of the recordings performed in a wild-type mouse. Baseline stimulation frequency has been kept at 1Hz. In order to assess the effect generated by higher frequency to A δ -fibers the same frequency has been pushed to 50Hz for 3 minutes. The horizontal lines represent the discharge of A δ -fibers. Indeed, being those discharges in a range between 3 and 9ms, and considering about 10cm between stimulating and recording electrodes the conduction velocity is about 11 - 33m/s, namely A δ fibers. They show an activity-dependent slowing like that of C fibers (figure 4.8). An exponential decay in the conduction velocity can be easily seen between minutes 40 and 45 of the elapsed time.

4.2.6 Marking technique of C-fibers and A δ -fibers

The marking technique can be applied with the SPiike software, in fact this does not require a software implementation since natural stimuli are applied externally through ice, hot rods and forceps. The only implementation needed for the use of this technique is the possibility of adding comments to the raster plot. In this case the reaction of the fibers following the marking stimulation can be assessed. Indeed sometimes spurious discharges due to noise or other factors such as ectopic activity or a too low temperature of the skin can arise, so during analysis is important to know what made the fiber to discharge. Comments can be easily added through the SPiike command window. Figure 4.9 is an example of a marking technique applied on A δ -fibers. The fiber at a latency of 8ms reacts to the mechanical stimulation, hot rod and ice application suggesting that this might be a polymodal A δ fiber. Other fibers at latencies of about 3 and 4 ms have an activity-dependent slowing but they do not respond to the markings, meaning that either they might be silent A δ nociceptors or the stimuli did not hit the receptive field of those fibers.

4.2.7 Recovery cycle of C-fibers

The recovery cycle has been implemented in the SPiike software, therefore this stimulation protocol can be used for assessing the functionality and healthiness of the fibers under investigation. SPiike can read a excel file in which all the interstimulus intervals are stored. Hence this gives to the users some flexibility. Indeed, they can change the interstimulus intervals for skipping some values and speed up the recovery cycle protocol. If other fibers or protocols must be tested the values can be changed to suit best the needs of every experiment. For instance, the recovery cycle of A δ -fibers has not been generated yet but it can be included in the future. This would need a lot of trials since due to their conduction velocity the behavior of A δ -fibers may have a different recovery cycle than those of C fibers. In fact within slower fibers, every C-nociceptor type and sub-population has got its own recovery cycle pattern, as shown in figure 4.8. Therefore, A δ -fibers will most likely have different behaviors according to their type.

4.3 Spiike, analysis module

Additional functions not available in the QTrac software have been successfully implemented in the SPiike tool. Among them, the users can now select a specific fiber to perform spike sorting and fiber classification. Another feature is the possibility

of selecting the sweeps to analyze and the generation of additional plots in which spike extraction and counting are performed.

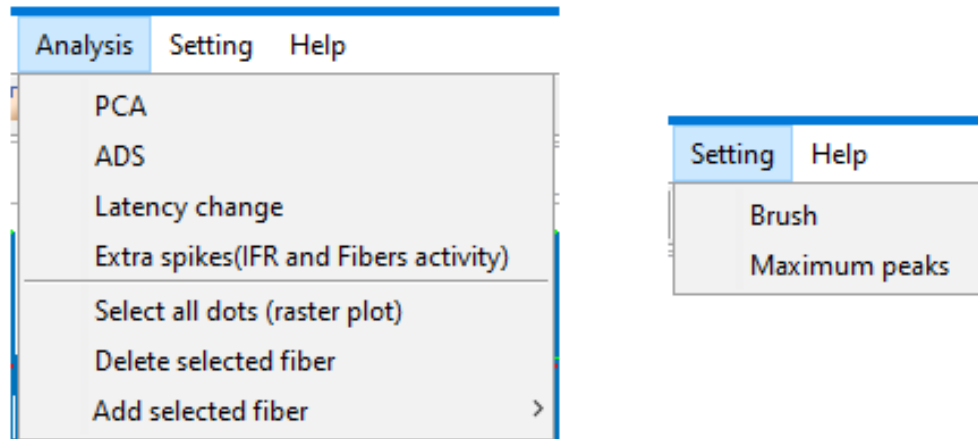


Fig. 4.10: Analysis module menubar differences

4.3.1 Menu and toolbar - SPiike Analysis module

The menu and toolbar of the SPiike analysis module are pretty similar to those of the recording module, as shown in figure 4.1. However, some differences exist.

The toolbar is composed by some of the recording module tools such as a save as, print, zoom in, zoom out, pan, data cursor icons as well as the options for changing the thresholds of the filtered data, the button to show/hide comments and the peaks location however others have been implemented. Among them, the option to change the sweep displayed in the filtered plot, by hitting the raster plot in the point in which the sweep must be shown. Once it is selected a cross-like pointer is displayed in the raster plot and by using the arrow it can be changed. The horizontal line of this pointer in the raster plot is converted into a vertical line in the filtered data and it is used as a pointer for checking the peak of the fiber under analysis. The vertical line of the cross-like pointer is instead used to point to the sweep that is shown in the filtered data and it can be changed to the previous nearest one by using the left arrow or the next nearest sweep by using the right arrow. Furthermore, an option to hide the dots in the raster plot and show only the brushed dots (the selected ones) has been implemented as well. Lastly an option to brush (select) the wanted dots, used for the PCA algorithm, is shown on this toolbar and also the tool for clearing this selection allowing the user to highlight other dots.

Regarding the menu, it lacks of the recording and the stimulus tabs since this module cannot stimulate the fibers of interest but it is only used for analysis purposes.

Quite the opposite, it is provided with analysis and setting tabs as shown in figure 4.10 and the Edit tab has been expanded. Indeed it is worth pointing out that sometimes the fibers can have some jumps in the recordings due to a poor insertion of the stimulating electrode in the skin and to changes in the electric field by external factors. This forces different branches of the same nociceptor free ending to start discharging. Since their lengths, even within the same nociceptor, are slightly different the latency is affected since the action potential needs to travel a shorter or longer distance. Therefore during the analysis this must take into account and sometimes corrected to avoid wrong results. The Edit tab of the analysis module allows to change the position of the selected dots in order to cope with this problem.

The analysis tab instead is composed by a PCA option that allows to invoke the principal components analysis algorithm for spike sorting and fiber classification. A ADS option that can be used for fiber classification by means of the ADS behavior. When this is selected the software is asking to hit 5 points in the raster plot that allow the software to evaluate the latency change following changes in the stimulation frequency. The 5 points are respectively: last peak before 0Hz, first peak after 0Hz, last peak of 0.25Hz, last peak after 2Hz, asymptotic baseline after 2Hz. This is meant to be used for C fibers classification, that is why these values of stimulation frequency, however it can also be used for other fiber analysis taking into account that other frequencies may be used. The following option, namely the latency change entry, is used to make a quick evaluate of two points and the extra spikes option is meant to evaluate the instantaneous firing rate and the fiber activity. Additional options are provided as well such as the selection of the all dots in the raster plot without the need of selecting them and the possibility of adding the selected fiber to a excel file (first column: X axis; second column: Y axis). In this way the fiber of interest can be extract from the software and plotted without the background noise. Moreover in the menu has been implemented a setting tab to change the way the brush tool is selecting the dots (i.e. brush option) and the minimum latency at which the peaks algorithm starts scanning each sweep to look for maxima. This is useful for eliminating the spurious signal coming from the stimulus artifact. The brush option instead allows the user to select the dots in a arbitrary shape or with a rectangular box. All the other tabs are basically the same as the SPIike recording module with the addition of the open and import option in the file tab for the opening of the saved recordings and the Labchart recordings.

Moreover, once the PCA option in the analysis tab is selected another GUI is displayed, as shown in figure 4.12. From here Spiike software is computing the PCA and the K-means algorithm is applied on this. This is well explained in the following section (sec. 4.3.2). However, sometimes this algorithm does not work properly, for instance when the clusters are too much superimposed or the cluster are in a circular

disposition. Thus other clustering algorithm has been added in the final version of the SPIke software. The DBSCAN clustering algorithm [Clu] is one of them and it works well for circular clusters, thus in all the cases in which the K-means algorithm has some difficulties. Also the EM [Clu] and wavelet clustering algorithm [SCZ00] have been added and they can be selected once the other two are unable to provide satisfactory results. Furthermore, sometimes by eye the clusters are well defined but for some reasons the algorithms cannot differentiate well enough the clusters, this is why also a manual selection of the cluster has been added, both in the PCA space and in the raster plot space. In the latter case, if the fiber is well characterized and it is pretty clear that the dots shown in the raster plot belong to the same fiber, the fiber can be selected in the raster plot space and the algorithm is showing the points in the PCA space that belong to this fiber. Thus also the functionality of the PCA algorithm can be checked since if the discharges are of the same fiber in the PCA space the highlighted points must belong to the same cluster. Another useful tool is the possibility to eliminate the outliers from the PCA space. Indeed sometimes spurious discharges are shown on it and the real waveform can be obscured by this noise.

4.3.2 Spike sorting and fiber classification – C-fibers of a mouse recording

Figure 4.11 shows a plot with the filtered data and a raster plot, the same as figure 4.1, but with a selected fiber on it (the one that is red highlighted). On top, the modified data plot shows the recorded signal already filtered out and on it a threshold (red line) can be found at a high of 10mV. The recording module uses this threshold to populate the raster plot below. In this raster plot the neural discharge of some C-nociceptors (the lines characterized by a fin-like shape) is shown. It is worth pointing out that for visualization purposes the highest peaks are colored differently (green dots), thus during the stimulation is a good practice to look for fibers that shown a strong and clear signal. In figure 4.11 two fibers have been selected for sorting (the two horizontal red lines). The vertical red line selects the sweep of interest and the raw data is visualized on the plot above. The module can in addition down-sample the filtered data in order to speed-up computation and visualization. This can provide an overview of fiber behaviors, however if a high sampling rate is required the down sampling can be switched off and the analysis can be performed with better results. In this case, unlike figure 4.1 the marking technique has not been used but the activity dependent slowing (ADS). Using this effect, the module can estimate the fiber type (4 types of C-fibers) through a suited function in the analysis tab. This algorithm looks at latency changes following shifts in the stimulation frequency. This is a well-established technique however it is a manual isolation that requires a massive time load. Thus, we looked for other ways

to speed up the pipeline. A possible solution is to use a different approach, based on the fiber action potentials. A clustering algorithm has been implemented. The community not only can exploit this as a remedy for the ADS technique but even for other classification problems.

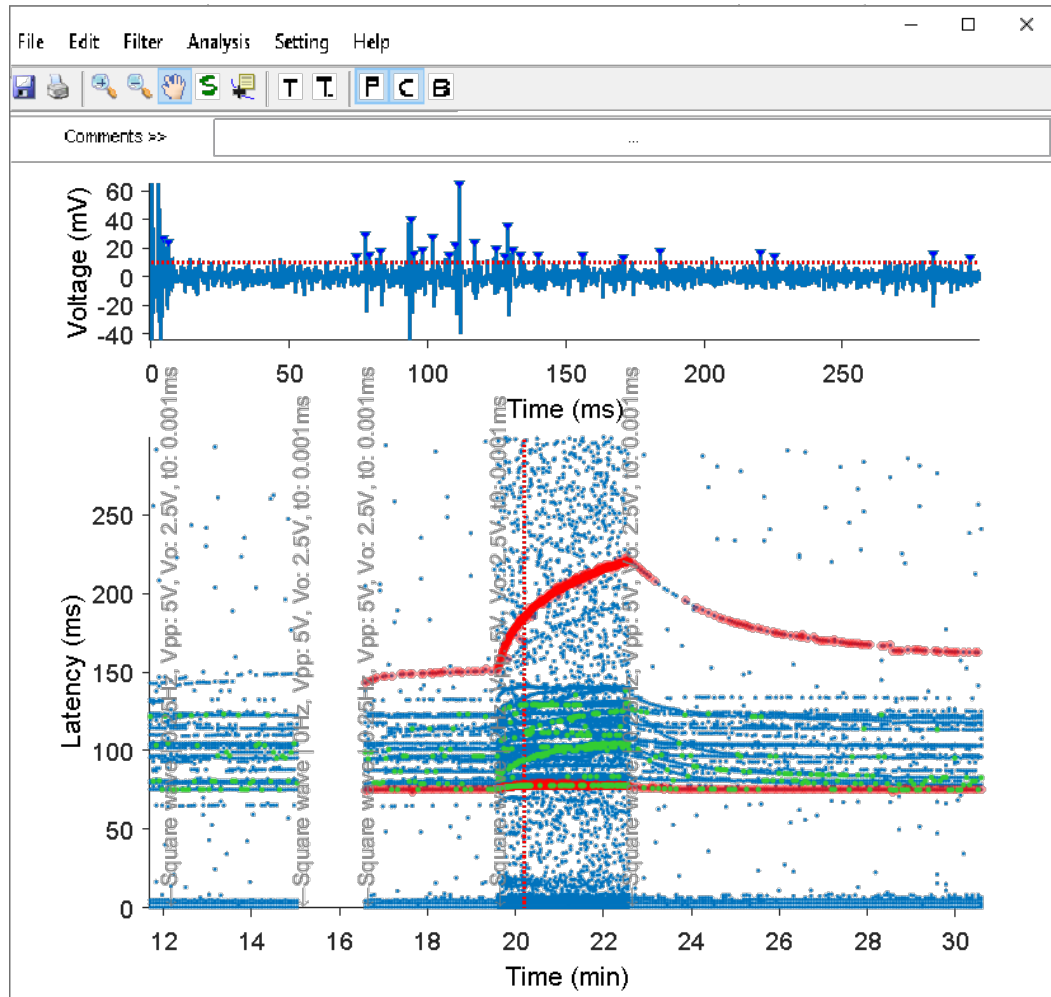


Fig. 4.11: Fiber extraction. The plot above shows a modified recorded data with the threshold (red line) at 10mV. The raster plot below shows the activity-dependent slowing (ADS) of some C-fibers. Two of them have been selected (red dots) for sorting.

Mainly, a spike sorting has been implemented through a PCA and K-mean analysis (Figure 4.12). On the top left, all the selected action potentials (the horizontal red lines of figure 4.11) are superimposed on the same plot. Top right, a plot related to the PCA analysis with the first three principal components (PC1-3). The selected action potentials are firstly analyzed by the PCA to find out differences in the action potential waveform. Secondly, these spikes are visualized in a different space (principal components) that emphasizes characteristics that were hidden before. This hidden space will lead to grouping of fibers into different clusters (the blue

clusters on the off-diagonal plots). The diagonal shows the histograms related to the first three principal components. Two peaks are shown on it showing that there are clearly two different fiber populations. However, in this step the K-means algorithm did not assign them yet. Bottom right, a K-means algorithm performs the task of splitting and classifies these clusters. This can hopefully speed up the pipeline and provide information regarding fibers of interest in one-step computation. The two colors are related to the two different fiber populations found by the algorithm. Now, the two peaks have different colors, as it should be. It is worth pointing out that not always the classification can be done by eye, thus this algorithm must be added to the pipeline.

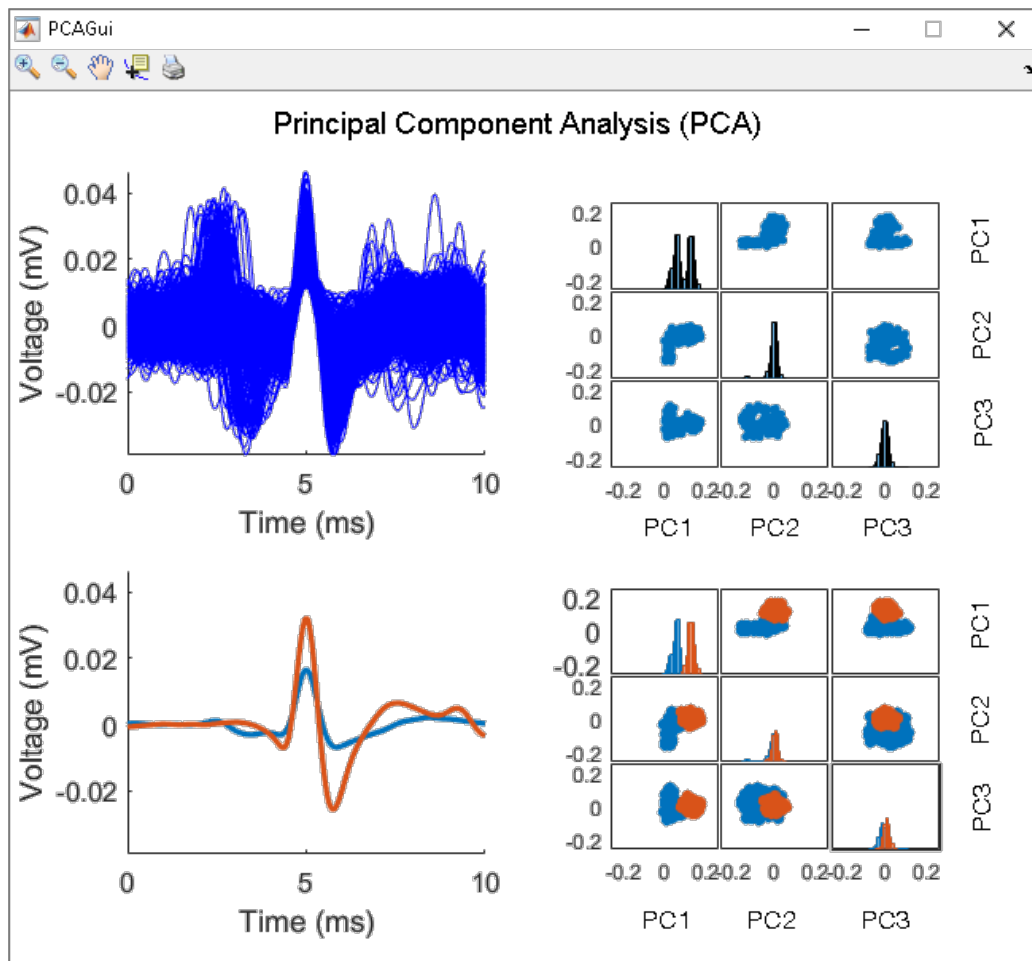


Fig. 4.12: Principal component analysis (PCA) and K-means. These techniques are applied on the selected fibers (red dots) of Figure 4.11. Top left, action potentials of these two fibers, superimposed. Top right, first three components (PCs 1-3) of the PCA algorithm. Bottom right, K-means applied to the PCA clusters for sorting. Bottom left, average of the action potentials related to the first and second cluster (C-fiber 1,2).

On the bottom left, the action potentials are averaged considering the two fiber populations separately. Furthermore, as mentioned before a function able to convert data gathered in Lab Chart archives into information readable by the analysis module has been successfully added. This allows researcher to exploit the abovementioned analysis not only on archives recorded by these modules but even by third-part software such as Lab Chart datasets.

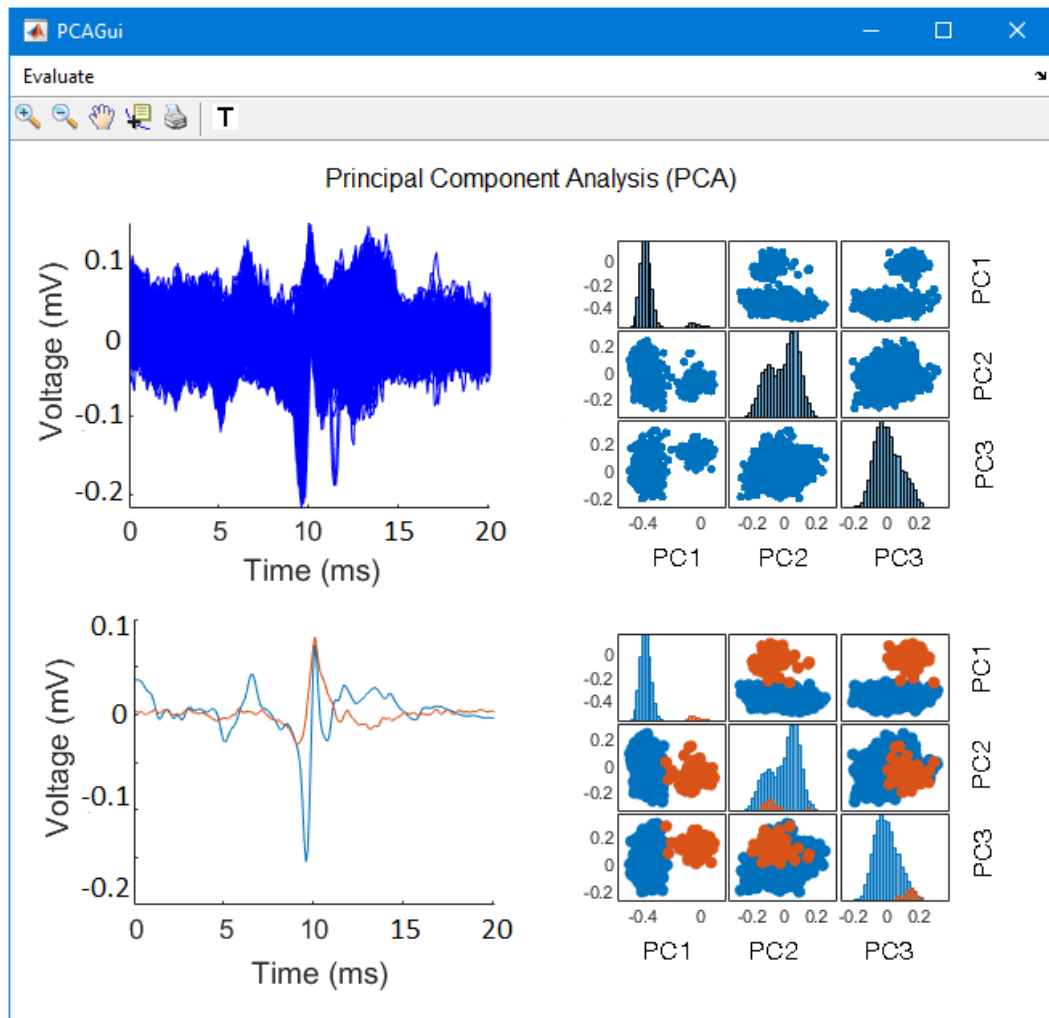


Fig. 4.13: PCA and K-mean of C vs Adelta fibers. These techniques are applied to the A δ -fiber at 8ms latency of figure 4.9 and a C fiber in the same recording. Top left, action potentials of these two fibers, superimposed. Top right, first three components (PCs 1-3) of the PCA algorithm. Bottom right, K-means applied to the PCA clusters for sorting. Bottom left, average of the action potentials related to the first and second cluster (C-fiber 1,2). The two fibers show different action potentials, and this resemble the literature for myelinated and unmyelinated fibers.

4.3.3 Spike sorting and fiber classification – C fiber vs. A δ -fiber

Figure 4.13 instead shows a PCA applied to A δ -fiber and C fibers of the recording shown in figure 4.9, the A δ -fiber at a latency of about 8ms and another C fiber that appear in the same recording. The action potentials of these two fibers have been selected all together as shown in the top left of figure 4.13. Performing a PCA on them two clusters appear (top right, figure 4.13) meaning that there are clearly two different fiber populations, C and A δ fibers respectively. After applying the K-means algorithm on them and separating the two fiber populations and making an average of their action potentials the shape of their spikes is shown (bottom left, figure 4.13). It is worth pointing out that the two potentials of myelinated (type A δ) and unmyelinated (type C) fibers have two opposite polarities as described in the literature [Val18]. In the myelinated fiber (blue line, bottom left, figure 4.13) there is a downward peak right before 10ms followed by another one at 10.5ms, meaning that the recording electrode has been probably inserted between two nodes of Ranvier, as described in the literature [Val18] and in the introduction (sec. 1.9.4). The PCA analysis works fine in the classification of these two-fiber type, having that their potentials have such different morphology.

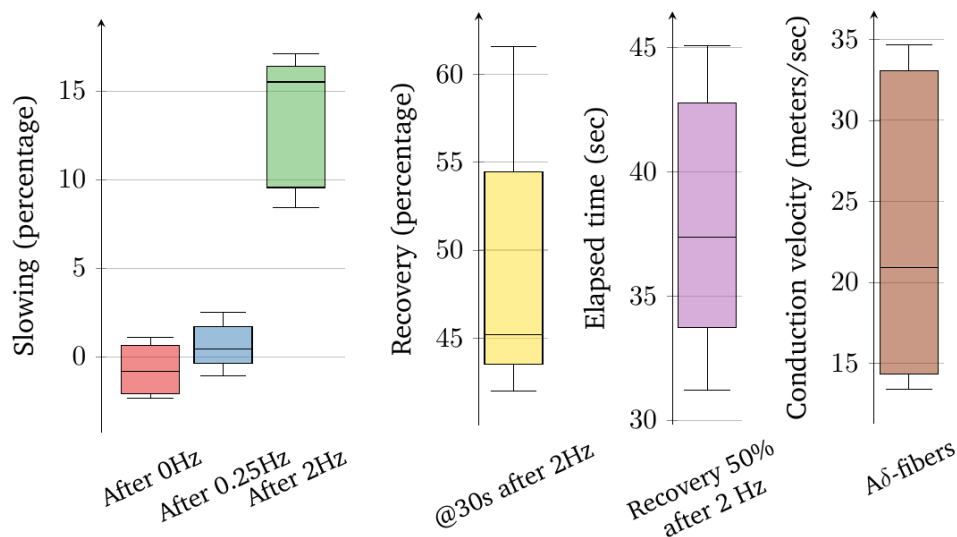


Fig. 4.14: A δ -fibers statistical analysis

| | Median (25th,75th percentile) | | |
|-----------------------------|----------------------------------|-------------------------|------------------------|
| | Percentage | Seconds | Meters/sec |
| Latency change after 0Hz | -0.82 (-2.08, 0.63) | | |
| Latency change after 0.25Hz | 0.45 (-0.38, 1.69) | | |
| Latency change after 2Hz | 15.51 (9.55, 16.4) | | |
| 30s recovery after 2Hz | 45.18 (43.49, 54.47) | | |
| 50% recovery after 2Hz | | 37.37 (33.73, 42.78) | |
| Conduction velocity | | | min:13.22 max:34.63 |

Tab. 4.1: A δ -fibers statistical analysis

4.3.4 Statistical analysis of Adelta fibers

Furthermore, additional information of A δ -fibers can be extracted through the SPiike software, such as the latency changes after the pause, the first 0.25Hz stimulation, the 2Hz stimulation, and the recovery to the initial baseline latency after the 2Hz stimulation at a 30s and at 50% respectively. Figure 4.14 and table 4.1 show all these parameters extracted from the 5 visible A δ fibers on figure 4.9. As comparison figure 4.15 shows the percentage of slowing @0.25Hz, @2Hz, the recovery at 30s, the time to 50% recovery and the conduction velocity of C nociceptors. As it can be seen on it the percentages of slowing of the recorded A δ -fibers approach those of type 1A nociceptors more than those of type 1B C-fibers even though they are almost half of them. Also the recovery at 30s and the time to 50% recovery is pretty similar to those of 1A nociceptors. The conduction velocity as expected is bigger for the A δ -fibers. With a conduction velocity ranged between 13.22 and 34.63 m/s and considering the polarity of the action potential it is pretty clear that the recording of Adelta fibers and faster fiber can be achieved with the developed software. It is worth noting that due to a low availability of mice for recordings and being microneurography a extremely time consuming technique even more when an unknown fiber population needs to be studied, a statistical analysis with a bigger sample size could not be performed. In this case as specified before only the extraction of 5 A δ -fibers parameters has been possible. Thus these values might be verified through multiple trials, however the values are congruent to what has been expected from the literature and this is the first time a A δ fiber has been recorded through the microneurography technique. However, as occurred for C-nociceptors (i.e. type 1A and 1B) there might be subclass of A δ fibers, this is why more trials

are needed for the right classification of A δ fibers. This however needs a sufficient number of experiments that could not be performed within this project, being this also not one of the main objectives. Nevertheless, as demonstrated, the software is able to stimulate faster fibers giving to the research community a powerful tool for the study of the peripheral nervous system through the microneurography technique. This will lead to improvement in the quality of drug development.

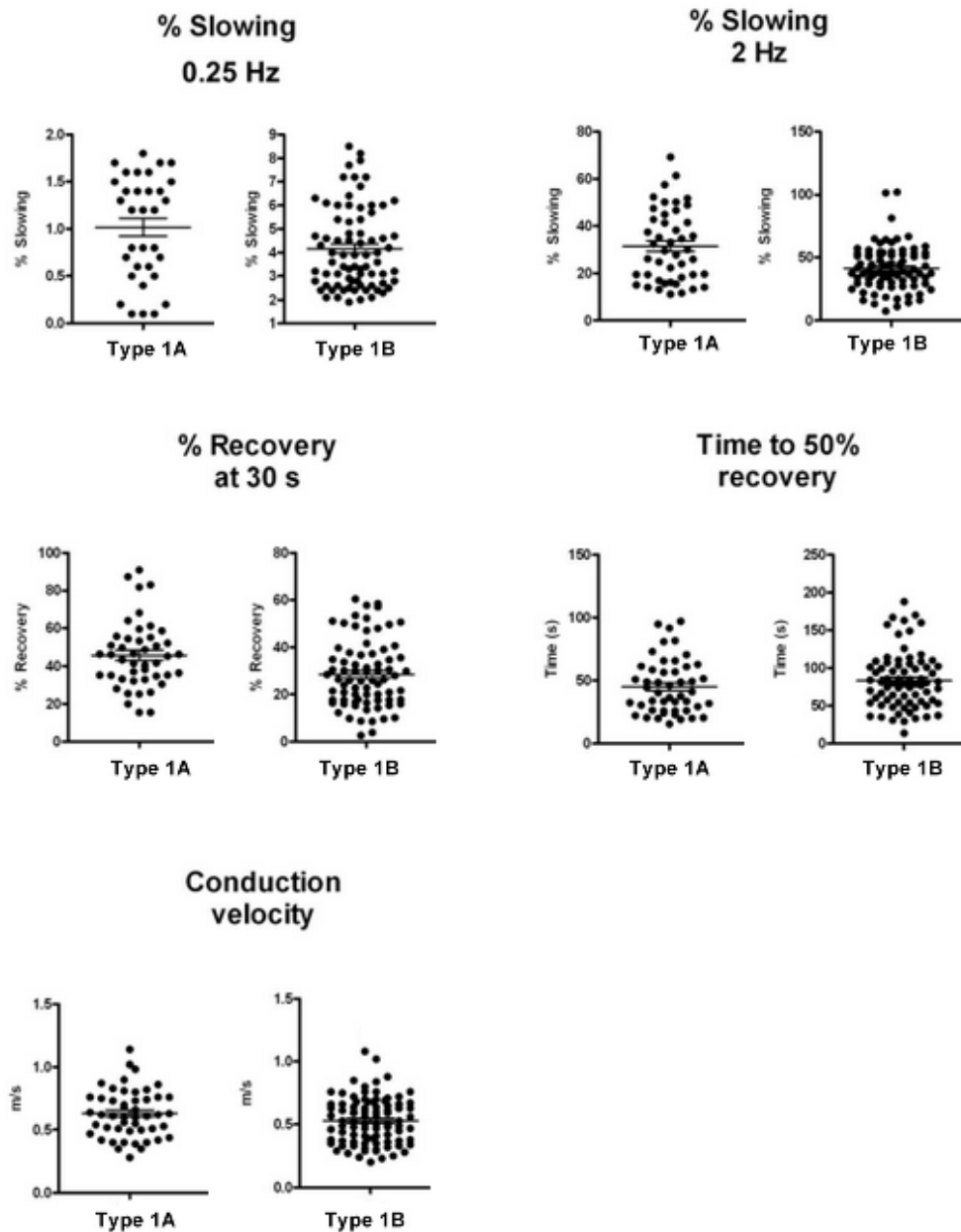


Fig. 4.15: C-nociceptors parameters (Adapted from [Ser+11])

4.4 Spike extraction - an example of a cold hyperalgesia patient

Another possibility of the software is the analysis of recordings performed in patients, through a utility that allows the researchers to import LabChart recordings. Indeed, SPiike cannot be used for the direct stimulation and recording of human patients, but it can surely be used for analysis purposes. This is due to ethical problems that need a previous validation of the software by the ethics committee.

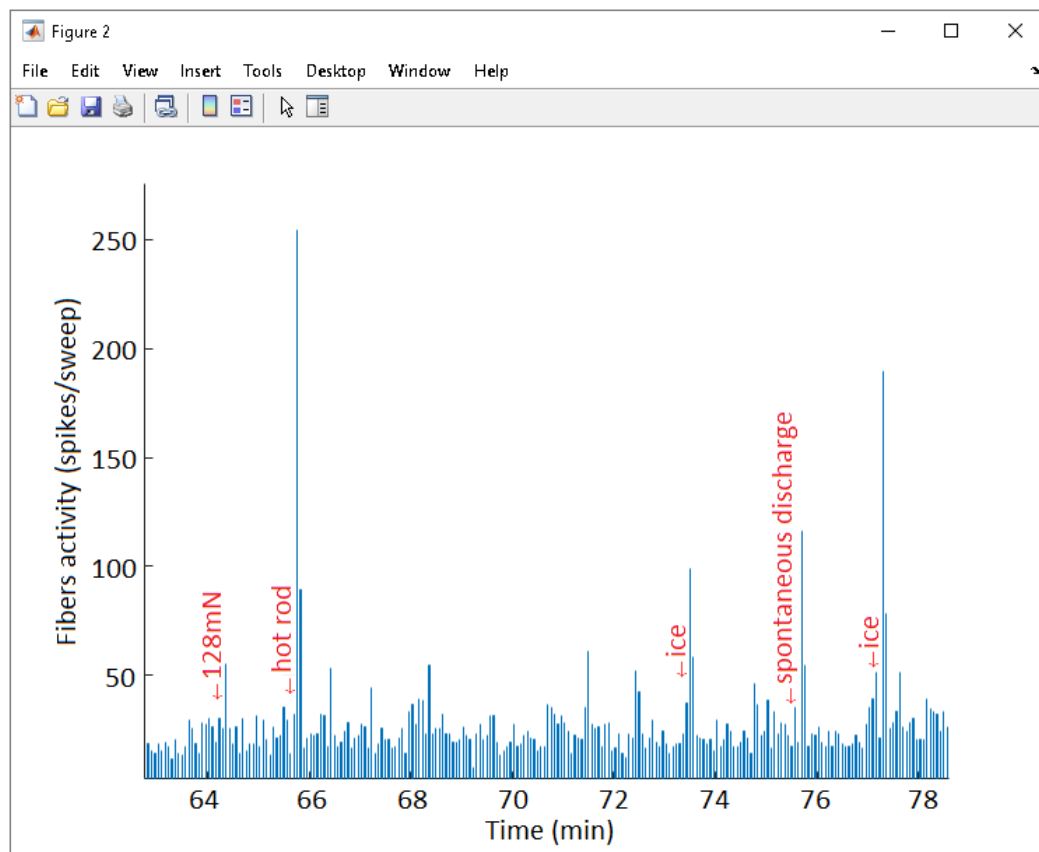


Fig. 4.16: The graph shows the number of spikes per sweep -of the fibers under investigation- as function of the elapsed time. The spikes represent abrupt changes in the neurons discharge. They follow marking stimuli and accidental events (e.g. patient movement or noisy discharges).

4.4.1 Fiber activity

In figure 4.16 the fibers activity of a recording done in a cold hyperalgesia patient (figure 4.1) is depicted. In this specific case natural stimuli (i.e. hot rod, ice, 128mN) are applied and the transitional states can be evaluated looking at the peaks shown

on it. Every peak corresponds to an increase in the number of spikes generated by the fibers. The selected action potentials have been counted sweep by sweep, therefore this graph represents the number of spikes per sweep. Around minute 64 there is a peak following the 128mN mechanical stimulation, around minute 66 another peak that is generated by the hot rod stimulus. The same can be seen in figure 4.1 with the characteristic jump of the fibers at these elapsed time and their exponential recoveries. Instead, ice application has been provided around minutes 73,5 and 77. It is worth noting that in figure 4.16 at minute 76 there is a peak that is not due to natural stimuli but to a spontaneous discharge (i.e. patient movement, noise, burst discharge, etc. . .) that sometime can happen.

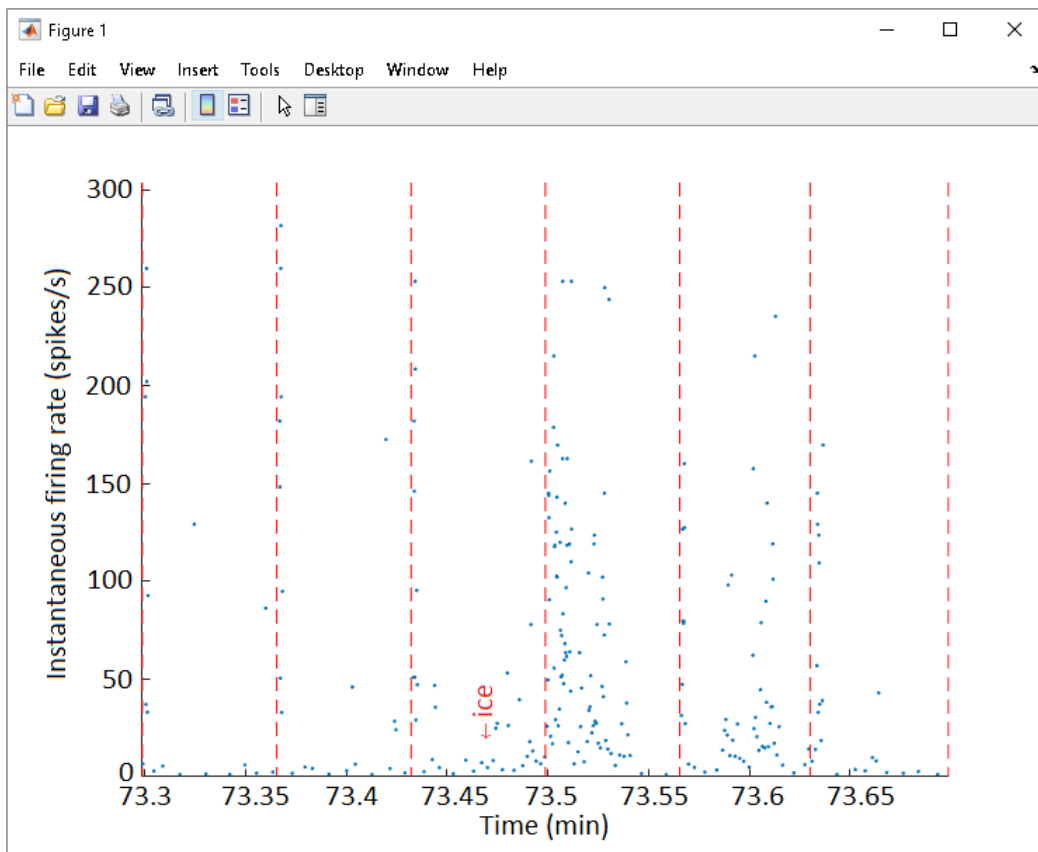


Fig. 4.17: The graph shows the spikes per second of the stimulated fibers upon marking stimulation. It has been performed with ice, applied directly to the receptive field of the neurons under stimulation. Through this feature a dynamic change in the IFR can be noticed and studied. Basically, in this specific case a slowly adapting behavior can be observed. Vertical red lines represent the sweeps onset.

4.4.2 Instantaneous firing rate (IFR)

Figure 4.17 shows the instantaneous firing rate (IFR) of the peripheral neural network following stimulation by ice. The stimulus has been applied directly to

the receptive field of the neurons under stimulation and a response can be noticed at minute 73,5. This is a powerful feature for characterizing fibers behavior upon stimulation, and to assess their responsiveness and recovery following natural stimuli. From figure 4.17, the adaptation curve of these fibers can be easily extract. It resembles the accommodation curve of a free nerve endings nerve fiber with its characteristic slowly adapting behavior. The stimulus was applied for just couple of seconds, but SPiike software can be also used for studying dynamic changes in the firing rate of fiber populations following more prolonged stimuli.

4.4.3 IFR statistical analysis

Furthermore, SPiike can extract information from the fibers activity plot and make a statistical analysis on it. This has been done considering 6 cold allodynia and cold hyperalgesia patients and evaluating the fibers activity following the marking by mechanical, ice and hot rod stimulations. The marking of mechanical stimulation has been performed with von Frey Filaments (128 to 512 mN), hot rod at 41-48°C, ice cubes or air-puff (below 15°C). Menthol was applied on the receptive field of the nociceptors under investigation and the quantification of the extra spikes generated by the marking technique has been compared before and after this menthol application. The goal of this study was to check if the menthol was able to change the pain sensation perceived by these patients. Figure 4.18 and table 4.2 show the statistical analysis of the 128mN mechanical, hot rod and ice application.

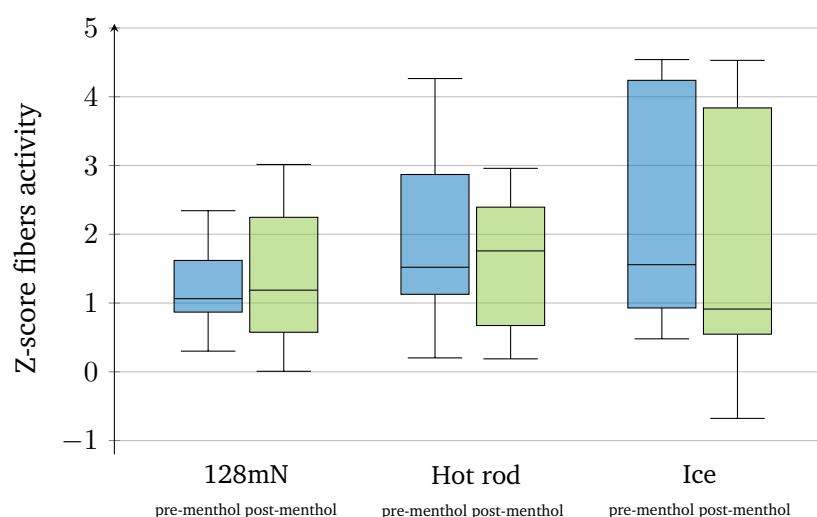


Fig. 4.18: Z-score fibers activity statistics

For every stimulation type the boxplots have been calculated considering all the stimulations performed in these 6 patients and dividing them into 2 groups (pre and post menthol application). On the left, the two boxplots shown the fibers

activity Z-score of the 128mN mechanical stimulation considering as baseline the number of spikes generated by the fibers under investigation at rest and before the menthol application. The two boxplots in the center show the one of the hot rod stimulation and on the right the same statistics done on ice stimulation. Table 4.2 shows all the data regarding median, 25th percentile, 75th percentile of the boxplots depicted in figure 4.18. No statistical differences were reported in the extra spikes generation upon heat ($p=0.42$), cold ($p=0.596$) and 128mN mechanical stimulation ($p=0.68$) comparing pre and post menthol application in cold allodynia/hyperalgesia patients.

| Z-score fibers activity | Pre menthol | | | Post menthol | | |
|-------------------------|-------------|------|--------------|--------------|------|--------------|
| | Hot rod | Ice | Mech (128mN) | Hot rod | Ice | Mech (128mN) |
| Median | 1.52 | 1.56 | 1.06 | 1.76 | 0.91 | 1.19 |
| 25th percentile | 1.13 | 0.93 | 0.87 | 0.67 | 0.55 | 0.57 |
| 75th percentile | 2.87 | 4.24 | 1.62 | 2.39 | 3.84 | 2.25 |

| | Hot rod | Ice | Mech (128mN) |
|---------|---------|-------|--------------|
| p-value | 0.42 | 0.596 | 0.68 |

Tab. 4.2: Median, 25th percentile, 75th percentile and p-value of the boxplots shown in figure 4.14

Even if the results do not show a statistically relevant change before and after menthol application, it is clear that the software is now able to evaluate the fibers activity following marking stimulation. Thus, the change in the number of spikes generated within a sweep can be easily evaluated and analyzed through the SPiike software. This may be used for assessing the effectiveness of a new developed drug and in any sort of application that requires such an analysis.

4.4.4 Correlation between SPiike and QTrac outcomes

With the aim of validating the results obtained within the SPiike software and those extracted from the QTrac a correlation analysis has been conducted. Basically some recorded fibers of the 6 aforementioned patients have been used for this purpose. Parameters such as the slowing after the 2Hz stimulation, the 30 seconds recovery after the 2Hz stimulation and the elapsed time needed to recover the 50% of slowing after the 2Hz stimulation have been compared. These are the same parameters discussed in the previous paragraphs (sec. 4.3.3) and more specifically in figure 4.14. These parameters are the most important ones in the fiber characterization having the C-fibers can be subdivided into the different sub-classes just evaluating the slowing forced by the 2Hz stimulation. Figures 4.19a, 4.19b and 4.20 show

the correlation between the Qtrac and the SPiike software. In all parameters the correlation is linear meaning that the two software give the same results.

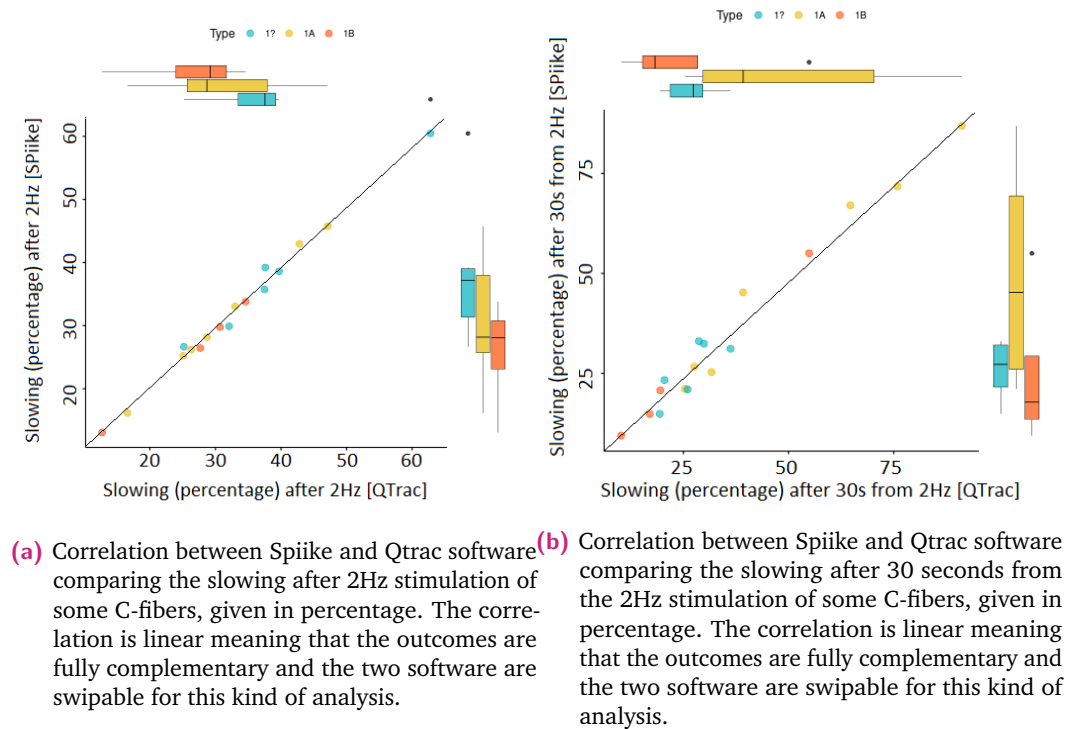


Fig. 4.19

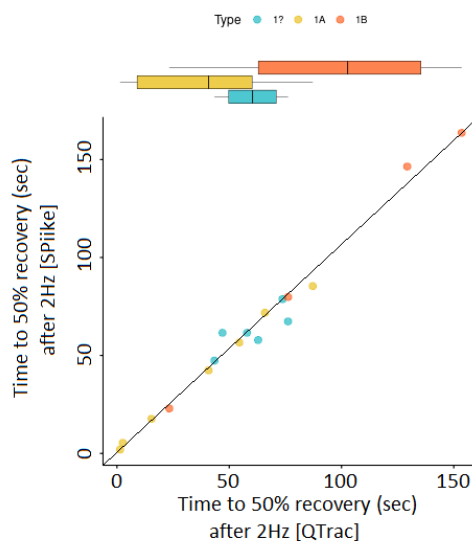
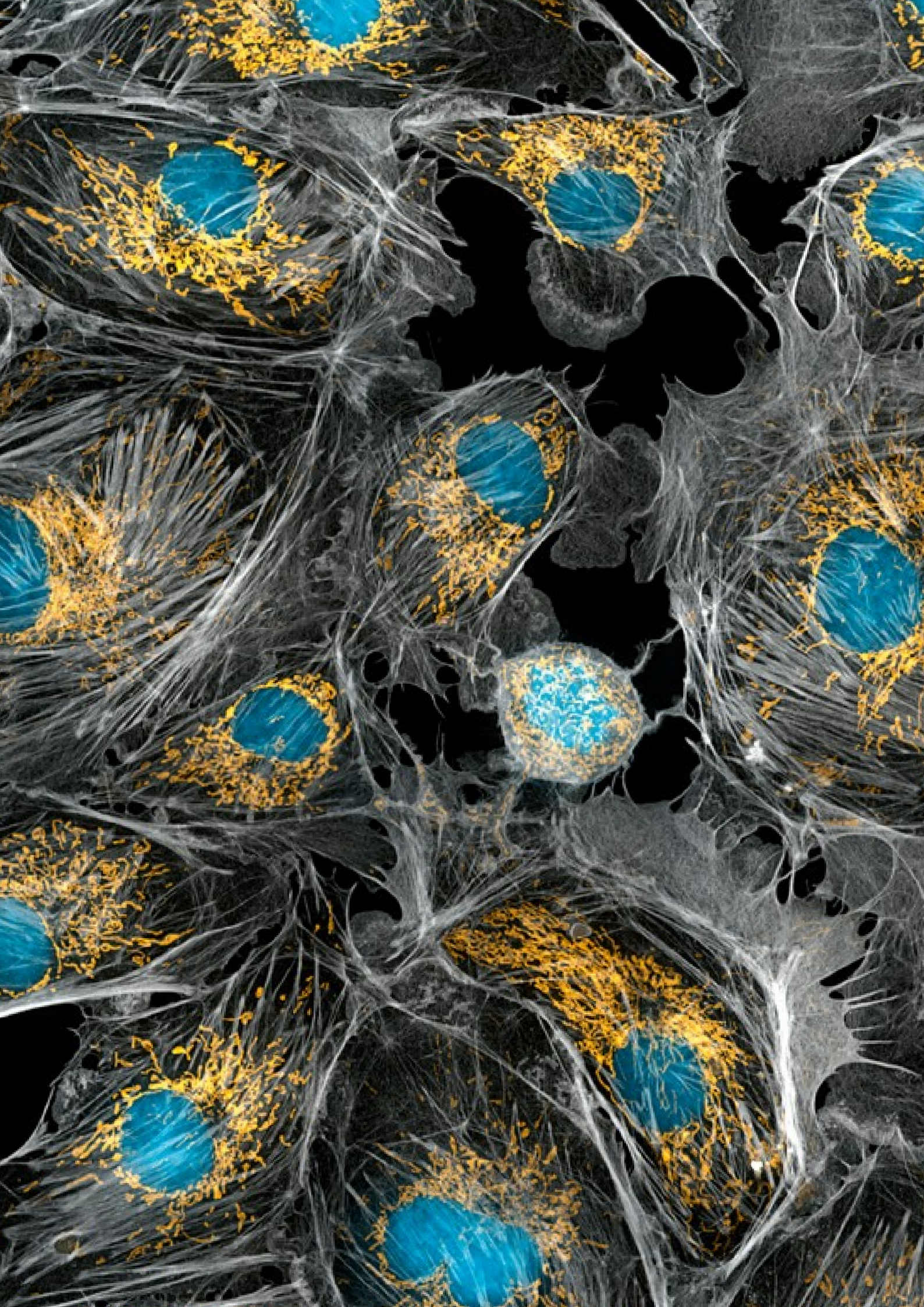


Fig. 4.20: Correlation between Spiike and Qtrac software comparing the time to recovery to 50% after 2Hz stimulation of some C-fibers, given in s. The correlation is linear meaning that the outcomes are fully complementary and the two software are swappable for this kind of analysis.

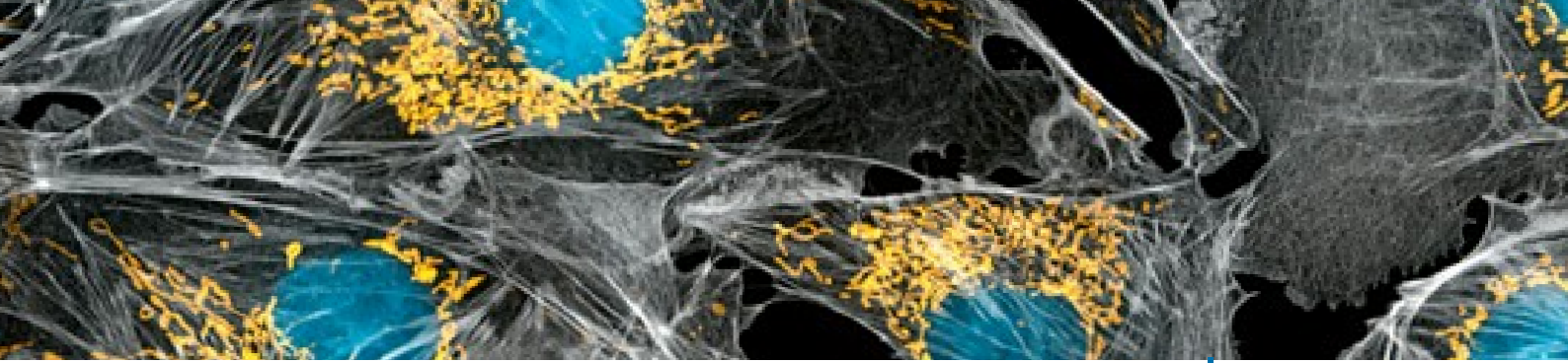
As mentioned before (sec. 4.3.1) sometimes some jumps can occur. However, for this comparison, in both software the fiber discharges have been taken without any

manipulation since this could have altered the results. In any case, even though the correlation analysis in such a way is the most reliable possible these results must be checked if some statistically analysis must be conducted, as shown in the previous paragraphs. Therefore SPiike can be used as a substitute of the QTrac software having that the results are almost the same, and moreover it can be used for additional analysis such as spike sorting and the evaluation of the fibers activity among others, functionalities that were not possible in other software packages.



Your Body Under The Microscope

[<https://pics-about-space.com/cool-space-sky-stars-galaxy?p=4>]



5

Discussion

” *The human brain has 100 billion neurons, each neuron connected to 10 thousand other neurons. Sitting on your shoulders is the most complicated object in the known universe.*

— **Michio Kaku**
Universe, Complicated

SPiike software have been developed taking into account that nowadays peripheral nervous system recordings can be used to study the physiology and pathophysiology of several diseases in preclinical studies as well as as exploration and diagnostic technique in clinical trials. This experiments aim to understand how external noxious and no-noxious stimuli are transduced and sent to the brain. The peripheral nervous system is the first level of a more complex neural system and must be understood firstly since the building block of higher central processing relays. Some diseases and symptoms that can be attributed to the central nervous system sometimes originate in the peripheral system. Understanding its functioning is fundamental for more targeted drugs and cures. However, microneurography software already available in the market can only stimulate and record slow conducting fibers (i.e. C-fibers). Thus, to improve our knowledge, enhanced and faster algorithms for fiber recording and analysis need to be implemented. This is the goal of this project that ended up with the making of the SPiike software.

5.0.1 [SPiike overview](#)

SPiike software comes with a graphical user interface as shown in figure 5.1, this makes the program very easy to interact with. The user can use the software

easily without the need to learn nothing about programming languages since all the commands are easy and self-explanatory. In any case in the results section (sec. 4) a brief description of all the commands available in the last version can be found and in the software a manual has been added. The software has got shortcuts, in such a way that recording and analysis can be sped up and some functions can be called directly through the keyboard. The software will be distributed in its standalone version, this means that it can be installed without the need of buying Matlab licenses or other alternative software. The only requirement is to have a internet connection for the downloading of the Matlab runtime that is free of charge. The free space needed is about 1Gb, having that the Matlab runtime weights almost 800Mb, and Spiike software weights less than 10Mb. However, enough free space for saving the recording is required.

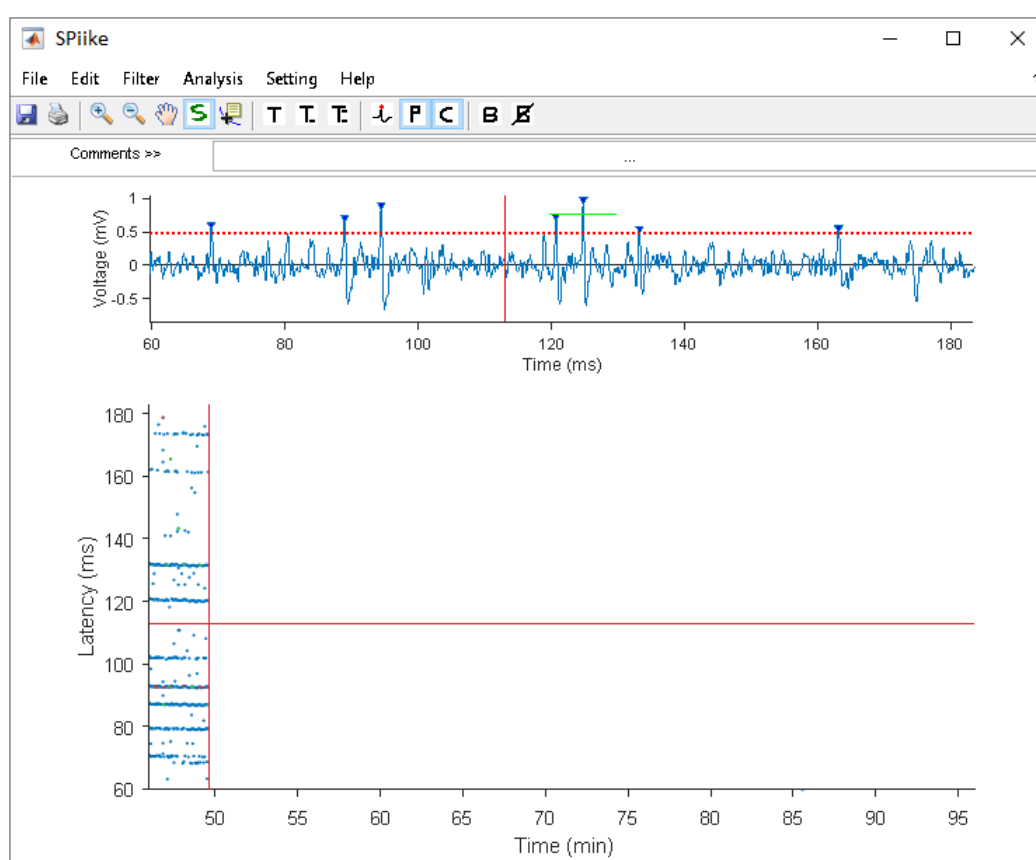


Fig. 5.1: SPIike software graphical user interface (GUI).

SPIike software has been developed in a modular way to allow high performances even when run in computers that do not have a very powerful hardware. This is why, it is split into two modules, a recording and a analysis module.

5.0.2 Recording module

When the recording module is used, through the menu bar the recording can be saved and a screenshot of the window can be taken for post-analysis purposes. The menu bar allows also to set the filter applied to the raw data, to change the sampling frequency, the auto save settings, the threshold for the raster plot algorithm and to change how the waveform and the dots are displayed in the graphs. Furthermore, the stimulus waveform and some parameters linked to it can be tuned as well. The prompt command instead allows the user to insert commands that afterwards can be retrieved through the history button and saved in a text file. In such a way, a macro can be fed to the software for the automatization of the recording steps. Lastly, the stimulation of the fibers under investigation can be looped until the stop button is hit or a protocol can be used. Usually the protocol is a well defined sequence of stimuli with different stimulation frequencies applied for a certain interval of time. This allows the characterization of the fibers through the activity-dependent slowing behavior, an intrinsic fiber characteristic that give insights on their type. However, since the software is reading a excel file with the information regarding stimulation frequency and stimulation time this can be changed at will by editing the input file, allowing researchers to add different protocols that best suits with the type of fiber they need to investigate and record.

Additionally, the maximum stimulation frequency sustained by SPiike has been pushed to 1000Hz. This allows the users to assess the behavior of C fibers as well as faster fibers (e.g. Adelta, Abeta, Aalpha fibers), which was not possible in previous software. Previous software used in microneurography studies such as QTrac [Cam+11; GP+15; Ser+12; Ser+09; SBN10] were indeed only able to push the stimulation frequency up to 10Hz and this is not suitable for fast conducting fibers, but only for C-fibers. The SPiike software has been developed taking into account that not only C-fibers but also other types should be included in the experiments. In the pain field the two fibers that alert the brain when a noxious stimulus touch the skin are indeed C and $A\delta$ fibers, instead the other fibers are important for the sensorial perception. Thus C and $A\delta$ fibers must be included in preclinical trials of pain studies in all those cases in which the efficacy of a developed drug should be assessed. However, since the SPiike software copes with a stimulation frequency up to 1000Hz, other types of fibers such as motor and sensorial fibers can be stimulate with this software as well. This open new possibilities for the experiment designers, since the microneurography technique along with the SPiike software will allow researchers to stimulate and record every fiber type. Indeed since the electrode is inserted directly into the nerve tuning properly the stimulus current and having a good separation between the recording and stimulating electrode single-unit recordings can be obtained. There are already some techniques that allow to record motor or

sensorial fibers (e.g. contact heat-evoked potential stimulator (CHEPS) [Lag+15], pain-related evoked potential (PREPs) [Han+15], etc.), however most of the time what is recorded is a compound action potential. The single-unit discrimination will then allow more suited experiments that will improve the quality of cures and diagnosis facing diseases and injuries.

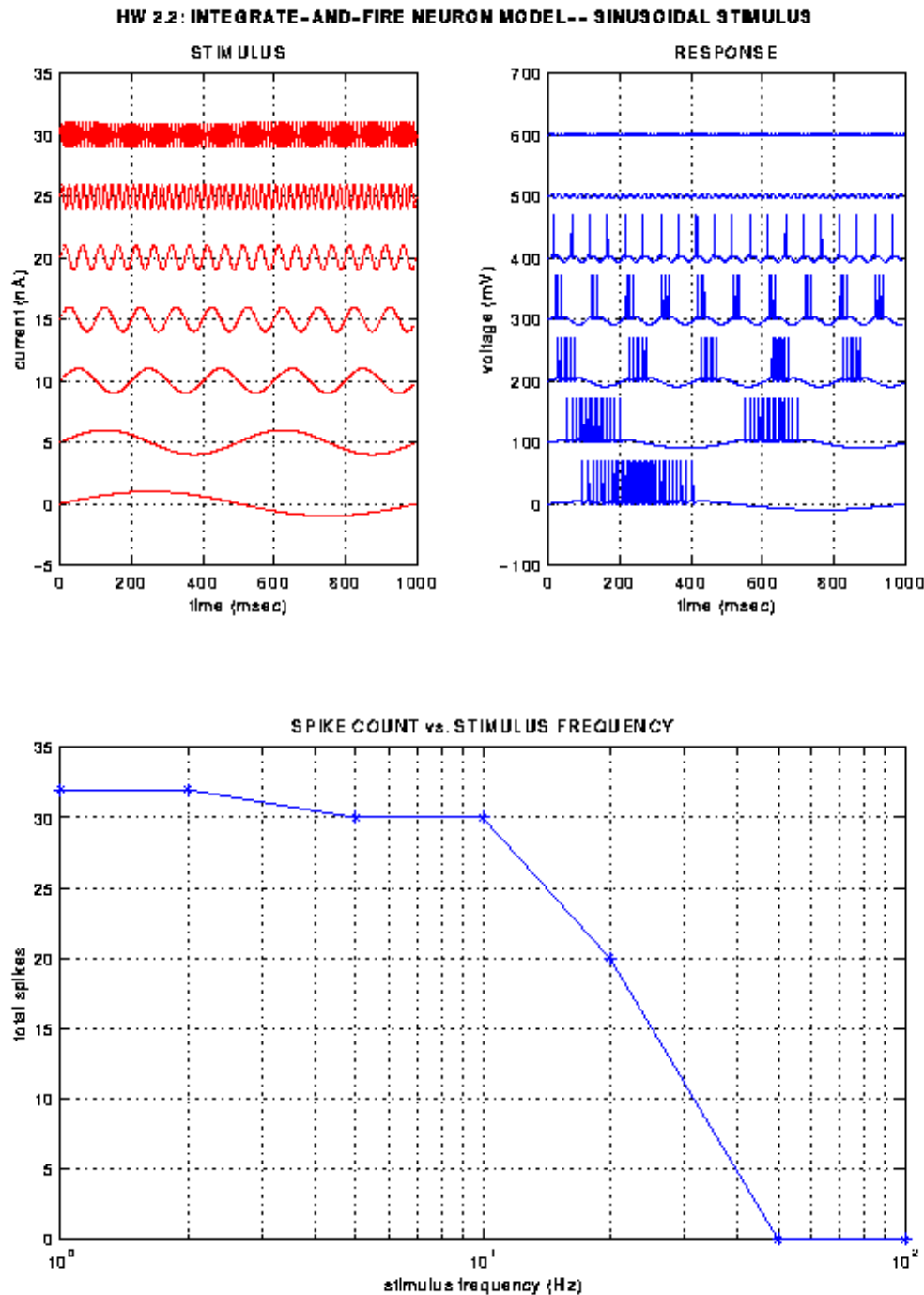


Fig. 5.2: Frequency response of neurons when stimulated with a sinusoidal function. [Sti]

5.0.3 Stimulus waveforms

As mentioned before another useful capabilities of the SPiike software is to possibility of changing the stimulation waveform. Normally a rectangular waveform is exploited for this kind of experiments [SBN10; Ond+16; Geo+07], however in the last version of the SPiike software this can be changed. Other types of waveform that can be added are: a square wave, a cosine, a sine, a sawtooth, a dirichlet or a chirp function, a linear progression of a conditioned stimulus and the usual recovery cycle through the importing of the delays from an external editable excel file. Moreover in the menu bar there is an option for changing the stimulus parameters. This allows to change the stimulus duty cycle (i.e. Dc; only available for the square waveform), the stimulus amplitude peak-to-peak (i.e. Vpp), the stimulus offset (Vo), the stimulus delay starting from the onset of the sweep (i.e. t0) and the number of the lobes when the Dirichlet and the Chirp functions are selected. This wide variety of stimulus types allows the researcher to check different properties of the fiber under investigations. For instance changing the duty cycle of the stimulus waveform the dynamic response of the fibers can be checked such as if they show a slow or a fast adapting behavior.

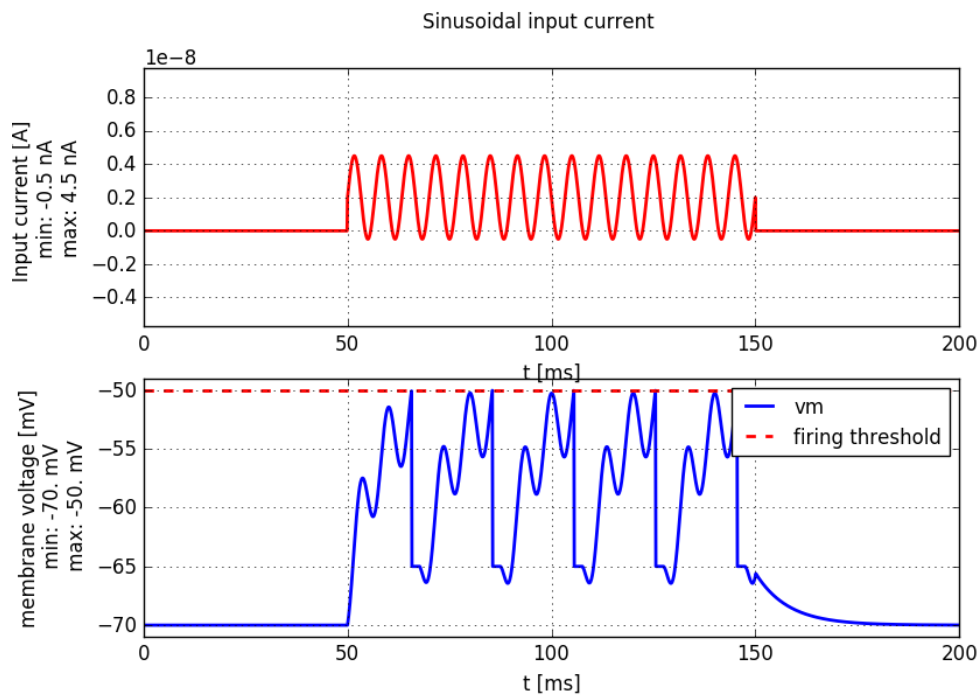


Fig. 5.3: Injection of a sinusoidal current and its effect on membrane potential. [Lif]

Furthermore a sinusoidal waveform is useful for checking the cutoff frequency of the neurons. Indeed, for any given time (e.g. 1000 msec) when neurons are stimulated with a sinusoidal waveform they respond with the same number of action

potentials even when the period is changed, however this happens up to a well specified frequency. Overcoming this frequency means that the neurons will start lowering the action potentials generated since they cannot cope anymore with a electrical perturbation that is changing too rapidly over time, as shown in figure 5.2. This behavior is due to the intrinsic property of a neuron. Indeed, as shown in a simulation of the response of a neuron model (figure 5.3), as already known the membrane potential needs to overcome a threshold in order to make the fiber to discharge. Therefore, when the sinusoidal stimulus has a slow frequency the current injected into the neuron is adequate to exceed this threshold, however when it gets faster the fluctuations happen below this level and this is the reason why at high frequency the neurons stop discharging. Instead, the sawtooth stimulus is actually a ramp stimulus that can be used for checking the threshold at which the fibers start discharging, the same effect that happens when the temperature is gradually increased. Some neurons will start discharging at a very specific temperature and in such a way they can be classified into a group or other. The same happens with a electrical stimulus however the discharge is generated by a flux of current. The same can be expected from a whole cell patch clamp study, however in this case the behavior of several neurons can be checked at once and not only the discharge of a single neuron. The Dirichlet function has instead a similar shape of an action potential, thus potentially using this type of stimulation that is less perturbative than a rectangular waveform the artifact generated by the flux of current can be lowered. However, this should be checked with further studies since no information has been found in the literature regarding this specific stimulus waveform. In the literature [NRH88] biphasic waveform are claimed to decrease the stimulus artifact since the current perturbation is both in the positive and negative side and this can somehow balance the disturbance. Therefore, playing with the stimulus parameters such as duty cycle, stimulus offset and stimulus amplitude peak-to-peak also the rectangular waveform could be used in a way that the stimulus artifact is decreased in intensity. Lastly, the Chirp function has the property of containing the whole spectrum frequencies within its signal so in this case it can be potentially used for checking the proper frequency at which the fibers respond most. For instance for testing the best stimulating frequency change during the ADS stimulation. However, it is worth noting that the device shown in the methods section, namely the Digitimer DS7a, can only be used as pulse generation. The DAQ board can be connected to this stimulator but the signal will be only used as a trigger. In order to make the most of this functionality of the SPiike software a voltage follower stimulator must be used, such as the Digitimer DS2A Isolated Voltage Stimulator.

5.0.4 Analysis module

The analysis module is instead meant to be used to analyze the recordings saved through the recording module. However, SPiike can also import third-party archives such as LabChart recordings. This can be used for analyzing data of recordings previously done in patients using other software packages, since direct stimulation of human subjects cannot be achieved using the developed software until it has been already validated. The graphical user interface of the analysis module resembles that of the recording module but some additional functions have been added such as a analysis tab that allows the user to perform several tasks. The fibers in this module can be selected through a dedicated brushed button and some analysis can be performed on these data. SPiike indeed can carry out sophisticated analyses having that machine learning capabilities have been implemented, such as a Principal Component Analysis (PCA) and a K-means algorithm for spike sorting and classification problems. These algorithms have been implemented to speed up the analysis of the recorded fibers. In previous software packages every single fibers needed to be selected before any sort of analysis could be performed on them. This was pretty easy for fibers with a good signal-to-noise ratio, however when the SNR drooped to a low level the separation of the fibers from the noise was difficult an extremely time consuming. Therefore, through spike sorting and fiber classification now the entire sweeps can be selected all at once and the software is taking care of separating the fibers automatically without the need to do it by eyes. This is a very powerful technique that was not available in previous software and will allow researchers to save time and to improve the quality of their outcomes.

Moreover, the evaluation of the fiber instantaneous firing rate and the fibers activity can be assessed as well as the fibers latency change and some information regarding their activity-dependent slowing. This can be iterated through trials and some statistical analysis can be extracted from the recordings.

Another important feature is that the stimulation frequency has been pushed to 1000Hz, now fast conducting fibers can be analyzed as well. C and A δ fibers are generally easier to check and to analyze since the stimulus artifact does not overlap with their action potentials [25, 26]. Indeed, they are slow enough to distance themselves from the stimulus artifact when the separation between stimulation and recording electrode is at least equal to 4-5 cm (distance that can be usually obtained with the smallest animals used in this study, namely mice). A α and A β fibers are faster than C and A δ fibers and they require more distance between the two electrodes to be able to distinguish them from the stimulus artifact, hence recordings performed in rats or even better in human patients have to be preferred if these faster fibers have to be analyzed. Figure 5.4 shows the different types of fibers that

can be stimulated through electrical stimulation [Oka+12]. They are subdivided into different sub-populations depending on their conduction velocities. It is clear that fast conducting fibers (i.e. $A\alpha$ -fibers) are almost superimposed to the stimulus artifact, while slow conducting fibers (i.e. C-fibers) are well separated.

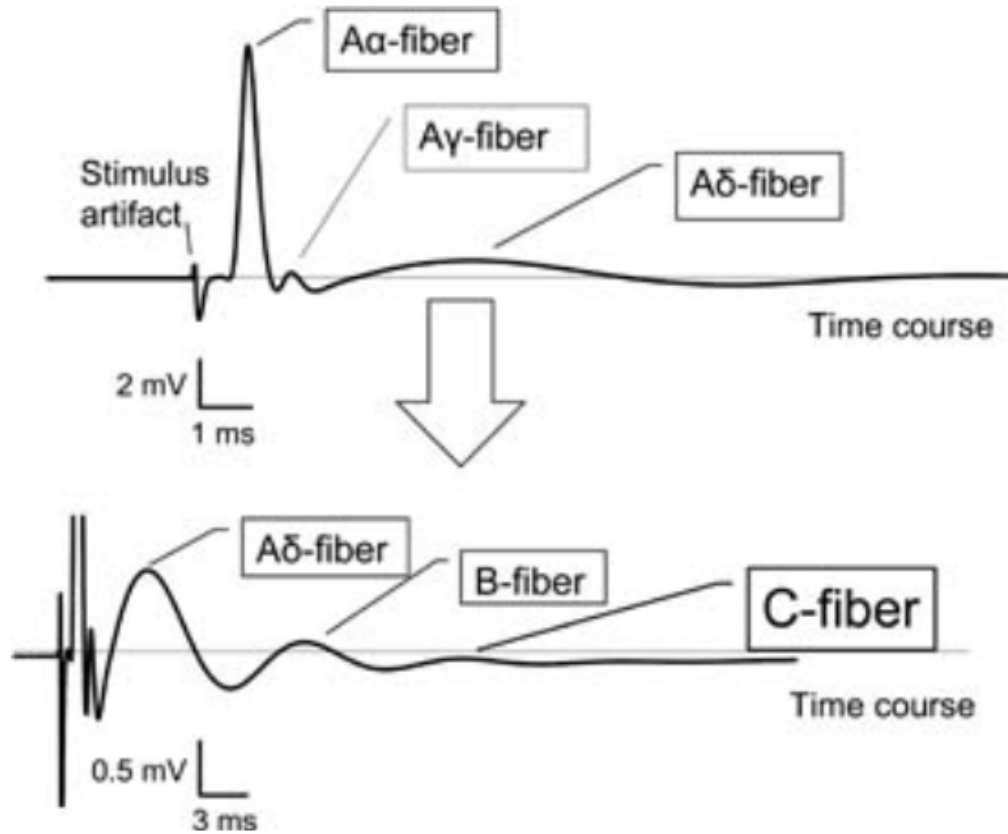
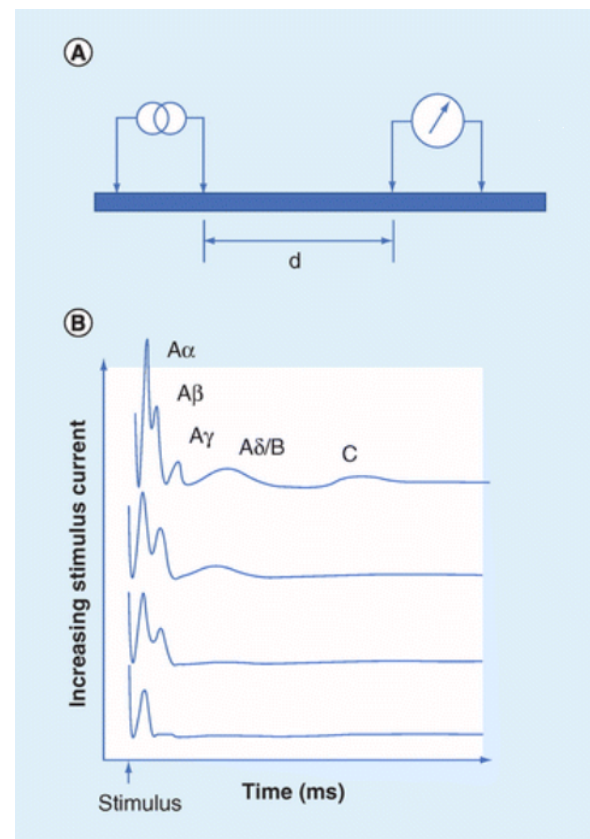
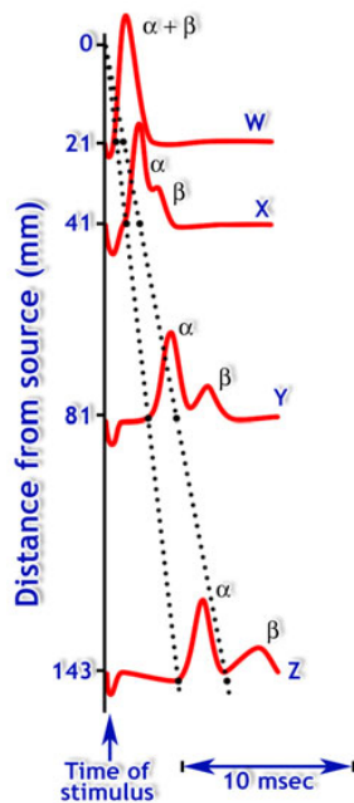


Fig. 5.4: Fibers subpopulation classified according to their conduction velocities. Namely, the elapsed time from the stimulus artifact at which they appear. [Oka+12]

Thus, if an experiment is focused on this fast conducting fibers some precautions must be taken. First of all the distance plays a key role in obtaining good outcomes. As shown in figure 5.5a $A\alpha$ and $A\beta$ fibers needs a distance between source and recording electrode of at least 8-9cm, otherwise they will overlap and the single-unit recording would be impossible [Cap]. Another important factor is that even if the different conducting fibers are well separated in the same sub-population there might be more then one fiber discharging. Therefore, the software instead of recording a single action potential it would be actually recording a compound of action potentials. This would be a problem during the ADS stimulation since the fibers react differently to changes in the stimulation frequency. Basically, during the increase in the stimulation frequency (e.g. 2Hz for C-fibers) they might split into single action potentials for then recovering back to the initial compound action potential once

the stimulation frequency is put back to baseline. This would complicate the post-analysis since the fibers could not be distinguished easily. A solution is to increase even more the distance from source but if this cannot be achieved another solution must be taken, namely to lower the current injected into the fiber receptive field or as mentioned before to use a different stimulus waveform. Figure 5.5b shows that fast conducting fibers are easier to stimulate than slow conducting ones [PSK18]. Therefore, depending on the type of fiber to stimulate the stimulus intensity must be chosen properly. Furthermore, not only the conduction velocity plays an important role in the easiness of generating an action potential, but also the distance between the stimulating electrode tip and the fiber receptive field is crucial. Indeed more current means a wider electric field and more fibers that are discharging. Therefore, the stimulus intensity must be increased gradually until few fibers are displayed on the raster plot. This is the right intensity that may avoid the problem of the compound action potential.



(a) Illustration of fibers action potential separations from both the stimulus artifact and each other, depending on the distance from source. [Cap] (b) Illustration of evoked compound action potentials according to the intensity of the stimulus current [PSK18]

5.0.5 A δ -fibers insight

Thanks to this cutting edge software, A δ fibers have been recorded and analyzed for the first time ever with the microneurography technique, as shown in figure 5.6. Their behavior resemble that of C fibers, they showed a ADS behavior and a

response to external stimuli such as hot rod, ice and mechanical stimulation. Indeed, figure 5.6 shows a recording of a $A\delta$ fiber obtained during a trial performed in a wild-type mouse. The baseline stimulation frequency has been kept at 1Hz, and with the goal of assessing the effect generated by higher frequency to $A\delta$ -fibers the same frequency has been pushed to 50Hz for 3 minutes. The horizontal line at a latency 8ms represents the discharge of a $A\delta$ -fiber. Indeed, considering a distance of about 10cm between stimulating and recording electrodes the conduction velocity of this fiber is equal to 12.5 m/s, namely $A\delta$ fiber. It shows an activity-dependent slowing like that of C fibers with its characteristic exponential decay that can be seen between minutes 40 and 45 of the elapsed time. It also reacted to mechanical, hot rod and ice application meaning that this might be a polymodal $A\delta$ -fiber. Some statistical analyses have been carried out using this fiber along with some others $A\delta$ -fibers and they showed some interesting results. During this analysis, the percentage of slowing @0.25Hz, @2Hz, the recovery at 30s, the time to 50% recovery and the conduction velocity have been extracted. The results showed that these fibers resemble more the behavior of type 1A C-nociceptors than type 1B. For instance the recovery at 30s and the time to 50% recovery is pretty similar to those of 1A nociceptors (1A C-nociceptors: ~45% and ~46sec, respectively [Ser+11]; $A\delta$ -fibers: 45% and 37sec, respectively) while the slowing after the 0.25Hz and the 2Hz stimulation are almost the half of those recorded in 1A C-fibers (1A C-nociceptors: ~1% and ~30%, respectively [Ser+11]; $A\delta$ -fibers: 0.45% and 15%, respectively). However, due to the low availability of mice for this kind of recordings and being the technique time consuming when new fibers must be studied the sample size was small. Further studies must be conducted to check if there might be sub-populations of $A\delta$ -fibers as in C-nociceptors.

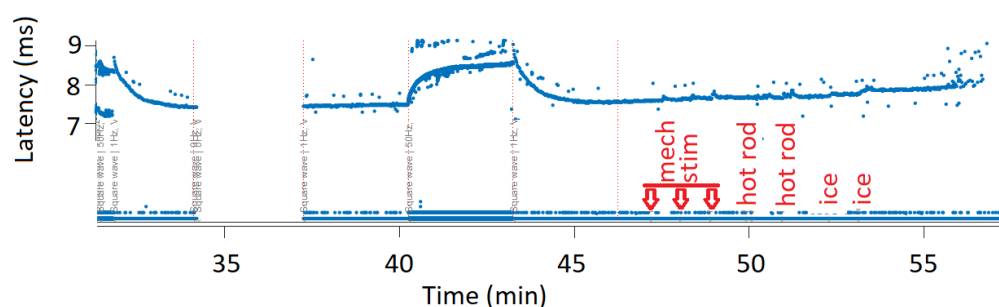


Fig. 5.6: At a latency of 8ms an $A\delta$ -fiber shows activity-dependent slowing and a response to different stimuli (mechanical stimulation, hot rod and ice application). This resembles the behaviour of a C-fiber.

However, the goal of creating a new software able to stimulate slow conducting fibers as well as faster fibers has been fully achieved and the software may be used by other researchers for tailoring their microneurography experiments towards $A\delta$ -fibers. This

should improve the knowledge on the peripheral nervous system and improve the quality of drug development.

5.0.6 Comparison between microneurography and other techniques

The microneurography technique has been developed by two researchers, Karl-Erik Hagbarth and Åke Vallbo, at the Department of Clinical Neurophysiology of the Academic Hospital in Uppsala, Sweden [Val18]. It is a *in vivo* extracellular single-unit recording technique. There exist other extracellular single-unit recording techniques but most of them are either *ex vivo* or *in vitro*. For instance in the epidermis-up ex-vivo skin-nerve preparation [Wel+10] the hindlimb skin of a mouse is dissected from the animal and placed in a perfusion chamber. The saphenous nerve is kept attached to the skin and then the tissue perfused with synthetic interstitial fluid. The bath temperature is monitored and kept at 32°C. This technique needs then an external organ bath and fluid circulation. The superfusion of isolated receptive fields is realized with metal rings and an application system connected to a roller pump, the electrical stimulation is performed through metal microelectrodes [Zim+09]. This means that this technique is more time consuming for the sample preparation than the microneurography and it needs additional instruments such as a chamber and a perfusion system. Furthermore, it is worth pointing out that there exist different tissue preparation techniques and all of them use different approaches and target different goals. The *in vitro* experiments are used in all those cases in which other options cannot be used or when a more detailed cellular and molecular analysis must be conducted however they are not ideal since the tissue is created artificially and is unrelated with the whole organism. *Ex vivo* experiments are instead still experiment done outside a living organism but with tissue taken from him, thus the experiment should give more detailed information regarding side-effects. However, if the experiment should target toxicity and interaction of compounds with the entire organism *in vivo* experiments must be preferred. However, sometimes the effects during *in vivo* experiments could be hard to identify since changes can be due to external factors as well. Therefore the three techniques should be used complementarily.

5.0.7 Overview of microneurography

The microneurography technique as explained before is a very advanced technique that allow translational studies. Indeed it is not a very invasive technique compared to the *ex vivo* skin nerve preparation, among others. However it is time consuming and the patients can get tired during the study. Indeed they must maintain their

foot still for at least an hour to avoid losing the recording due to movements of the electrodes. This can vary depending on the experiment but in any case the patient must be aware of this. Moreover, it can be a bit painful during the stimulation, mainly during the 2Hz of the ADS protocol. Indeed when the stimulation frequency is increased it generates a build up of action potentials at the medula level that enlarge the pain perceived by the patients due to temporal summation. A troubleshooting in this case is to lower the stimulation current but with the possibility of either losing some fibers or generating fiber jumps that can occur due to changes in the electric field intensity that alters the branches of the nerve endings being stimulated. This is why is a good practice to start the recording with the minimum current stimulation needed for having a fair number of fibers and without the inconvenience of the patient.

5.0.8 Comparison between *in vivo* and *ex vivo* software

Nowadays some software for *ex vivo* studies are already available in the market however for *in vivo* ones only the Qtrac and the Open-Ephys (<https://open-ephys.org/>) can be used. The Open-Ephys is a package software able to record neural activity, however is more suited for optical or even electrical recordings performed directly into the brain of the animal [Sie+ 17]. QTrac is instead more suited for studies in the peripheral nervous system in both animal models and human beings with all the advantages and disadvantages described before. Instead *ex vivo* software are the Spike 2 from Cambridge Electronic Design (<http://www.ced.co.uk>) and the DAPSYS data acquisition system (<http://www.dapsys.net>; Brian Turnquist, turnquist@bethel.edu). Spike 2 by CED is a free-running software such as the LabChart software, therefore only the recorded signal is displayed and some analysis can be performed but it lacks of a raster plot. It can perform spike sorting searching for neural discharges however it cannot track-back the action potential to their respective latency, indeed a raster plot is needed for this. Therefore QTrac and SPiike are more versatile in this regard, being SPiike even more powerful with its built-in PCA analysis capability. The DAPSYS software samples at 33kHz and it uses a standard PC running Windows XP and a Microstar DAP52000 data acquisition processing board. Even though the software is open-access the starter kit is kind of expensive (almost 5000 euros). The software can analyze the action potentials and assign an ID to it. The same ID means that the software recognized the action potential to belong to the same neuron. Furthermore, it assigns a timestamp to the action potentials, namely the time of occurrence. However as for SPiike 2 by CED a raster plot is not shown, thus further manipulations of the dataset should be performed in order to check the ADS behavior and other techniques explained in the methods section (sec. 3), such the recovery cycle and the marking technique.

Therefore, SPiike software can be considered an improvement of the QTrac software with extended functionalities that were not available before. Hence, Qtrac and the SPiike software by their own can be used to perform translational studies being that other software are too invasive for studies in living human beings. Indeed Open-Ephys targets central nervous system discharging that can be recorded directly from living animal models. However, drilling through the skull must be carried out and this is not admissible in human patients. Even worse for the software that works along with *ex vivo* tissues since they can be exploited for animal studies but not for recording in human beings. The only technique that allow to extract tissue from human patients in the pain field is the so-called skin biopsy. This technique checks if there is a reduction in the fiber density for the diagnosis of the small fiber neuropathy. However the tissue extracted from the patient is tiny, the punch biopsy is done with a circular blade ranging in size from 1 mm to 8 mm. This is due to the fact that fiber nerve endings are microscopic and just the dermis of the skin need to be studied. Instead, in neural studies the discharge pattern along the axon is targeted. The fibers most of the time discharge after being electrically stimulated, the so-called evoked potential. And for the reasons explained before there should be a considerable distance between the stimulating electrode and the recording one. This generates a problems in human studies since a large portion of the nerve should be removed generating impairments and tissue damage in the subject. Therefore, the Qtrac and Spiike software that are used along with the microneurography, one of the least invasive techniques for extracellular single-unit recording of small fibers such C and A δ nociceptors, are the preferred option for translational studies and experiments in living human beings.

5.0.9 SPiike advantages over QTrac

The development of SPiike software required an iterative procedure such as forward and backward steps due to the complexity of the task. However, SPiike has been developed accounting all the required constraints and it already reached its final version. The software can stimulate, record and analyze both C and faster fibers, mostly A δ fibers. SPiike is equivalent -with fully complementary outcomes- to another software available in the market (i.e. QTrac). However, SPiike can be used as an alternative to Qtrac software with several advantages. QTrac allows the user to do some tasks through a prompt command window, however all the commands have to be remembered or checked in a manual provided in the software, SPiike is more user-friendly and it has got a prompt window too but with the advantage of having a toolbar that can be used to speed up the process and the user can interact directly with the plots of the graphical user interface.

Also, a powerful signal conditioning is required for the purpose of extracting data from the noisy signal recorded by the electrode inserted inside the nerve. To this end, SPiike software implements two thresholds in the voltage domain (the y axis of the raw data) for the extraction of action potentials that lay within this window. And an enhanced wavelet-based filter can be activated to improve the quality of the signal and to help eliminating noise and spurious data.

As explained before, SPiike comes with advanced analysis capabilities such as machine learning algorithms (PCA and K-means) that allow the user to perform spike sorting and fiber classification. This was not possible with the Qtrac package and it will help to speed up the process of fiber characterization. Moreover, SPiike saves the entire sweep signal having that Qtrac is only saving the first 500ms. This allow the evaluation of the instantaneous firing rate and the fiber activity since the discharge throughout the entire sweep can be analyzed by SPiike.

Also the possibility of importing third-party archives such LabChart recordings is a novelty. Qtrac can indeed only analyze archives previously recorded through its own software. In such a way SPiike can be also used to perform enhanced analysis using previous recorded archives that can be retrieved from a database of previous LabChart recordings. Furthermore, it can be used to analyze recordings in all those applications in which the SPiike recording module can not be used so far, such as human patients recordings (sec. 4.4). This allows the researchers to wide the scope of microneurography recordings towards a wider range of experiment possibilities.

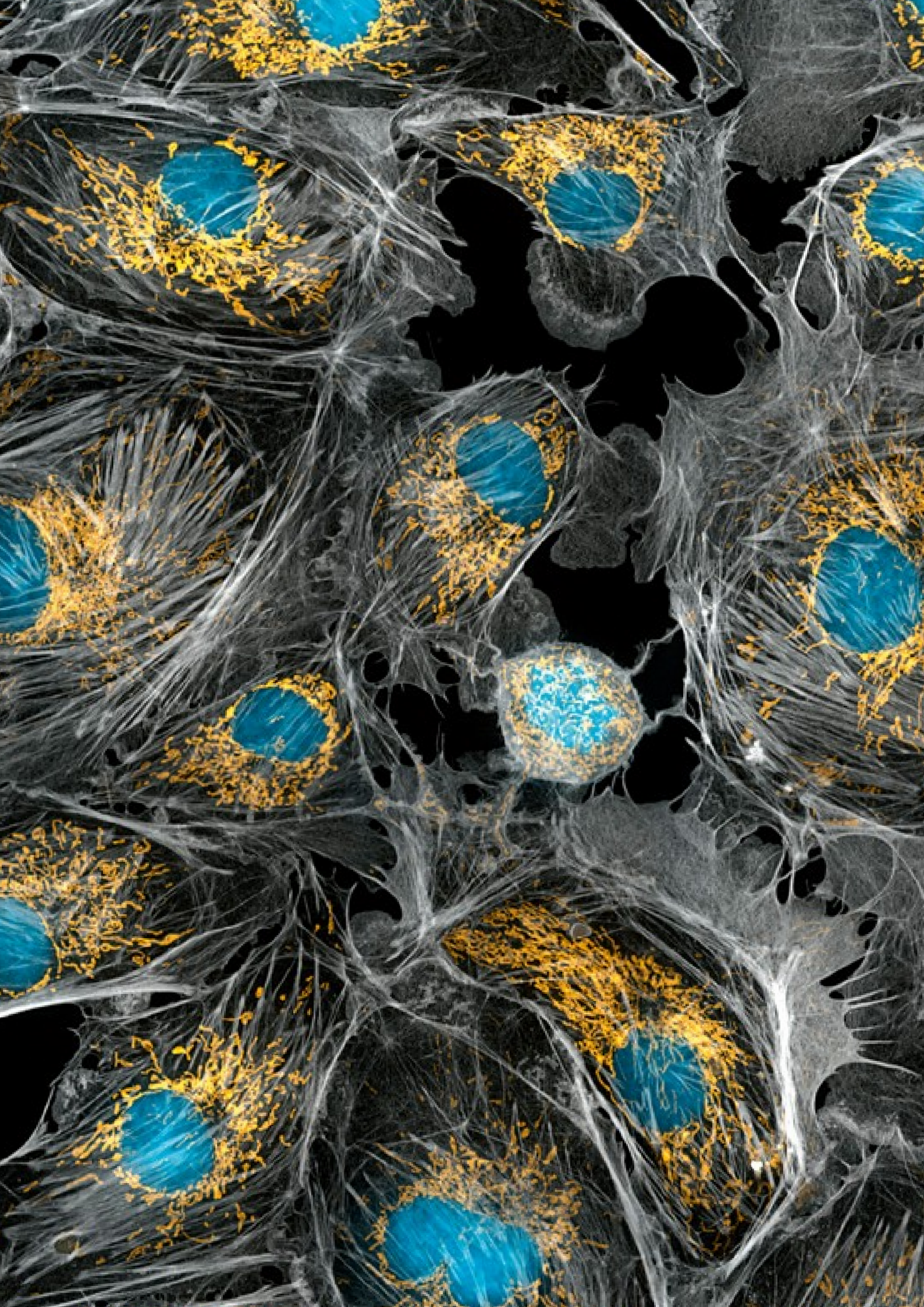
5.0.10 Software validation - Correlation between SPiike and QTrac

The SPiike software have been compared with the QTrac software, both qualitatively and quantitatively. Indeed as demonstrated in the previous chapter (sec. 4.1.3) the recording of a patient have been imported both in Qtrac and SPiike software and their raster plots provided the same view, meaning that quantitatively they are almost identical. Furthermore, a quantitative analysis have been conducted as well (sec. 4.4.4) and it showed that the extraction of the most important parameters such the slowing following the 2Hz stimulation of C-fibers, their slowing after 30s from the last 2Hz stimulus and the time to recovery to 50% after the 2Hz stimulation is the same for the two software. Thus, this demonstrates that the SPiike and Qtrac are interchangeable for these kind of analysis, however the SPiike software provides more advanced features that were not available in previous software packages.

5.0.11 Acknowledgments

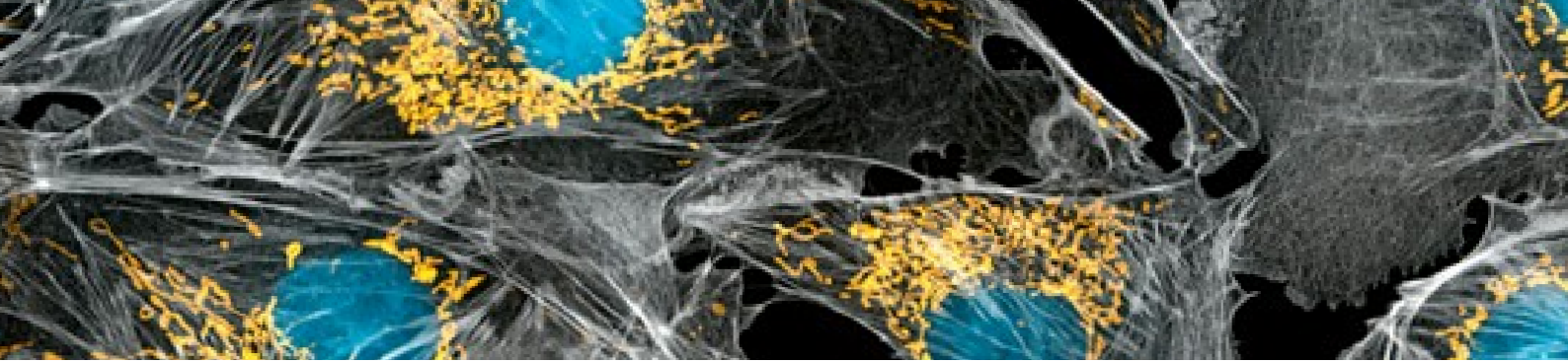
This software is part of a wider project that complement different approaches in the field of pain. The whole project has been carried out by other network partners (PainNet, EU funded ITN network) as well and it had been designed to integrate clinical and preclinical studies. This software development in particular spanned between several fields from software development through in vivo experiments. The objective was very ambitious. However, thanks to a highly competitive working environment we fully achieved all the objectives set.

This software will provide concealed features of nociceptor properties to the community.



Your Body Under The Microscope

[<https://pics-about-space.com/cool-space-sky-stars-galaxy?p=4>]



6

Conclusions

1. A new recording and analysis software (SPiike) has been developed, with a user-friendly interface, thus less code to write is needed.
2. SPiike contains a built-in PCA module with his K-means algorithm.
3. An improved stimulation frequency has been implemented in this software, it can reach 1000Hz of stimulation which is suitable for recording fast conducting fibers such as $A\delta$, $A\beta$ and $A\alpha$ fibers, a feature that was not possible in previous software.
4. A wavelet filter that can be activated by the user to enhance the filtering of the raw signal.
5. The software allows the use of two thresholds for the raster plot instead of one, to lower the likelihood of grabbing noisy data as action potentials.
6. SPiike has got additional analysis capabilities such as the extraction of the instantaneous firing rate and the evaluation of the fiber activity.
7. The capability of analyzing third-party archives such as LabChart recordings (suitable for human patients' recordings) extends the possible uses of the software.
8. Spiike is split into two modules (recording and analysis modules) such that the computational power required for running the software is lowered.

9. A δ fibers have been already recorded and they show a activity-dependent slowing and a exponential decay following the marking technique such that of C-fibers.
10. SPiike software outcomes have been compared with those of QTrac software both qualitatively and quantitatively and it showed that the two software are fully analogous.
11. SPiike software allows to extend microneurography recordings towards more suited experiments thanks to the possibility of recording and stimulating not only C but also A δ nociceptors among other fast conducting fibers.



Image of a human iris

[<http://ilmcity.co.uk/wp-content/uploads/2017/01/iris.jpg>]

Bibliography

- [Att11] Nadine Attal. „Assessment of neuropathic pain in the setting of intervention trials“. In: *Clinical Investigation* 1.4 (2011), pp. 501–507 (cit. on p. 19).
- [Bee56] Henry K Beecher. „Relationship of significance of wound to pain experienced“. In: *Journal of the American Medical Association* 161.17 (1956), pp. 1609–1613 (cit. on p. 18).
- [Ben15] Eduardo E Benarroch. „Ion channels in nociceptors: recent developments“. In: *Neurology* 84.11 (2015), pp. 1153–1164 (cit. on p. 10).
- [Ben+19] David L Bennett, Alex J Clark, Jianying Huang, Stephen G Waxman, and Sulayman D Dib-Hajj. „The role of voltage-gated sodium channels in pain signaling“. In: *Physiological reviews* 99.2 (2019), pp. 1079–1151 (cit. on pp. 11, 12).
- [Cam+11] Mario Campero, Hugh Bostock, Thomas K Baumann, and José L Ochoa. „Activity-dependent slowing properties of an unmyelinated low threshold mechanoreceptor in human hairy skin“. In: *Neuroscience letters* 493.3 (2011), pp. 92–96 (cit. on p. 113).
- [Dev+10] Emmanuel Deval, Xavier Gasull, Jacques Noël, et al. „Acid-sensing ion channels (ASICs): pharmacology and implication in pain“. In: *Pharmacology & therapeutics* 128.3 (2010), pp. 549–558 (cit. on p. 8).
- [Dha+09] Ajay Dhaka, Valerie Uzzell, Adrienne E Dubin, et al. „TRPV1 is activated by both acidic and basic pH“. In: *Journal of Neuroscience* 29.1 (2009), pp. 153–158 (cit. on p. 7).
- [Dic02] A. H. Dickenson. „Editorial I: Gate Control Theory of pain stands the test of time“. In: *BJA: British Journal of Anaesthesia* 88.6 (June 2002), pp. 755–757. eprint: <https://academic.oup.com/bja/article-pdf/88/6/755/11206400/880755ed1.pdf> (cit. on pp. 13, 14).

- [Die+03] André Diedrich, Warakorn Charoensuk, Robert J Brychta, Andrew C Ertl, and Richard Shiavi. „Analysis of raw microneurographic recordings based on wavelet de-noising technique and classification algorithm: wavelet analysis in microneurography“. In: *IEEE Transactions on Biomedical Engineering* 50.1 (2003), pp. 41–50 (cit. on p. 56).
- [Djo+06] Laiche Djouhri, Stella Koutsikou, Xin Fang, Simon McMullan, and Sally N Lawson. „Spontaneous pain, both neuropathic and inflammatory, is related to frequency of spontaneous firing in intact C-fiber nociceptors“. In: *Journal of Neuroscience* 26.4 (2006), pp. 1281–1292 (cit. on p. 19).
- [Dym+19] David A Dymment, Paulien A Terhal, Cecilie F Rustad, et al. „De novo substitutions of TRPM3 cause intellectual disability and epilepsy“. In: *European Journal of Human Genetics* 27.10 (2019), pp. 1611–1618 (cit. on p. 8).
- [Edg09] Leading Edge. „Cellular and Molecular Mechanisms of Pain“. In: *Cell* 139 (2009) (cit. on p. 7).
- [Fin+16] Nanna B Finnerup, Simon Haroutounian, Peter Kamerman, et al. „Neuropathic pain: an updated grading system for research and clinical practice“. In: *Pain* 157.8 (2016), p. 1599 (cit. on p. 19).
- [For17] Diego Fornasari. „Pharmacotherapy for neuropathic pain: a review“. In: *Pain and therapy* 6.1 (2017), pp. 25–33 (cit. on p. 19).
- [Fri12] Wilma Friedman. „Growth factors“. In: *Basic Neurochemistry*. Elsevier, 2012, pp. 546–557 (cit. on p. 9).
- [FW10] Tanya Z Fischer and Stephen G Waxman. „Neuropathic pain in diabetes—evidence for a central mechanism“. In: *Nature Reviews Neurology* 6.8 (2010), p. 462 (cit. on p. 19).
- [Geo+07] Annette George, Jordi Serra, Xavier Navarro, and Hugh Bostock. „Velocity recovery cycles of single C fibres innervating rat skin“. In: *The Journal of physiology* 578.1 (2007), pp. 213–232 (cit. on pp. 6, 63, 64, 89, 115).
- [GJ97] Bradley S Galer and Mark P Jensen. „Development and preliminary validation of a pain measure specific to neuropathic pain: the Neuropathic Pain Scale“. In: *Neurology* 48.2 (1997), pp. 332–338 (cit. on p. 19).
- [GP+15] Elizabeth Garcia-Perez, Romà Solà, Mireia Sumalla, and Jordi Serra. „Behavioral and electrophysiological abnormalities in two rat models of antiretroviral drug-induced neuropathy“. In: *Pain* 156.9 (2015), pp. 1729–1736 (cit. on p. 113).
- [Han+15] Niels Hansen, Ann-Kathrin Kahn, Daniel Zeller, et al. „Amplitudes of pain-related evoked potentials are useful to detect small fiber involvement in painful mixed fiber neuropathies in addition to quantitative sensory testing—an electrophysiological study“. In: *Frontiers in neurology* 6 (2015), p. 244 (cit. on p. 114).
- [HV68a] K-E Hagbarth and ÅB Vallbo. „Discharge characteristics of human muscle afferents during muscle stretch and contraction“. In: *Experimental Neurology* 22.4 (1968), pp. 674–694 (cit. on p. 25).
- [HV68b] K-E Hagbarth and ÅB Vallbo. „Pulse and respiratory grouping of sympathetic impulses in human muscle nerves“. In: *Acta physiologica Scandinavica* 74.1-2 (1968), pp. 96–108 (cit. on p. 25).

- [HV69] K-E Hagbarth and AB Vallbo. „Single unit recordings from muscle nerves in human subjects“. In: *Acta Physiologica Scandinavica* 76.3 (1969), pp. 321–334 (cit. on p. 25).
- [Jen06] Mark P Jensen. „Review of measures of neuropathic pain“. In: *Current pain and headache reports* 10.3 (2006), pp. 159–166 (cit. on p. 19).
- [Kie+00] Matthew C Kiernan, David Burke, Kjeld V Andersen, and Hugh Bostock. „Multiple measures of axonal excitability: a new approach in clinical testing“. In: *Muscle & Nerve: Official Journal of the American Association of Electrodiagnostic Medicine* 23.3 (2000), pp. 399–409 (cit. on p. 19).
- [Kie+20] Matthew C Kiernan, Hugh Bostock, Susanna B Park, et al. „Measurement of axonal excitability: Consensus guidelines“. In: *Clinical Neurophysiology* 131.1 (2020), pp. 308–323 (cit. on p. 43).
- [KK13] Matthew C Kiernan and Ryuji Kaji. „Physiology and pathophysiology of myelinated nerve fibers“. In: *Handbook of clinical neurology* 115 (2013), pp. 43–53 (cit. on p. 64).
- [Kle+12] Inge Petter Kleggetveit, Barbara Namer, Roland Schmidt, et al. „High spontaneous activity of C-nociceptors in painful polyneuropathy“. In: *PAIN®* 153.10 (2012), pp. 2040–2047 (cit. on p. 19).
- [KSJ91] Eric R. Kandel, James H. Schwartz, and Thomas M. Jessell, eds. *Principles of Neural Science*. Third. New York: Elsevier, 1991 (cit. on p. 9).
- [Lag+15] Vera Lagerburg, Mayienne Bakkers, Anne Bouwhuis, et al. „Contact heat evoked potentials: Normal values and use in small-fiber neuropathy“. In: *Muscle & nerve* 51.5 (2015), pp. 743–749 (cit. on p. 114).
- [Lew98] Michael S Lewicki. „A review of methods for spike sorting: the detection and classification of neural action potentials“. In: *Network: Computation in Neural Systems* 9.4 (1998), R53–R78 (cit. on p. 70).
- [Mag+13] Yael G Maguire, Mikhail G Shapiro, Thaddeus R Cybulski, et al. „Physical principles for scalable neural recording“. In: *Frontiers in computational neuroscience* 7 (2013), p. 137 (cit. on p. 56).
- [Mai+10] C Maier, R Baron, TR Tölle, et al. „Quantitative sensory testing in the German Research Network on Neuropathic Pain (DFNS): somatosensory abnormalities in 1236 patients with different neuropathic pain syndromes“. In: *Pain* 150.3 (2010), pp. 439–450 (cit. on p. 19).
- [McK05] David D McKemy. „How cold is it? TRPM8 and TRPA1 in the molecular logic of cold sensation“. In: *Molecular pain* 1 (2005), pp. 1744–8069 (cit. on p. 8).
- [Men10] S Mense. „Functional anatomy of muscle: muscle, nociceptors and afferent fibers“. In: *Muscle pain: understanding the mechanisms*. Springer, 2010, pp. 17–48 (cit. on pp. 7, 8).
- [Mou67] Vernon Mountcastle. „The problem of sensing and the neural coding of sensory events“. In: *The neurosciences: A study program* (1967), pp. 393–408 (cit. on p. 20).

- [MSM16] Aaron D Mickle, Andrew J Shepherd, and Durga P Mohapatra. „Nociceptive TRP channels: sensory detectors and transducers in multiple pain pathologies“. In: *Pharmaceuticals* 9.4 (2016), p. 72 (cit. on p. 7).
- [Nij+13] Tim HJ Nijhuis, Siebe AS de Boer, Abhijeet L Wahegaonkar, et al. „A new approach to assess the gastrocnemius muscle volume in rodents using ultrasound; comparison with the gastrocnemius muscle index“. In: *PloS one* 8.1 (2013), e54041 (cit. on p. 45).
- [NRH88] Jan Nilsson, John Ravits, and Mark Hallett. „Stimulus artifact compensation using biphasic stimulation“. In: *Muscle & Nerve: Official Journal of the American Association of Electromyography and Clinical Neurophysiology* 11.6 (1988), pp. 597–602 (cit. on p. 116).
- [Oka+12] Hideyuki Okano, Hiroyuki Ino, Yu Osawa, Toshiaki Osuga, and Hozumi Tatsuoka. „The effects of moderate-intensity gradient static magnetic fields on nerve conduction“. In: *Bioelectromagnetics* 33.6 (2012), pp. 518–526 (cit. on p. 118).
- [Ond+16] Akiko Onda, Sae Uchida, Harue Suzuki, and Harumi Hotta. „Stimulus frequency-dependent inhibition of micturition contractions of the urinary bladder by electrical stimulation of afferent A β , A δ , and C fibers in cutaneous branches of the pudendal nerve“. In: *The Journal of Physiological Sciences* 66.6 (2016), pp. 491–496 (cit. on pp. 42, 115).
- [PS06] Tim D Plant and Rainer Strotmann. „9 TRPV4: A Multifunctional Nonselective Cation Channel with Complex Regulation“. In: *TRP Ion Channel Function in Sensory Transduction and Cellular Signaling Cascades* (2006), p. 125 (cit. on p. 8).
- [PSK18] John L Parker, Nastaran H Shariati, and Dean M Karantonis. „Electrically evoked compound action potential recording in peripheral nerves“. In: *Bioelectronics in medicine* 1.1 (2018), pp. 71–83 (cit. on p. 119).
- [Pur+04] D. Purves, G. Augustine, D. Fitzpatrick, et al. „Neuroscience, 3rd ed.“ In: 2004 (cit. on pp. 6, 7, 15, 17).
- [Qui+10] Raimi L Quiton, Radi Masri, Scott M Thompson, and Asaf Keller. „Abnormal activity of primary somatosensory cortex in central pain syndrome“. In: *Journal of neurophysiology* 104.3 (2010), pp. 1717–1725 (cit. on p. 19).
- [Ros+18] Charlotte Rostock, Katrin Schrenk-Siemens, Jörg Pohle, and Jan Siemens. „Human vs. mouse nociceptors—similarities and differences“. In: *Neuroscience* 387 (2018), pp. 13–27 (cit. on pp. 26–30).
- [Rou+12] Yann Roudaut, Aurélie Lonigro, Bertrand Coste, et al. „Touch sense: functional organization and molecular determinants of mechanosensitive receptors“. In: *Channels* 6.4 (2012), pp. 234–245 (cit. on p. 9).
- [San+02] Massimo Santoro, Rosa Marina Melillo, Francesca Carlomagno, Alfredo Fusco, and Giancarlo Vecchio. „Molecular mechanisms of RET activation in human cancer“. In: *Annals of the New York Academy of Sciences* 963.1 (2002), pp. 116–121 (cit. on p. 10).

- [SBN10] Jordi Serra, Hugh Bostock, and Xavier Navarro. „Microneurography in rats: a minimally invasive method to record single C-fiber action potentials from peripheral nerves in vivo“. In: *Neuroscience letters* 470.3 (2010), pp. 168–174 (cit. on pp. 19, 45, 113, 115).
- [SCZ00] Gholamhosein Sheikholeslami, Surojit Chatterjee, and Aidong Zhang. „WaveCluster: a wavelet-based clustering approach for spatial data in very large databases“. In: *The VLDB Journal* 8.3 (2000), pp. 289–304 (cit. on p. 94).
- [Sèn18] Damien Sène. „Small fiber neuropathy: diagnosis, causes, and treatment“. In: *Joint Bone Spine* 85.5 (2018), pp. 553–559 (cit. on p. 19).
- [Ser+09] Jordi Serra, Romà Solà, Cristina Quiles, et al. „C-nociceptors sensitized to cold in a patient with small-fiber neuropathy and cold allodynia“. In: *PAIN®* 147.1-3 (2009), pp. 46–53 (cit. on p. 113).
- [Ser+11] Jordi Serra, Romà Solà, Jordi Aleu, et al. „Double and triple spikes in C-nociceptors in neuropathic pain states: an additional peripheral mechanism of hyperalgesia“. In: *PAIN®* 152.2 (2011), pp. 343–353 (cit. on pp. 100, 120).
- [Ser+12] Jordi Serra, Hugh Bostock, Romà Solà, et al. „Microneurographic identification of spontaneous activity in C-nociceptors in neuropathic pain states in humans and rats“. In: *Pain* 153.1 (2012), pp. 42–55 (cit. on pp. 19, 63, 113).
- [Ser+99] Jordi Serra, Mario Campero, José Ochoa, and Hugh Bostock. „Activity-dependent slowing of conduction differentiates functional subtypes of C fibres innervating human skin“. In: *The Journal of physiology* 515.3 (1999), pp. 799–811 (cit. on pp. 61, 63, 70, 81).
- [Sie+17] Joshua H Siegle, Aarón Cuevas López, Yogi A Patel, et al. „Open Ephys: an open-source, plugin-based platform for multichannel electrophysiology“. In: *Journal of neural engineering* 14.4 (2017), p. 045003 (cit. on p. 122).
- [Tal+68] William H Talbot, Ian Darian-Smith, Hans H Kornhuber, and Vernon B Mountcastle. „The sense of flutter-vibration: comparison of the human capacity with response patterns of mechanoreceptive afferents from the monkey hand.“ In: *Journal of neurophysiology* 31.2 (1968), pp. 301–334 (cit. on p. 20).
- [TH76] E Torebjörk and RG Hallin. „A new method for classification of C-unit activity in intact human skin nerves“. In: *Advances in pain research and therapy* 1 (1976), pp. 29–34 (cit. on p. 25).
- [Tor70] HE Torebjörk. „C-fibre units recorded from human sensory nerve fascicles in situ. A preliminary report“. In: *Acta Soc Med Ups* 75.1 (1970), pp. 81–84 (cit. on p. 25).
- [Val18] Åke Bernhard Vallbo. „Microneurography: how it started and how it works“. In: *Journal of Neurophysiology* 120.3 (2018), pp. 1415–1427 (cit. on pp. 20–25, 70, 98, 121).
- [VH68] ÅB Vallbo and K-E Hagbarth. „Activity from skin mechanoreceptors recorded percutaneously in awake human subjects“. In: *Experimental neurology* 21.3 (1968), pp. 270–289 (cit. on p. 25).

- [Wel+10] Scott A Wellnitz, Daine R Lesniak, Gregory J Gerling, and Ellen A Lumpkin. „The regularity of sustained firing reveals two populations of slowly adapting touch receptors in mouse hairy skin“. In: *Journal of neurophysiology* 103.6 (2010), pp. 3378–3388 (cit. on p. 121).
- [WGB08] Alexander B Wiltschko, Gregory J Gage, and Joshua D Berke. „Wavelet filtering before spike detection preserves waveform shape and enhances single-unit discrimination“. In: *Journal of neuroscience methods* 173.1 (2008), pp. 34–40 (cit. on p. 81).
- [WY15] Deric L Wheeler and Yosef Yarden. *Receptor tyrosine kinases: family and subfamilies*. Springer, 2015 (cit. on p. 10).
- [Yos+14] Naoki Yoshimura, Teruyuki Ogawa, Minoru Miyazato, et al. „Neural mechanisms underlying lower urinary tract dysfunction“. In: *Korean journal of urology* 55.2 (2014), p. 81 (cit. on p. 12).
- [Zim+09] Katharina Zimmermann, Alexander Hein, Ulrich Hager, et al. „Phenotyping sensory nerve endings in vitro in the mouse“. In: *Nature protocols* 4.2 (2009), p. 174 (cit. on p. 121).

Websites

- [Adi] [Online; accessed 20-January-2021]. ADInstruments. URL: <https://m-cdn.adinstruments.com/product-data-cards/MLT185-DCW-18B.pdf> (cit. on p. 47).
- [Adn] [Online; accessed 14-January-2021]. ADInstruments. URL: <https://www.adinstruments.com/products/neuro-amp-ex> (cit. on p. 47).
- [Bnc] [Online; accessed 14-January-2021]. National Instruments. URL: <https://www.ni.com/pdf/manuals/372121f.pdf> (cit. on p. 44).
- [Cap] [Online; accessed 27-April-2021]. Biopac. URL: <https://www.biopac.com/wp-content/uploads/a03.pdf> (cit. on pp. 118, 119).
- [Clu] [Online; accessed 12-April-2021]. towards data science. URL: <https://towardsdatascience.com/the-5-clustering-algorithms-data-scientists-need-to-know-a36d136ef68> (cit. on p. 94).
- [Coma] [Online; accessed 21-December-2020]. Program Creek. URL: <https://www.programcreek.com/2011/02/how-compiler-works/> (cit. on pp. 52, 53).
- [Comb] [Online; accessed 21-December-2020]. Slide Share. URL: <https://slideplayer.com/slide/7022986/> (cit. on p. 52).
- [Daqa] [Online; accessed 14-January-2021]. National Instruments. URL: <https://www.ni.com/en-us/support/model.pci-6221.html> (cit. on p. 44).
- [Daqb] [Online; accessed 27-January-2021]. Matlab. URL: https://www.mathworks.com/help/pdf_doc/daq/daq_ug.pdf (cit. on pp. 56, 57).
- [Dev] [Online; accessed 11-January-2021]. tech lobsters. URL: <https://www.techlobsters.com/software-development-methodology-what-is-waterfall/> (cit. on p. 54).

- [Ds7] [Online; accessed 14-January-2021]. Digitimer. URL: <https://www.digitimer.com/product/human-neurophysiology/peripheral-stimulators/ds7a-ds7ah-hv-current-stimulator/> (cit. on p. 43).
- [Fhca] [Online; accessed 14-January-2021]. FHC. URL: <https://www.fh-co.com/product/microelectrode-neurography/> (cit. on p. 46).
- [Fhcb] [Online; accessed 20-January-2021]. FHC. URL: <https://www.phymep.com/wp-content/uploads/2014/09/un-spec-2012.pdf> (cit. on p. 46).
- [Gui] [Online; accessed 1-February-2021]. Matlab. URL: <http://www.apmath.spbu.ru/ru/staff/smirnovmn/files/buildgui.pdf> (cit. on pp. 58, 59).
- [Hom] [Online; accessed 14-January-2021]. Harvard Apparatus. URL: <http://www.harvardbioscience.ca/HAC-Homeothermic-Blanket-System.html> (cit. on p. 45).
- [Hum] [Online; accessed 14-January-2021]. Digitimer. URL: <https://www.digitimer.com/product/life-science-research/mains-noise-eliminators/humbug-noise-eliminator/> (cit. on pp. 48, 49).
- [Irg] [Online; accessed 21-December-2020]. Tutorials point. URL: <https://dev.to/lefebvre/compiler-104---ir-generation-39e8> (cit. on p. 54).
- [Kme] [Online; accessed 5-February-2021]. kaggle. URL: <https://www.kaggle.com/questions-and-answers/156142> (cit. on p. 68).
- [Laba] [Online; accessed 25-January-2021]. ADInstruments. URL: <https://www.adinstruments.com/sites/default/files/wysiwyg-resources/images/labchart-screen-video-capture-zoom-view-channel-calculations.jpg> (cit. on p. 50).
- [Labb] [Online; accessed 21-January-2021]. ADInstruments. URL: <https://www.adinstruments.com/products/labchart> (cit. on p. 50).
- [Lif] [Online; accessed 19-May-2021]. URL: <https://neurondynamics-exercises.readthedocs.io/en/latest/exercises/leaky-integrate-and-fire.html> (cit. on p. 115).
- [Mat] [Online; accessed 11-February-2021]. Eva Maria Kiss. URL: <https://www.evamariakiss.de/tutorial/matlab/> (cit. on p. 52).
- [Mic] [Online; accessed 15-January-2021]. Trittech Research. URL: <https://www.tritechresearch.com/MM-3.html> (cit. on p. 47).
- [MMSD15] University of Minnesota Medical School Duluth. *Gate-control theory of pain*. [Online; accessed 18-November-2020]. 2015. URL: <https://www.d.umn.edu/~jfitzake/Lectures/DMED/Somatosensation/Somatosensation/GateTheory.html> (cit. on pp. 13, 14).
- [Ner17] Ninja Nerds. *Endocrinology | Receptor Pathways*. [Online; accessed 24-November-2020]. Youtube. 2017. URL: <https://www.youtube.com/watch?v=RMV130vU8gA> (cit. on p. 8).
- [Oop] [Online; accessed 10-February-2021]. kaggle. URL: <https://www.w3resource.com/java-tutorial/java-object-oriented-programming.php> (cit. on p. 71).

- [Pca] [Online; accessed 1-February-2021]. BuiltIn. URL: <https://builtin.com/data-science/step-step-explanation-principal-component-analysis> (cit. on p. 67).
- [Pow] [Online; accessed 14-January-2021]. ADInstruments. URL: <https://www.adinstruments.com/products/powerlab-daq-hardware> (cit. on p. 49).
- [Sch] Matthias Scholz. [Online; accessed 26-January-2021]. Max Planck Institute of Molecular Plant Physiology. URL: <https://www.adinstruments.com/sites/default/files/wysiwyg-resources/images/labchart-screen-video-capture-zoom-view-channel-calculations.jpg> (cit. on p. 66).
- [Sem] [Online; accessed 21-December-2020]. Tutorialspoint. URL: https://www.tutorialspoint.com/compiler_design/compiler_design_semantic_analysis.htm (cit. on p. 53).
- [Sha] Slide Share. *Generation and conduction of action potentials*. [Online; accessed 16-November-2020]. URL: <https://www.slideshare.net/CsillaEgri/action-potentials> (cit. on p. 13).
- [Sti] [Online; accessed 19-May-2021]. URL: http://nelson.beckman.illinois.edu/courses/physl317/part1/hw2/hw2p2_prob.html (cit. on p. 114).
- [Tho] Dr. James Thompson. *Chapter 13: Peripheral Nerve Histology*. [Online; accessed 25-November-2020]. Austin Peay State University. URL: https://www.apsubiology.org/anatomy/2010/2010_Exam_Reviews/Exam_4_Review/CH_13_Peripheral_Nerve_Histology.htm (cit. on p. 22).

List of Figures

| | | |
|-----|--|----|
| 1.1 | An experiment for demonstrating that noxious and non-noxious sensations has got two different pathways (A) The setup: a noxious and non-noxious receptor are recorded, heat is applied on the skin. (B) The discharge pattern of these two neurons following temperature increases. (C) The number of action potentials against stimulating temperature. [Pur+04] | 6 |
| 1.2 | The pain sensation experienced by the human body is subdivided into a first sharp and intense pain followed by a second more delayed and diffuse pain sensation. These is due to differences in the conduction velocity of the two types of nociceptors that arise from the dorsal root ganglia, namely <i>Aδ fibers</i> and <i>C fibers</i> [Pur+04] | 7 |
| 1.3 | Ion channels involved in the nociception. Some transmembrane receptors that convert chemical, mechanical and temperature stimuli into ions flux can be found in the free nerve endings of the nociceptors. Among them there are acid-sensitive cation channels (ASIC), transient receptor potential (TRP) vanilloid type 1 (TRPV1) and ankyrin 1 (TRPA1) channels, G-protein-coupled receptors channels (GPCR), transmembrane protein 16 channels (TMEM16A) and tyrosine kinase A channels (TrkA). TRPV1 and ASIC can detect changes in the pH of the extracellular environment, TRPV1 furthermore detects heat, capsaicin, anandamide, 12-hydroperoxyeico-satetraenoic acid (12-HPETE) and mechanical stimuli. TRPA1 detects reactive oxygen species (ROS), nitric oxide (NO) and thiols. GPCR detects Bradykinin, ATP and PgE2. TrkA detects nerve growth factors (NGF). After the transduction of the external stimuli, action potentials are generated through the help of sodium and potassium channels and at the synopsis level the nociceptor releases a wide spectrum of ions such as GABA _B , Opioids (μ), Cannabinoids (CB1) and Adenosine (A1) for signal propagation to the second order neuron. [Ben15] | 10 |

| | | |
|------|--|----|
| 1.4 | Ion channels involved in the rising phase of an action potential. Na _v 1.9 and Na _v 1.3, involved in the amplification of sub-threshold stimuli. Na _v 1.7 contributes to the rising phase as well as it helps Na _v 1.3 and Na _v 1.9 to amplify subthreshold stimuli. Na _v 1.6 is the channel able to produce a resurgent current in some cells and with the help of Na _v 1.8, it contributes to the rising phase of the action potential. [Ben+19] | 11 |
| 1.5 | Post synaptic potential. (A) No summation: a single action potential coming from a single pre-synaptic neuron is not enough for the second order neuron to fire, since the post-synaptic potential does not reach threshold. (B-C) Spatial summation: several pre-synaptic neurons fire at the same time and make connection with the same second order neuron increasing its likelihood to fire. (D) Temporal summation: the same pre-synaptic neuron consecutively fires building up the post synaptic potential [Sha] | 13 |
| 1.6 | Gate control theory. (A) Unmodulate pain. The nociceptor is connected through a excitatory synapses to the second-order neuron and through a inhibitory synapses to the inhibitory neuron. Therefore, when the nociceptor is excited it makes the second order neuron to discharge a strong signal towards the thalamus. (B) Modulated pain. Same principle of unmodulated pain with the exception of having a mechanoreceptors connected to the inhibitory neuron through an excitatory synapses. Thus when both the nociceptor and the mechanoreceptor are stimulated a weaker signal is sent to the brain. [Dic02] [MMSD15] | 14 |
| 1.7 | Major pathways for the central transmission of pain and temperature. These pathways run along the spinothalamic (or anterolateral) system and they are centrally projected. (A) The sensory discriminative component. (B) The affective-motivational component. [Pur+04] | 15 |
| 1.8 | Inflammatory soup following tissue injury. Some chemicals released by the nociceptors (e.g. Substance P, CGRP, etc..) and the body (e.g. ATP, histamine, prostaglandin, etc..) enhance the activity of nociceptors contributing to a temporary allodynia and hyperalgesia in the site of damage. This effect allows the body to heal and to avoid further damages. [Pur+04] | 17 |
| 1.9 | Schematic view of a nerve and its comparison with the tip of the electrode used for microneurographic studies. | 22 |
| 1.10 | Typical action potential (AP) shapes recorded during microneurographic studies. (A) Unmyelinated neuron AP, such as that of a <i>C fiber</i> . (B) Thinly myelinated neuron AP, such as that of a <i>Aδ fiber</i> . [Val18] | 23 |

- 1.11 Peak separation of a myelinated fiber during microneurographic studies. If the electrode is inserted between two nodes of Ranvier at time 0 the recorded action potential (AP) has got a biphasic shape. However, as the time goes by the downstream node due to the damage generated by the electrode starts slowing down and the upstream and downstream AP shapes are no longer synchronized. This generates a quadriphasic shape complex that starts to be more evident until the downstream node fails and the complex becomes again biphasic. [Val18] 24
- 1.12 Comparison of TrkB/TrkA and TrkC/TrkA double positive sensory neurons in mice and humans, in the dorsal root ganglia. Scale bar = 100 μ m. The images (A,B,E,F) shows a representative dual-cloro fluorescence in situ hybridization for the detection of TrkA (in red) against TrkB (in green in A and B) and TrkC (in green in E and F). The insertion in (E, F) shows double-positive cells. (C) Quantification of double-positive TrkB cells against TrkA cells as scatter blots (mean \pm SEM). (G) Quantification of double-positive TrkC cells against TrkA cells represented as scatter blots (mean \pm SEM). No significant (n.s.) difference has been found. Differently oriented squares/triangles shaded or filled represents different subjects. (D,H) Venn diagrams showing the percentage of TrkB/TrkA (D) and TrkC/TrkA (H) from all TrkA expressing cells. [Ros+18] 27
- 1.13 Comparison of TRPV1/TrkA double positive sensory neurons in mice and humans, in the dorsal root ganglia. Scale bar = 100 μ m. The images (A,B) shows a representative dual-cloro fluorescence in situ hybridization for the detection of TrkA (in red) against TRPV1 (in green). The insertion in (A, B) shows double-positive cells. (C) Quantification of double-positive TRPV1 cells against TrkA cells. Significant difference has been found ($p = 0.0003$). Differently oriented squares/triangles shaded or filled represents different subjects. [Ros+18] 28
- 1.14 Comparison of RET/TrkA double positive sensory neurons in mice and humans, in the dorsal root ganglia. (G) Quantification of double-positive RET cells against TrkA cells. Significant difference has been found ($p = 0.002$). Differently oriented squares/triangles shaded or filled represents different subjects. (H,I) Analysis of the relative RET and TrkA transcript expression levels in humans (H) and mice (I), evaluated through fluorescent intensities. In (H) a large group of RET/TrkA double-positive neurons is detectable, but it is not in mice DRGs [Ros+18] 28

| | | |
|------|---|----|
| 1.15 | Comparison of Na _v 1.6- Na _v 1.9/TrkA double positive sensory neurons in mice and humans, in the dorsal root ganglia. (G) Quantification of double-positive RET cells against TrkA cells. Significant difference has been found ($p = 0.002$). Differently oriented squares/triangles shaded or filled represents different subjects. (H,I) Analysis of the relative RET and TrkA transcript expression levels in humans (H) and mice (I), evaluated through fluorescent intensities. In (H) a large group of RET/TrkA double-positive neurons is detectable, but it is not in mice DRGs [Ros+18] | 29 |
| 3.1 | The experimental approach of this study is composed by a stimulation module, animal models, recording module, software development (machine learning and data analysis capabilities) that may led to some discoveries. | 42 |
| 3.2 | Setup for a microneurography recording (adapted from [Kie+20]) . . | 43 |
| 3.3 | | 45 |
| 3.4 | Functional elements of a Digitimer Hum Bug. [Hum] | 48 |
| 3.5 | Labchart software. [Laba] | 50 |
| 3.6 | Matlab IDE. It is composed by four windows. A command window that shows commands and output as well as it can be used for inserting some inputs. A workspace window that displays functions and variables of the running scripts. A folder view that shows all the saved scripts and subfolders. A editor window that displays the content of the scripts, and allows the user to change it. [Mat] | 52 |
| 3.7 | The flowchart of a compiler, from the source code to a machine code readable from the hardware. [Coma] | 53 |
| 3.8 | Basic waterfall model for software development [Dev] | 54 |
| 3.9 | | 56 |
| 3.10 | A data acquisition system. [Daqb] | 57 |
| 3.11 | Guide layout for the design of a GUI. [Gui] | 58 |
| 3.12 | Guide graphical user interface example. [Gui] | 59 |
| 3.13 | Raster plot extraction. (A) Sweep traces with two action potentials on it. They are first increasing their latency and they then recover back. (B) A raster plot extracted putting a horizontal threshold on all the traces above and plotting a dot only when the signal is exceeding this value. On it two horizontal thin-like lines are shown, those correspond to the two neurons that were discharging in the graph above. [Ser+99] | 61 |

| | | |
|------|---|----|
| 3.14 | Activity dependent slowing and marking technique. [Ser+99] (A) A type 1 fiber is shown, its latency increases during the 4Hz stimulation and it recovers to the baseline when the stimulation frequency comes back to 0.25Hz, this phenomenon is called activity dependent slowing. Then 4 natural stimuli are applied in the so-called marking technique, at a) by a metal rod (ca 25 °C), at b) by ice, at c) by Von Frey hair (24 bar) and at d) by heating to 48 °C for 5 s. (B) A type 2 unit is shown on it instead and its ADS is totally different with respect to the type 1 fiber, moreover at a) and b) a metal rod (ca 25 °C) is applied. | 63 |
| 3.15 | Working principle of the recovery cycle. [KK13] | 64 |
| 3.16 | Working principle of a principal component analysis (PCA). [Sch] . . . | 66 |
| 3.17 | Object-oriented programming. [Oop] | 71 |
| 4.1 | SPiike software analysis module - Graphical User Interface (GUI). On the top, a graph showing the filtered data recorded by the recording electrode. On the bottom, the raster plot of the fibers under investigation, 9 fibers are shown on it an the marking technique has been applied. After 128mN, hot rod and ice application a exponential decay of some fiber latency can be noticed, meaning that the fibers reacted to the stimulation. | 80 |
| 4.2 | QTrac software, with the same pattern discharge of the SPiike software (figure 4.1) | 81 |
| 4.3 | Installation of the standalone SPiike software | 82 |
| 4.4 | Graphical user interface of SPiike recording module. | 83 |
| 4.5 | Tabs of the menu bar. | 84 |
| 4.6 | Setting of some menu bar options. | 85 |
| 4.7 | Stimulus type parameters. | 86 |
| 4.8 | Activity-dependent slowing of C fibers innervating rat skin [Geo+07]. The figure shows the activity-dependent slowing of C fibers innervating rat skin. This is also used as a comparison for the figure 4.9 in which faster fibers (A δ -fibers) have got the same ADS behavior, meaning that with SPiike software faster fibers can be recorded and analyzed as well. | 89 |
| 4.9 | Adelta fibers showing an activity-dependent slowing such as C fibers. In the raster plot, on top at a latency of 8ms an A δ -fiber shows activity-dependent slowing and a response to different stimuli (mechanical stimulation, hot rod and ice application). On the bottom, other A δ -fibers do not respond to the marking stimulation however they have got an ADS with his characteristic exponential decay slowing. | 90 |
| 4.10 | Analysis module menubar differences | 92 |

| | | |
|------|--|-----|
| 4.11 | Fiber extraction. The plot above shows a modified recorded data with the threshold (red line) at 10mV. The raster plot below shows the activity-dependent slowing (ADS) of some C-fibers. Two of them have been selected (red dots) for sorting. | 95 |
| 4.12 | Principal component analysis (PCA) and K-means. These techniques are applied on the selected fibers (red dots) of Figure 4.11. Top left, action potentials of these two fibers, superimposed. Top right, first three components (PCs 1-3) of the PCA algorithm. Bottom right, K-means applied to the PCA clusters for sorting. Bottom left, average of the action potentials related to the first and second cluster (C-fiber 1,2). . | 96 |
| 4.13 | PCA and K-mean of C vs Adelta fibers. These techniques are applied to the A δ -fiber at 8ms latency of figure 4.9 and a C fiber in the same recording. Top left, action potentials of these two fibers, superimposed. Top right, first three components (PCs 1-3) of the PCA algorithm. Bottom right, K-means applied to the PCA clusters for sorting. Bottom left, average of the action potentials related to the first and second cluster (C-fiber 1,2). The two fibers show different action potentials, and this resemble the literature for myelinated and unmyelinated fibers. | 97 |
| 4.14 | A δ -fibers statistical analysis | 98 |
| 4.15 | C-nociceptors parameters (Adapted from [Ser+11]) | 100 |
| 4.16 | The graph shows the number of spikes per sweep -of the fibers under investigation- as function of the elapsed time. The spikes represent abrupt changes in the neurons discharge. They follow marking stimuli and accidental events (e.g. patient movement or noisy discharges). . . | 101 |
| 4.17 | The graph shows the spikes per second of the stimulated fibers upon marking stimulation. It has been performed with ice, applied directly to the receptive field of the neurons under stimulation. Through this feature a dynamic change in the IFR can be noticed and studied. Basically, in this specific case a slowly adapting behavior can be observed. Vertical red lines represent the sweeps onset. | 102 |
| 4.18 | Z-score fibers activity statistics | 103 |
| 4.19 | | 105 |
| 4.20 | Correlation between Spiike and Qtrac software comparing the time to recovery to 50% after 2Hz stimulation of some C-fibers, given in s. The correlation is linear meaning that the outcomes are fully complementary and the two software are swipable for this kind of analysis. | 105 |
| 5.1 | SPiike software graphical user interface (GUI). | 112 |
| 5.2 | Frequency response of neurons when stimulated with a sinusoidal function. [Sti] | 114 |
| 5.3 | Injection of a sinusoidal current and its effect on membrane potential. [Lif] | 115 |

| | | |
|-----|---|-----|
| 5.4 | Fibers subpopulation classified according to their conduction velocities. Namely, the elapsed time from the stimulus artifact at which they appear. [Oka+12] | 118 |
| 5.6 | At a latency of 8ms an A δ -fiber shows activity-dependent slowing and a response to different stimuli (mechanical stimulation, hot rod and ice application). This resembles the behaviour of a C-fiber. | 120 |

Publications

P46-S RP11-819C21.1 and ZNRD1-AS long non-coding RNA changes following experimental pain correlate with laser-evoked potential habituation—Catello Vollono^{a,*}, Costanza Pazzaglia^a, Massimo Santoro^b, Enrica Di Sipio^b, Rocco Giordano^a, Luca Padua^a, Lars Arendt-Nielsen^c, Massimiliano Valeriani^{d,e} (^aDepartment of Geriatrics, Neuroscience and Orthopedics, Fondazione Policlinico Universitario 'A. Gemelli' IRCCS - Università Cattolica del Sacro Cuore, Rome, Italy, ^bDepartment of Neurology, Don Carlo Gnocchi Onlus Foundation, Milan, Italy, ^cLaboratory for Experimental Cutaneous Pain Research, SMI, Department of Health Science and Technology, Faculty of Medicine, Aalborg University, Aalborg, Denmark, ^dNeurology Unit, Ospedale Pediatrico Bambino Gesù, IRCCS, Rome, Italy, ^eCenter for Sensory-Motor Interaction, Aalborg University, Aalborg, Denmark)

* Corresponding author.

Background: Long non-coding RNAs (lncRNAs) are a group of non-coding RNAs acting as regulators of gene expression, through interaction with histones or through interaction with complementary DNA sequences, implicated in various human diseases such as cancer, cardiovascular diseases, autoimmune and neurodegenerative disorders and have been reported to be involved in the modulation of neuropathic pain.

We recorded Laser Evoked Potentials (LEPs) in order to study: (1) lncRNAs modifications in experimental pain model; (2) correlation between the lncRNA changes and objective measure of pain perception.

Material and methods: LEPs were recorded in 11 healthy subjects after hand and perioral region stimulation. Three consecutive series were recorded for each stimulation site in order to investigate the habituation. Blood samples were collected immediately before LEP recording (baseline) and after 30-min (post-pain). We screened 84 lncRNAs, involved in autoimmunity and inflammatory response.

Results: We identified 2 lncRNAs up-regulated at the post-pain time: RP11-819C21.1 (fold change = 8.2; $p = 0.038$) and ZNRD1 antisense RNA 1 non-protein coding (ZNRD1-AS) (fold change = 6.3; $p = 0.037$). The up-regulation of both lncRNAs showed a significant positive correlation with the LEP habituation to perioral region stimulation ($p = 0.04$ and $p = 0.01$, respectively).

Conclusions: This is the first study showing lncRNA changes in a pain experimental model. RP11-819C21.1 and ZNRD1-AS shows as direct target miR-19a and miR19b, a class of microRNAs involved in modulation of multiple potassium channel α -subunits.

lncRNAs could be involved in the pathophysiology of painful diseases characterized by reduced habituation to pain.

doi:10.1016/j.clinph.2019.04.582

P47-S Cold C-fibers sensitization to warm stimulation after ultraviolet B and heat-capsaicin exposure—Lenin Reyes-Haro^{*}, Federico Ponente, Romà Solà, Jordi Serra (Neuroscience Technologies, Barcelona, Spain)

* Corresponding author.

Background: Capsaicin, UV-B irradiation and electrical stimulation methods have been used to develop experimental hyperalgesia in Phase-I human studies. These sensitization models contribute to

the study of the functional behavior of small fiber C-nociceptors. However, there is no published literature about functional changes of cold C-fibers using these models.

Material and methods: Skin sensitization was induced at the dorsum of the foot (superficial peroneal nerve) in two healthy volunteers using ultraviolet B radiation in one female and heat/capsaicin in one male. Microneurographic recordings were performed in the intermediate branch of the superficial peroneal nerve. Then trains of cold and warm stimuli, from 32 to 4 and 32 to 48-Celsius degrees respectively, were applied in the skin area of interest before and at least 45 min after induction of the skin sensitization models.

Results: Preliminary results showed a single cold C-fiber recorded in each subject. During cold stimulation, there were not functional variations in the cold receptors. Warm stimulation induced a reduction of the spontaneous firing rate of the cold fibers during the baseline recording in both models (room temperature at 25 °C). After the UVB and heat-capsaicin induction, the firing rate of the cold C-fibers in response to cold stimuli was increased. All cold C-fibers recorded became also sensitized to warm stimuli.

Conclusions: The ultraviolet B radiation and the heat-capsaicin sensitization models sensitize cutaneous cold C fibers to warmth. Some cases of warm allodynia in humans could partially be explained by skin sensitization after inflammatory processes (e.g., sunburn or thermal/chemical exposure).

doi:10.1016/j.clinph.2019.04.583

P48-S Obstructive sleep apnea in Myasthenia gravis patients—Ho-Won Lee^{*}, Ji-Sung Park (Kyungpook National University Chilgok Hospital, Daegu, South Korea)

* Corresponding author.

Background: Myasthenia gravis (MG) is autoimmune diseases that manifest clinical symptoms including diurnal fatigability, ptosis, diplopia, dysarthria and rarely respiratory failure. Few studies have demonstrated a high prevalence of obstructive sleep apnea (OSA) in MG. The aim of this study was to elucidate the clinical and polysomnographic difference between clinically stable Korean MG patients with and without OSA.

Objectives and methods: Total of eighteen stable MG patients were enrolled. The clinical parameters including sex, age, duration of the disease, prescribed medication status, thymectomy status and antibody status were obtained. The overnight polysomnography (PSG) was performed in all patients.

Results: We compared MG patients with and without OSA in relation to the baseline characteristics and overnight PSG parameters. Among the clinical parameters, male sex and body mass index showed a statistically significant difference between the two groups. The PSG showed eleven times higher apnea-hypnea index (AHI) in MG with OSA. AHI was further analyzed with supine and non-supine position and 70% of the MG with OSA manifested supine OSA.

Conclusions: This study demonstrated male sex and body mass index as significant clinical risk factors of OSA in MG and PSG data showed a high prevalence of supine dominant OSA.

doi:10.1016/j.clinph.2019.04.584

Colophon

This thesis was typeset with L^AT_EX 2_ε. It uses the *Clean Thesis* style developed by Ricardo Langner. The design of the *Clean Thesis* style is inspired by user guide documents from Apple Inc.

Download the *Clean Thesis* style at <http://cleanthesis.der-ric.de/>.

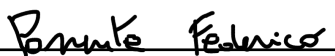
Declaration

I declare that I have completed this work solely and only with the help of the mentioned references as well as my supervisors.

Universitat de Barcelona, Facultat de Medicina

Barcelona, Spain

May 26, 2021

A handwritten signature in black ink, reading "Ponente Federico", is written over a horizontal line.

Federico Ponente

